FREQUENCY AND TEMPERATURE DEPENDENCE OF DIELECTRIC PROPERTIES OF SOME COMMON ROCKS

by

Marcel St. Amant

B.Sc., Physics, University of Montreal
(1967)

SUBMITTED IN PARTIAL FULFILLMENT
OF THE REQUIREMENTS FOR THE
DEGREE OF MASTER OF
SCIENCE

at the

MASSACHUSETTS INSTITUTE OF
TECHNOLOGY
August, 1968

Signature of Author_____
Department of Geology and Geophysics, August , 1968

Certified by_____
Thesis Supervisor

Accepted by_____
Chairman, Departmental Committee on Graduate Students

Lindgren

FREQUENCY AND TEMPERATURE DEPENDENCE OF DIELECTRIC PROPERTIES OF SOME COMMON ROCKS

by
Marcel St.-Amant

Submitted to the Department of Geology and Geophysics, Massachusetts Institute of Technology, August 1968, in partial fulfillment of the requirements for the degree of Master of Science

Abstract

As part of an investigation of the possible dielectric behaviour of lunar surface materials and in order to understand the mechanism of these effects, the dielectric constant, the dielectric loss, the resistivity in powder and in solid forms as a function of temperature and frequency in vacuum, have been measured on some geologic materials. A basalt, a granite and a dunite were the three rocks tested in solid forms while several others were tested only as powders. The temperature range used was 27°C to about 400°C, with the exception of a basalt where temperatures down to -60°C were also investigated. The frequency range used is about 50Hz to 3MHz.

The results show that most of the macroscopic dielectric properties of dry rocks are manifestations of the classical or the non-classical Maxwell-Wagner effect. Among these are: 1) a loss tangent rise at low frequency, 2) one or more relaxation peaks observed in powdered rocks, 3) a lower value of A.C. resistivity at low frequency than expected, and 4) a relatively frequency-independent loss

tangent at low frequencies.

At high frequencies, the frequency-independent loss tangent is, for the present time, best explained with the help of Garton's theory. In his model, the polarizable elements are dipoles consisting of double potential wells where one well is very much deeper than the other in the absence of a field and is stable. The shallow well is thermally activated. Garton shows that this leads to an exactly frequency-independent imaginary dielectric constant for a frequency range which may be chosen as wide as desired.

Investigations have also been made on the effect of a very small amount of water on a basalt sand, with some unexpected results. The most striking one is that below a critical concentration, the presence of water results in an increase of the loss tangent, independent of the frequency, and with a corresponding increase of dielectric constant. A relaxation peak was observed also at 0.5% water concentration.

Thesis Supervisor: David W. Strangway
Title: Assistant Professor of Geophysics

Table of Contents

		Page
Abstract		ii
Table of Contents		iv
Acknowledgements		vi
List of Tables		vii
Table of Symbols		viii
I.	INTRODUCTION	
	1. Purpose of the Investigation	1
	2. Review of the Dielectric Mechanism	2
	3. Other Similar Investigations	5
II.	THE EXPERIMENTAL WORK	
	1. Description of Instruments	8
	2. Experimental Procedure	12
	3. Quality of Data	18
III.	DESCRIPTION OF RESULTS	
	1. The Basalt AA Sample	20
	2. The Powder Samples	22
	3. The Solid Samples	24
IV.	DISCUSSION	
	1. General	26
	2. The Frequency Independent Loss Tangent	27
	3. The Effect of Water	31
	4. The Relaxation Peak in Powdered Rocks	33
	5. The Relaxation in Pyroxenes	34
	6. Behaviour at Low Frequency	36
	7. Difference Observed Between Powder and Solid Forms of the Same Material	38

8. The Dielectric Constant Value 39
9. The Irreversible Thermal Effect 44
10. Other Effects 45

V. CONCLUSIONS 46

References 48

Appendix A: Computer Output 51
B: Graphs
Explanation and List 63
C: Table and Illustration of
Instruments, Fig. 1 to Fig. 7 122
D: The Determination of K, tan from
the Experimental Data 131
E: Proposed General Form of tan
for Dry Sand and Low Density
Rock (at 27°C) 132

ACKNOWLEDGEMENTS

This investigation has been supported by NASA under project NGR 22-009-257 as part of a lunar electromagnetic study. Instrumentation was made available from NASA project NGR 22-009-176.

I am very grateful to my thesis advisor, Dr. David W. Strangway, for his many thoughtful suggestions and guidance throughout this work.

Also, this work has been possible with the help of numerous kind people in the department and to whom I am greatly indebted:

To Dr. G. Simmons who provided some of the rock samples and many electronic instruments which were intended for the research project of Dr. K. Horai whom I also thank.

To Dr. D.R. Wones who provided mineral samples.

To David Enggren for his kind assistance and helpful technical advice.

To Sara Brydges who typed this work and helped me to improve the English quality of the text.

To Dr. C. Wunsch, Dr. W.F. Brace, Dr. R.S. Naylor and Dr. H.W. Fairbairn for their advice, the use of their machine shop and their sample preparatory laboratory.

My friend Yves Pelletier did the mineralogic analysis and the sample holder #4 was machined by Dave Riach and Jock Hirst.

List of Tables

		Page
Table I.	Table of Symbols	viii
Table II.	Physical Parameters of Samples	13
Table III.	Electrical Parameters of Samples	23
Table IV.	Mineralogic Analysis of Basalt M	41
Table V.	Mineralogic Analysis of Granite	42
Table VI.	Calculated and Measured Values of the Dielectric Constant of Powders	43
Table VII.	Table of Instruments Used	129

Computer Outputs

Table CO-1.	Basalt AA: Powder form	52
Table CO-2.	Plagioclase: Powder form	53
Table CO-3.	Hypersthene: Powder form	54
Table CO-4.	Dunite: Powder form	55
Table CO-5.	Basalt M: Powder form	56
Table CO-6.	Granite: Powder form	57
Table CO-7.	Augite: Powder form	58
Table CO-8.	Diabase P: Powder form	59
Table CO-9.	Basalt M: Solid form	60
Table CO-10.	Granite: Solid form	61
Table CO-11.	Dunite: Solid form	62

Table I

Table of Symbols

Symbol	Definition
C	Capacitance in picofarads
d	Thickness in cm
e	2.71828
E	Activation energy related to the relaxation
ev	Electron volt
f	Frequency in Hz
G(y)	Distribution function in respect to variable y
Hz	Hertz (cycles/sec)
KHz	Kilohertz
MHz	Megahertz
I	Electrical current in amperes
k	Boltzmann constant
K or K'	Real dielectric constant
K"	Imaginary dielectric constant
K*	Complex dielectric constant
P	Polarization value of a dielectric
Q	Electric charge in coulombs
t	Time in seconds
T	Temperature in degrees Kelvin (unless otherwise indicated)
tan δ	Loss tangent = $\frac{K'}{K''}$
U	Activation energy related to the concentration of lattice defects
u	Activation energy related to the mobility of the charge carriers
v	Packing factor or the volume fraction of a given material
V	Potential difference in volts
w	Activation energy related to the conductivity or resistivity

Symbol	Definition
y	Dummy variable
σ	Conductivity in mho/cm
σ_∞	Conductivity in mho/cm at $\frac{1}{T} = 0$
ρ	Resistivity in ohm-cm
ρ_∞	Resistivity in ohm-cm at $\frac{1}{T} = 0$
τ	Relaxation time in seconds
τ_∞	Relaxation time in seconds at $\frac{1}{T} = 0$
ν	Relaxation frequency in Hz
ν_∞	Relaxation frequency in Hz at $\frac{1}{T} = 0$
ν_m	Frequency of a loss tangent maximum
$\nu_{\infty m}$	Frequency of a loss tangent maximum at $\frac{1}{T} = 0$
ω	Angular frequency in rad/sec
η	Porosity = (1-V)

SUBSCRIPTS

s	Static value or low frequency limit
∞	High frequency limit
ac	Alternative current
dc	Direct current

I. INTRODUCTION

I.1. Purpose of the Investigation

The purpose of this research is to study the dielectric behaviour of dry rocks, and the effect of a very slight amount of water, and to look for correlations between different electrical properties of the sample and their composition. These data may be very useful for dielectric studies of the lunar materials since the upper parts are considered to be very dry. Because it is believed that an appreciable depth of loose materials may be found in parts of the lunar surface, both powder and solid forms were studied.

In other investigations, some questions remained unsolved. Measurements made on "dry" rocks at room temperature show a dispersion of the dielectric properties at low frequency, usually thought to be due to a residual tightly bonded water effect. It is also believed that if the rock was truely dry, no such dispersion would appear. It will be shown in this investigation that this is not the case.

An attempt to explain the universally observed relatively constant value of loss tangent with frequency in dry rocks over a wide frequency range at room temperature was also made.

It has been suggested (6) that the resistivity of the lunar surface rocks may have been overestimated by many orders of magnitude since an extremely low conductivity is expected for dry powders.

Much experimental work in this investigation has been done at high temperature in vacuum for two reasons: 1) to get the relation $K(f,T)$, $\tan\delta(f,T)$ and $\rho(T)$, 2)to be sure that the sample is adequately dried and to measure the effect of the remaining bondedwater. Such a rigorous dehydration seems important. Some experimental observations

made by Howell and Licastro (14) found that a sample, when left in the atomosphere, increases its dielectric constant value within a matter of minutes due to water absorption.

I.2. Review of the Dielectric Mechanism

Most dielectric properties of materials can be explained in terms of relaxation or of resonance effects. In fact, these phenomena are mathematically the end limit of a single general mechanism (5), (9), involving an array of independent oscillators which respond to an electric field change with various amounts of damping. The resonance effect is only observed in the optical region and will not be discussed further here.

Widely different hypotheses lead to the same mathematical formulation known as a Debye-type relaxation phenomena (5) which is:

$$K^*(\omega) - K_\infty = \frac{K_s - K_\infty}{1 + i\omega\tau}$$

$$\tan\delta = \frac{(K_s - K_\infty)\omega\tau}{K_s + K_\infty\omega^2\tau^2}$$

for simgle relaxation time case. These relations are illustrated in Figure G1.

One interesting hypothesis which does assume any relaxation mechanism is:the rate of approach to equilibrium is proportional to the distance from equilibrium.

$$\tau \frac{dP(t)}{dt} = P_s - P(t)$$

where τ is constant.

Other elementary models are discussed in text books (4), (19). All microscopic mechanisms which explain dielectric

relaxation at low frequency in crystalline solids involve impurities or defects in the crystal (1), (2), (22),(21).

Another well known relation in dielectric studies is the one referred to as the Kramers-Kronig relation. It is

$$K'(\omega) - K_\infty = \frac{2}{\pi} \int_0^\infty \frac{yK''(y)}{y^2 - \omega^2} dy \qquad \text{for real component}$$

and

$$K''(\omega) = -\frac{2\omega}{\pi} \int_0^\infty \frac{K'(y) - K_\infty}{y^2 - \omega^2} dy \qquad \text{for complex component}$$

which holds for all linear systems (9 , for derivation of formulas), and is more general than the preceding one.

All molecular models give a temperature-dependence of relaxation time of the type

$$\tau = \tau_0 e^{E/kT}$$

Usually τ_0 is constant or varies as T^{-1}, and has a value of about $10^{-13\pm4}$ sec. (5).

In general, measurements show a broader maximum than that predicted by the Debye curve. One reason for this broadening is the interaction between polarizable oscillators such as in the case of polymer chains (8). Another interesting observation is the close correlation between dielectric loss and sonic and ultrasonic mechanical loss. A maximum in tan δ (f) is often reproduced when measuring its mechanical loss dependence on frequency (2), (25).

A very interesting observation made on dielectric materials is that most of them show a fairly constant value of tan δ over a wide frequency range. The relaxation

mechanisms discussed do not directly explain this, but a distribution of relaxation times $G(\tau)$ can be used as an explanation. A relatively constant value of tan δ is observed in many rocks and a theoretical understanding of this is of geophysical interest.

The distribution of τ may come from either of the parameters in the equation $\tau = \tau_0 e^{-E/kT}$.

Gever and du Pre (11), (12) give an interesting relation between electrical properties of such dielectrics which suggests that the distribution of τ is due to a distribution $G(\ )$ which slowly varies with E. For dielectrics where $\frac{\partial K}{\partial T}$ due to thermal expansion is small:

$$\frac{\partial K}{\partial T} \frac{1}{K \cdot \tan\delta} = -\frac{2}{\pi} \frac{\ln \tau_0 \omega}{T}$$

They do not explain the source of this large range. Garton (10) also gives an interesting explanation. He considers the case of a bistable model where potential wells are asymmetrical, the smaller one being thermally activated and having a range of energy values. The deeper well is stable as illustrated below, for the case of a dipole.

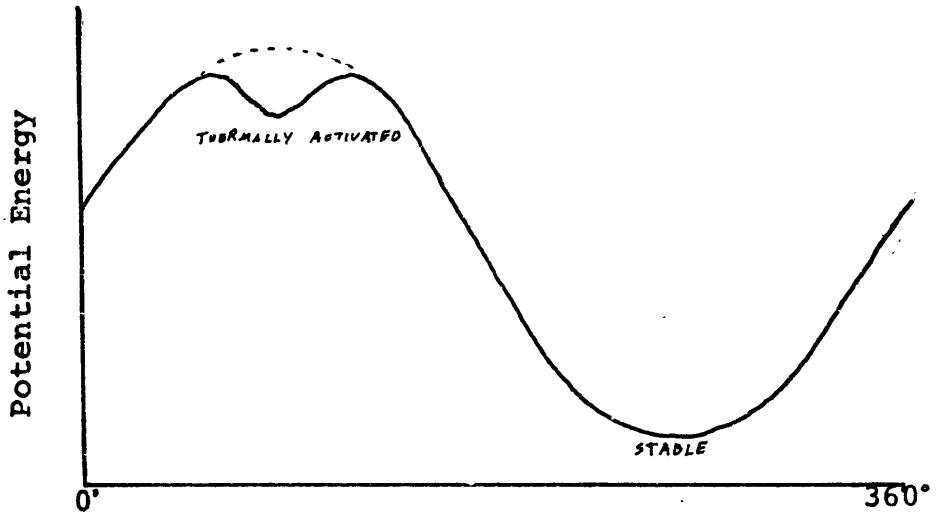

Angle of Rotation of a Dipole

This can readily lead to a frequency-independent imaginary dielectric constant (10). It has not been proved experi-

mentally, but it is likely to be important in amorphous materials or in disordered regions of a crystal (5), (10).

As we have said above, widely differing hypotheses can result in relaxation process. If we find a Debye peak, this does not prove that the effect is due to the microscopic structure of the material but may be due to its microscopic imperfection (5), (26), classical Maxwell-Wagner effect of inhomogeneous material (21) or a reversible trapping of charge carriers at domain interfaces or imperfections (28).

Attention must be given to the electrical contact at the electrodes which can lead to large errors in conductivity measurements (15) or dielectric measurements (5). These effects are non-linear.

I.3. Other Similar Investigations

Frequency and temperature dependence of dielectric properties of earth materials have been investigated since about 1945, mostly by Russians.

This type of research is as yet relatively rare, and may not well apply to the lunar problem.

The geologic material on which the dielectric properties have been studied as a function of temperature and frequency are: quartz (25), ice (7), (13), water (13), kaolinite (17), granite, quartz sand, microcline, muscovite. Parkhomenko (24) gives a good review of this kind of research. The quartz is the only one investigated in both powder and solid forms over a wide range of frequency and temperature.

Howell and Licastro (14) published an experimental study of the frequency dependence of the dielectric constant for a large variety of geologic material. They

observe a dispersion at low frequency in all "dry" rocks, and interpret this as being the effect of a remaining tightly bonded water. They verify the accuracy of some formulas for predicting the value of the dielectric constant of a mixture and found that measured values are always higher than the calculated ones for the porosity range investigated. They observed also that a very small moisture content in a rock drastically affects its dielectric properties, especially at low frequency. They found that the Keller and Licastro theory (explained below) did not explain their observations and concluded that some interfacial polarization occurs and probably also some electrode polarization.

Keller and Licastro (16) put forward a theory which may explain the very large dispersion in their sedimentary wet rock sample. They exclude the electrode polarization effect (p.266), and put forward a dispersion mechanism which is in fact a variation of the membrane polarization theory for the IP effect developed by Marshall and Madden (20). The difference is that the former theory involves a storage pore. This model requires that the rock has at least a large salt water content. They observe also a drastic change of the dielectric properties of sedimentary rocks around a critical value of water concentration. It is interesting to note in their results, a loss tangent maximum at $10^{4\pm1}$ Hz in many samples.

Such observations were also made by Chelidge (see Parkhomenko, 23) for many rock samples. He proves experimentally that such effects are volume effects and not electrode effects. Figure G2 (Fig. 92 in ref. 23), is also a very good example. It shows other interesting features which will be discussed later.

Jiracek reports some dielectric measurement on three basaltic rocks. It is interesting to note a break in their loss tangent curve at 10^4Hz in some of their

moistened samples. This result has been used for some lunar models (27).

II. EXPERIMENTAL WORK

II.1. Description of Instrument

In Figure 7, (the photograph) instrumental configuration is shown and Table VII gives the list of the instruments. Ground loops were eliminated by careful shielding and interference between instruments was found to be small. A small voltage due to high impedance coupling was found between the Variac, feeding the furnace, and the electrometer (Keithley 600A), probably due to a residual transformer effect between the anti-inductive winding of the furnace and the sample holder. When low voltages were measured, the powerstat was shut (1-2 min.) and the temperature did not vary more than 5°C during the reading.

a) The Sample Holder #1

The first sample holder was a simple cylindrical container with a central electrode. For resistivity measurements, the central electrode was smaller and two other concentric electrodes, made of very coarse aluminum screen were added to make a four-electrode configuration (the holes of the screen were squares with 1.5 cm. side, and the ratio: area of holes over total area, was about 80%.)

b) The Sample Holder #2

This sample holder (not drawn) is a rectangular aluminum box, 115mm x 115mm x 15mm inside dimensions, with a plate of aluminum 95mm x 95mm x 1.5mm held in place by 4 small teflon legs at its corners, inside the chamber, parallel to the large faces of the box, without touching any wall of the interior of the chamber. This plate plays the role of the active electrode of the capacitor, the chamber itself being the ground electrode. A small wire connected to this active plate passes through

an opening (5mm. diam.) of the aluminum box. It was possible to open the box to put in the sample powder. Large errors may be present due to electrode effects, as investigated by Scott et al (24) but they found that for a small concentration of water, non-contact and contact electrodes give very similar results, if not identical. In the present investigation slightly humid basalt sand was tested over a temperature range from 27°C to -60°C and from 100Hz to 3MHz. For water concentration less than 1% weight basis, no serious electrode polarization effects are believed to occur.

c) The Sample Holder #3

This sample holder, (Figure 1) is used only for dry powdered materials, from 27°C to 350°C and from 50Hz to 2MHz. It is cylindrical and consists of [1] a high temperature, vacuum-tight ceramic feed-thru; [2] a steel vacuum chamber plated with gold, acting as part of the ground electrode of this capacitor; [12] an active electrode holder, [4] removable active electrode; [6] removable ground electrode; [10] a retaining screen; [8] a retaining porous stone; [9] a nickel plated copper vacuum seal; [5] an inner thermocouple head;[3],[11] a protective ceramic tube with its lead in; [7] a vacuum tight stopper, acting as a pressure plate to squeeze the seal, and the sample space in between the electrodes.

All electrodes were gold plated, attention being given to protecting the ceramic feed-thru during plating. Its useful volume capacity was 12.3 ± 0.2 cc of the sample. Its useful empty capacitance was 30.4 ± 0.2 pf., the effective ceramic feed-thru capacitance is 3.0 pf., adding to the preceding capacitance value for an overall value of 33.4 pf. The effective feed-thru capacitance is defined as that part of the capacitance of the sample holder which is independent of the dielectric constant

of the sample which fills this instrument. The vacuum reached at room temperature was better than 1 micron and was probably about 0.1 micron.

This instrument has been partially damaged in two ways. During the calibration process at elevated temperature, up to 500°C, the instrument was contaminated for unknown reasons. A deposit was formed, slightly orange to brown in color. Vacuum oil vapors, or copper oxide from copper seals are possible sources. Examination of these seals showed a very strong change in color on heating. The ceramic feed-thru was short circuited by this deposit and so a vacuum trap was added, and the vacuum seals, plated with nickel. Decontamination was done in the following way. First, the ceramic feed-thru was heated in a bunsen flame, with the vacuum on the instrument. The short circuit was eliminated after a few treatments like this and its resistance, as well as its temperature dependence returned to its nominal value. Second, the contaminated gold surfaces were sanded with very fine emery paper and glass wool. The gold surface regained its color and became shiny.

The decontamination process was not ideal because the vacuum became temperature dependent, due to a small leak in the ceramic as shown in Figure 2, but completely reversible, at room temperature it was as good as initially.

At the end of the vacuum pipe, Figure 5, a ceramic vacuum-tight tube acted as vacuum tubing and as thermal insulator.

d) The Sample Holder #4

This instrument was made for measurement of solid samples in vacuum at high temperature, theoretically up to 700°C.

It has 5 discrete pieces (Figure 3).

1) The base parts are: [7] a ceramic feed-thru similar to the preceding instrument; [8] a stiff steel needle; [12] the base itself.
2) The upper plate: [2] thermocouple hole, [9] ceramic vacuum-tight tube for thermal insulation which terminates the vacuum pipe; [3] the plate itself; [10] an L joint.
3) [4] nickel plated copper seal.
4) [5] ventilated upper vise jaw.
5) [6] removable ventilated vise jaw

[1] and [11] are thermocouples.

This instrument just held the sample in place, and gave a 0.1 micron vacuum with the maximum of aeration to help remove moisture from the sample. No direct electrical contact was made between the sample and this instrument, but contact was made with removable platinum electrodes described later.

The ceramic feed-thru capacitance was 1.6 pf (less than the preceding instrument due to the smallness of the needle). The sample holder #4 has a large thermal inertia but also a good internal thermal conductivity which helps to reduce thermal gradients within the sample, when in thermal equilibrium.

e) The Furnace

Figure 5 shows a cross section of the furnace in operating position with sample holder #3. In this figure, the scale is 1 cm:1 in. The chromel wire winding embedded in the alundum paste is of anti-inductive type. The furnace was designed for low thermal inertia, to minimize eddy currents in the sample holder due to the winding of heating wires, and was well insulated for good low-temperature gradients (Figure 6).

II.2. Experimental Procedure

a) Sample Preparation

Samples were prepared in various ways, depending on size, form and availability. Basalt AA was bought in sand form from Lane and Sons Construction Company, Westfield, Mass. and sifting was the only operation necessary. The three rocks used as solid samples were drilled with a diamond drill and then were cut into slices 0.080" thick, with parallel polished faces.

Augite, as well as diabase P were crushed in a ceramic mortar and pestle. Surface alterations and impurities were removed by hand picking when the powder was still coarse-grained, but not all impurities could be removed, especially for the augite sample as explained later. Later observations under the microscope revealed at most 10% by volume of impurities of green color in the augite sample. All other materials were crushed with steel mechanical crushers and pulverizers to a mean mesh size of 20-24. The instruments were cleaned and brushed each time and all iron chips found in the sample from the grinders were removed with a magnet. For basalt, more attention was given so as not to remove all the magnetite. Probably half of magnetite content was removed in that way, but it appears to be unimportant in determining the dielectric properties. Visible impurities were hand picked at each stage of grinding and pulverizing process and the pure powder sifted to various upper diameter sizes (see Table II). The coarser grains were crushed in a ceramic mortar and pestle and sifted again. All sand samples were stored in polyesterene bags, "Baggies".

b) Procedure with sample holder #2

Basalt samples AA of mesh sizes #100 to #48 were oven dried in vacuum at about 150°C for 3 hours, then kept in

Table II

Physical Parameters of Samples

Name	Powder Solid	Solid Density	Powder Density	Source	Mesh Size Microns	Remarks
Augite	P	$3.25 \pm .29$	2.02	unknown	<420	not very pure
Basalt AA	P	3.0 -3.1	1.46	Mass.	100-200	commercially available
Basalt M	P S	2.95	1.40	Mass. Cape Neddick	<297	see mineralogical analysis
Diabase	P		$1.55 \pm .05$	New Jersey Pitsbury Mine	<420	not analyzed
Dunite	P S	3.32	1.82	Twin Sisters Colorado	<420	2% magnetite ?
Granite	P S	2.71	1.44	unknown	<420	see mineralogical analysis
Hypersthene	P	$3.4 \pm .2$	1.67	unknown	<297	2% impurity of chlorite
Plagioclase	P	2.64-2.7	1.58	unknown	<297	mostly albite

metal boxes with silica gel for one day or more. At the same time, the sample holder was filled with silica gel to keep it dry. To wet the samples, a known amount was put in a one liter conical flask and a measured amount of distilled water was added (from 0.4cc to 8cc). Then the flask was stoppered, shaken, slightly heated while the stopper was held in place, shaken again, then allowed to cool without removing the stopper. When ready, the silica gel was removed from the sample holder and the wetted sample was put in and shaken for the best packing possible. The packing factor was about 50% $\pm$ 5%. For low-temperature measurements, the filled sample holder was placed in a styrofoam box and surrounded with coarse aluminum screen to reduce the temperature gradient. This styrofoam box had ventilation openings for air flow cooled with liquid nitrogen vapor. Two-low temperature thermometers were used to check for gradient and average temperature value, one near the center of the sample holder, the other at one of its corners. Measurement was made when both thermometers were within 1 1/2 °C. The temperature difference was probably less than 4°C within the sample at -45°C, and less than 6°C at -50°C and -60°C. At this time, the low frequency bridge used was a G.R. 1650A, and the frequencies used were 300Hz, 1KHz, 3KHz, 10KHz, 100KHz, 1MHz, and occasionally 100Hz and 3MHz. Dry powder measurements were repeated at 27°C and good reproductivity found. Other mesh sizes were measured at 27°C and little differences found if the mesh sizes were not large in comparison to the electrode spacing. Results are shown in Graph Series C and F. This series of measurements is considered as semiquantitative.

c) Procedure with sample holder #3

Table II shows that 8 different samples were measured with this instrument. As soon as an experiment with this instrument ended, the sample holder was emptied of its

former content which was weighed and preserved in a paper bag, then disassembled for drying and cleaning with air, glass wool and cleaning paper on the gold surfaces. No fingerprints were put on these surfaces. Both electrodes were reassembled and the thermocouple hole of the removable ground electrode was stoppered to prevent the penetration of the sand. A small quantity of the sample was then poured into the sample holder and the holder was shaken to pack the sample. This procedure was repeated until the instrument was filled. A small plastic hammer was used to help pack the sample in. The packing factor (powder density to solid density ratio) obtained in this way is about 50% $\pm$ 5%. The stopper was removed and the screen, the porous stone and the nickel plated copper seal installed, The vacuum stopper was screwed to the chamber to squeeze the vacuum seal and this instrument placed in the furnace after installation of thermocouples. It was then connected to the vacuum which was held overnight.

Measurement was made of $\rho_{DC}(T)$, $\tan\delta\,(f,T)$, $K(f,T)$ with increasing temperature and decreasing temperature to see if some thermal hysteresis effect could be detected. Resistance values were taken before and after the dielectric measurement at one temperature. If polarization was present, the effect was subtracted as follows. The potential difference V_1 across the sample was read before resistance measurement, then the resistance measurement V /I was made during 1 min. and a few seconds later (2-5) the voltage V_2 across the sample was again measured. The electrode polarization effect was V_1-V_2

then we get $R = \frac{V_R - V_1 + V_1}{I_R}$ = the true sample's resistance

where R is the resistance of the sample.

V_R is the potential difference across the sample holder when taking the resistance value.

I_R is the current through the sample when taking the resistance value.

After the maximum temperature was reached, the Ohm's Law was tested at 200°C by measuring the voltage across the sample vs. the current drawn through the sample.

Each cycle included overnight pumping and lasted for 24 hours. At each temperature setting, the temperature gradient was checked from time to time and showed a maximum variation of 10°C for the external thermocouple with few exceptions, and 3°C for the internal thermocouple. The rate of external variation was somewhat higher since the thermal inertia of the metal sample holder was high.

Powder measurements were not repeated on this instrument, but the results from basalt AA could be compared with those measured on sample holder #2. The results were the same at high frequency but at low frequencies the dielectric loss is 30% lower in vacuum (compare Figure A with C1 and Figure A2 with C2). This is believed to be due to the effect of a small amount of bond water. The capacitance value of the sample holder with no sample, is slightly temperature-dependent but is less than 2%. This change was not considered important.

d) Procedure with sample holder #4

A slot 1/8" long and 1/32" in depth and width was made with a carbide point scriber on one sample (see Figure 4) to allow a steel needle to be inserted between the two pieces to be tested without separating the two rock sample pieces from the platinum foil electrode. The slabs were then cleaned with acetone to remove fingerprints, and with water. They were kept in a hermetic box with

silica gel.

Small tools were built to handle the samples and sample holders without fingerprint contamination. Figure 4 shows the sample set up: [11] a stainless steel ventilated lower vise jaw which has three circular grooves and a cross-shaped groove for ventilation to help eliminate the remaining bond water; [10] a thin platinum foil was pressed gently on the lower vise jaw to give it the same grooving pattern but with less relief and with many small holes at the bottom (as illustrated); [9], [4] platinum 80 mesh screen, these screens have been tapped with a small stainless steel hammer and anvil to get rid of their humps and make them flat, air spaces occupy 60% of the total area; [8], [5] the samples; [7] platinum thin foil, 0.0005" thick and 7/8" diam., with a small key for contact with the steel needle. It plays the role of active electrode of the capacitor; [3] platinum foil strip for electrical contact; [6] platinum collar; [2] porous ceramic dish for good pressure distribution on the sample and ventilation; [1] a stainless steel ventilated upper vise jaw to provide pressure for good contact and also to provide good ventilation. As we can see, the ventilation was a very important problem and is well illustrated in the section: Description of Results.

When this was completed, copper seals, vacuum stopper and the thermocouples were installed (Figure 3) and a stiff stainless steel wire was screwed on the live end of the feed-thru. All was put in the furnace. Since the capacitance of the wire depends on its geometry, only stiff wires were used on this instrument to reduce the statistical errors caused by a variation in capacity due to the wire bending. The theoretical effective air capacitance of this instrument (i.e. if the sample had a dielectric constant = 1) was about 3.34 pf, calculated

using the formula for parallel plates capacitors.

A.G.R. standard capacitor of 100 pf was connected in parallel to the low frequency capacitance bridge connector as the unknown capacitor, and a dry-air capacitor, with a nominal value of 151.6pf was connected in parallel to the high-frequency capacitance bridge as the unknown capacitor (the G.R. bridge measured capacities from 100 pf to 1100 pf by the direct method). Both capacitors were tested for capacitance and for loss tangent values for correction purposes.

The ground electrodes were the platinum collar [6] and screens [9], [4]. To evaluate the error introduced by the mesh size, since the dielectric constant values are calculated by taking as an hypothesis that the electrodes are flat plain surfaces, two platinum foils of the same size as the screens were cut. At atmospheric pressure, at room temperature, both screen and foils were measured to see if large errors were introduced. With the foil, the dielectric constant masured was 6% higher. The repeatability of the dielectric constant measurement with the screens was 6% (extreme cases on 4 measurements) so that the dielectric constant of samples are given without a screen effect correction.

II.3. Quality of Data

The temperatures given are measured on the inside thermometer of sample holders #3 and #4 with a thermocouple calibration error of 3/2%. Frequencies given are good to $\pm$5% and tan δ measured to $\pm$0.0005 (except at 100Hz and 2MHz which are good to $\pm$0.001 and at 50Hz which is good to $\pm$0.005). The capacitance reading was very precise, the major errors introduced being due to wire arrangements.

The values were stable to $\pm$0.5pf for sample holder #3 and to $\pm$0.2pf for sample holder #4. The resistance value quality varied considerably due to electrode polarization and is believed to be accurate to $\pm$20% in the worst cases (particularly in powders at temperatures less than 125°C). Stable values are found on solid samples. The resistance of the ceramic feed-thru as a function of temperature is known to $\pm$5%. Tanδ measurements made with sample holder #2 had much larger uncertainties at 10KHz and 100KHz as explained in Appendix B for Graph Series C and F.

III. DESCRIPTION OF RESULTS

III.1. The Basalt AA Sample

The first measurement series was made using the sample holder #1 and showed that the dielectric constant of a basalt sand is relatively independent of grain size if all grains are about the same size, for mesh sizes #10-#25 to #45-#100, but depend more strongly on the packing factor or on the porosity. The packing factor does not depend very much on the grain size, but more strongly on the distribution of these. An approximate value of resistivity was measured at room temperature and found to be 10^{15} ohm-cm, after 24 hours and about 10^{14} ohm-cm after a few minutes for field strength of about 10 volt/cm, when the material has been vacuum-oven dried at 150°C for 3 hours. This ageing effect is not due to electrodes since four-electrode configuration was used. The resistivity values are more dependent on grain size. The data are presented in Appendix A and B together with notes and explanations, for the following data.

Following these preliminary experiments, low-temperature effects and the effect of moisture were investigated. These results are shown in Appendix B in Graph Series C, F and Figure E4.

Before commenting on these curves, a few remarks on the stability of other parameters are necessary, as well as the goal of this specific investigation.

Grain sizes used were about 200 microns with a distribution of sizes around this value, but all measurements were made on the same sifted sand batch, and have the same grain size distribution. The value of the packing factor is about 50% $\pm$ 5%, but for each set of measurements, the packing process used was the same and was made in such a way that the maximum possible value

was reached. Then, using the same material with the same grain size distribution, it is believed that this gives a constant value within $\pm$2%. For this investigation, only the relative variation of dielectric properties with temperature, frequency and small moisture constant are important, keeping all other parameters as constant as possible. All measurements were made on the basalt AA.

The most interesting observation is that very small water content, up to 0.1%, adds a frequency independent contribution to the loss tangent, at least for the frequency and temperature range investigated. There is a critical moisture content, which may depend on the texture, the mineralogy, the weathering and the grain size. This moisture content was about 0.5% in our case. This observation is clearly shown in Figures C8 and C9, the complete F series and a comparison of C7 with C5. Keller and Licastro (16) also found such a critical value which was about 3% for sedimentary rocks. In Figure C7, a relaxation phenomena is well observed, even with only a few experimental points. It is possible to determine a rough value of activation energy (see Figure E4). The curve grouping in Figure C8 at 0.5% water and for -15°C to 27°C is due to the relaxation maximum observed. Above 0.5%, at a low temperature, the water concentration has little effect, but above a critical temperature, drastic changes are observed.

The main work has been done to find the relations of $K(f,T)$, $\tan\delta\ (f,T)$ and $\rho_{DC}(T)$, to look for a relation among these values as well as for differences between powders and solid samples of the same rock. Irreversible changes on heating could also be important.

III.2. The Powder Samples

Powders exhibit a loss tangent and dielectric constant properties which are much different than the solid samples. Relaxation peaks are often found in the powder. Irreversible changes on heating were observed in all samples at low frequencies, showing in most cases a decrease in the value of $\tan\delta$ and K, and at high frequency for low-loss and relaxation-free samples such as olivine and plagioclase. Release of strongly-bonded water may explain part of these phenomena, but not in all cases. A good correlation is found between K(f) and $\tan\delta$ (f) and the powders seem to show another relaxation peak, at very low frequency with a very high value. In this case, $\tan\delta$ rises at low frequency but this is not due to D.C. conductivity; this will be discussed later. A good correlation is also found in the irreversible thermal effect on K(f) and $\tan\delta$ (f).

No correlation is found between DC and AC resistivity (50 to 100 Hz), the latter being much lower and less temperature dependent. However, these two curves approach each other at high temperatures. Double relaxation peaks are observed in granite and are real though small. The D.C. resistivities of basalts are very strongly dependent on their thermal history. The parameters calculated from this series are given in Table III and the physical parameters are given in Table II.

A Note about Possible Contamination of the Samples

There is a possible effect of impurities in the samples investigated, due to insufficient cleaning of the instruments. The amount of impurities introduced during the crushing process is less than 1%, as observed microscopically. Mixture tests show that 1% of active impurities in the samples make only a very small contribution to dielectric properties. Unwanted materials

Table III

Electrical Parameters of Tested Samples

Name	ν_{om} Hz	E ev	w ev	ρ at 27°C ohms-cm extrapolated	K_∞	G.d.P. cst.* A 27°C 1MHz	tan δ at 10^5Hz
POWDERS							
Augite	$(7\pm3)\times10^9$	$0.385\pm.01$	$0.52\pm.07$		$4.4\pm.1$		
Basalt AA	not measurable	-	$0.59\pm.03$ $\underline{.39\pm.02}$	8×10^{14}	$3.1\pm.1$	0.011 0.03 at 3KHz	.011
Basalt M	$(9\pm1.4)\times10^{10}$	$0.65\pm.02$	$0.66\pm.04$ $\underline{0.86\pm.03}$	5×10^{16}	$3.2\pm.1$	0.021	.015
Diabase P	not measurable	-	too high resistivity		$3.4\pm.1$	0.014	.005
Dunite	no relaxation	-	$0.74\pm.07$	-	$2.9\pm.1$	0.03 at 10^5Hz	.001
Granite	10^{10}-10^{12}	$0.6\pm.1$	$0.76\pm.16$	5×10^{18}	$3.11\pm.03$	0.045	.004
Hypersthene	$(9.5\pm0.5)\times10^7$	0.445	too high resistivity		$3.11\pm.03$	-	.001
Plagioclase	no relaxation	-	$0.59\pm.02$	4×10^{16}	$3.25\pm.03$	-	.003 $\underline{0.007}$
Quartz	no relaxation	-	0.66 ± 0.02	3×10^{17}	-	-	
SOLIDS							
Basalt M	no relaxation	-	- $\underline{0.59\pm.03}$	$\underline{4\times10^{11}}$	$10.1\pm.2$	0.024 at 10^5Hz	.035
Granite	no relaxation	-	$0.86\pm.01$	10^{14}	8.08	0.028	.020 .030
Dunite	no relaxation	-	$0.58\pm.02$	10^{17}	$6.4\pm.2$	0.048 at 185°C and 10^5Hz	$\underline{.003}$ at 100°C

*Gever & du Pre constant $A = \frac{\partial K}{\partial T}\frac{1}{K\cdot\tan\delta}$ which must be about 0.04 to 0.09 at room temperature.

General comment: Underlined numbers are values taken after reaching the maximum temperature.

from the sample itself occur due to weathered portions, but this is usually in small amounts and care is taken to avoid or discard them. The sample of augite used was not pure and found to be rich in biotite and had a slight amount of hematite as well as another unidentified mineral. The biotite was removed by hand and an x-ray pattern of the remaining sample did not show any. However, it did show an unexpected peak at 15.5° from the maximum peak of the direct beam, probably due to the unidentified, green mineral. Experiments showed that impurities from the preceding sample did not contaminate the following samples. All iron filings were removed with a magnet and microscopic observation showed no trace of these.

All of the dielectric observations, as well as the shape of the curves are believed to be free from impurity effects.

III.3. The Solid Samples

The final measurement series was made with solid samples, and shows quite a different electrical behaviour than powders. No relaxation effects are detected in the solid form of those samples while such effects are easily observed in the powder form; the temperature dependence of their resistivity shows a different activation energy and a smaller irreversible effect of ρ_{DC} on heating. The dehydration process described below shows dramatically the necessity of a highly ventilated sample holder.

On the computer outputs, Table CO-9, the measurement series made on the first day are shown in the first 10 rows; the tenth is the one at temperature 100°C. The last four rows of data were taken four days later. During

these four days, the basalt was kept in dry air with silica gel. It is interesting to see the similarity of results at the same temperature after heating to 508°C. It was particularly difficult to remove bond-water in this sample. The sample was left for two days in a vacuum, heated twice to 150°C and once to 230°C before taking these measurements. The stability of measurements with time was the criterion used to decide if measurements would be taken or if another dehydration cycle would be done.

The granite was easier to dehydrate. It was heated to 150°C in vacuum twice, although the second one was not necessary.

The olivine was heated twice to 150°C in vacuum, before the measurement series shown in Table CO-11. No graph was made for it. The two heating cycles were not enough to produce stable measurements as may be seen in this table. At 100°C after being heated to 290°C, the loss tangent is smaller than those measured at 27°C before the final cycle and the dielectric constant shows less dispersion. More data would have been interesting but instrumental problems occurred at this time. The resistance values of these samples are shown in Appendix B, Graph Series D.

IV. DISCUSSION

IV.1. General

The results described above are quite varied, but there is a common link between them. It is possible from these results to find an explanation for some of these phenomena and to limit the number of possible mechanisms which explain others.

Let us summarize the general remarks which may be derived from these results.

a) In industrial dielectric materials and in most geologic materials, there is a frequency domain where the loss factor is relatively independent of the frequency, especially at low temperature.

b) A relaxation peak is found at low frequency in most minerals and dry rocks, at least in powder form.

c) The source of the relaxation peak in powdered rocks comes from one or a few specific minerals (see Fig. A16, A17 and the related explanation in Appendix B), but not from the general texture and composition of the rocks or from some contact phenomena.

d) Very small water content contributes to the frequency independent part of the loss tangent but a large water content contributes mostly to the low frequency loss tangent and dielectric constant.

e) At some critical value of water content, another relaxation peak appears.

f) There is a rise of loss tangent as well of the dielectric constant at low frequency.

g) There is a large difference in behaviour between AC and DC resistivity; the former has a lower value and is less dependent on temperature than the latter.

h) The temperature dependence of DC conductivity of powders and solids is different for the same igneous rock material.

i) Powders and solids have quite different dielectric properties.

j) 2.8-3.5 is the usual value of the dielectric constant for a rock powder with a packing factor 50%.

k) Irreversible thermal effects are observed in all samples, especially in the low-frequency-high-temperature range, and in the frequency independent part of their dielectric loss and conductivity.

l) A good correlation exists between K(f) and $\tan\delta$ (f), even with irreversible thermal effects.

IV.2. The Frequency Independent Loss Tangent

We have seen in the introduction that this behaviour means a wide distribution of relaxation time τ. This relaxation time depends on temperature with the usual relation $\tau = \tau_0 e^{E/kT}$ where τ_0 is constant or varies as T^{-1} (in some cases, much faster, as in the case of temperatures near the glass transition for some polymers (5)). This means that τ_0 or E is distributed, or both. In the case where the source of this relaxation involves thermally activated movements of ions or molecules, τ_0 is about $10^{-13\pm4}$ sec. (5). A distribution of E where G(E) varies slowly will lead to the Gevers and du Pre relation, given as:

$$\frac{\partial K}{\partial T}\,\frac{1}{K\cdot\tan\delta} = A = -\frac{2}{\pi}\,\frac{\ln\omega\tau_0}{T}$$

where $\tau_0 = 10^{-13\pm4}$ sec as indicated above.

Let us examine the significance of the applicability of this relation.

This relation holds if:

a) There is a wide scattering of activation energy E.

b) The distribution function G(E) varies slowly with E in the interval in which $\frac{\omega\tau}{1+\omega^2\tau^2}$ differs appreciably from zero.

c) τ_∞ and the polarizability of each particle do not depend strongly on E.

d) The dielectric constant change due to the dilatation of the material is small compared to the same change due to the distribution of activation energies.

Also, with the above hypothesis, they prove that tan δ is practically independent of f, and the dielectric constant increases slightly when decreasing f. Looking at the specific conditions b) and c), it may be useful to look at the mean parameter value τ_∞ of the relaxation mechanism which is mainly responsible for the loss tangent near the frequency, f, at a given temperature, T, to see if a slight variation of τ_∞ appears. This method has been used on rock samples where there is no large contribution from a relaxation peak. Fig. E5 shows a graph $\log_{10} \tau_\infty$ vs. f, although the uncertainty is very large. $\text{Log}_{10} \tau_\infty$ is known to ± 2; the source of this error comes from the poor precision with which $\frac{\partial K}{\partial T}$ is known. It can be seen that $\tau_\infty = 10^{-11\pm2}$ and there seems to be a trend to a lower value at lower frequency although there are not enough data points to establish this conclusion.

Fig. E6 shows the effect of temperature on the value τ_∞, and even though the uncertainties are extremely large, they are not enough to hide a large trend. τ_∞ has

smaller values at low temperature while Fig. E7 shows that τ is more constant at high temperature.

Thus the Gevers and du Pre relation holds from 27°C to 300°C and from 10^2Hz to 10^6Hz, probably more. Only one experiment was done at low temperature and no conclusions can be drawn for this case. Since a large variety of samples gives a value of $\tau = 10^{-11\pm2}$ sec., with the possible exception of solid dunite, a common cause must explain all these cases.

The Gevers and du Pre theory is quite general, no hypothesis is made about the mechanism of the wide scattering in the value of activation energy E. They observe also their theory applies particularly well to amorphous materials.

Garton (10) introduced a model of relaxation mechanism which invclves particularly a thermally activated temporary potential well (see Introduction). These wells become semi-permanent if the structure of the material is viscous enough, such as in a vitreous state. The frequency-independent tan δ behaviour is well explained in amorphous materials but less in crystalline substances. Garton suggests that such semi-permanent wells exist also at planes of imperfection in the crystal structure and in amorphous material between crystallites in a polycrystalline substance. The following experimental observation; (olivine, granite and minerals, which have coarser grains than basalts and diabase, show a lower value of the frequency-independent part of their loss tangent) is in accordance with the Garton's interpretation.

With such a model and with the help of some approximations, Garton proves that this model leads to a frequency independent tan δ , but as he writes, this theory is too crude to make any reasonable quantitative prediction.

There is another mechanism to account for a frequency independent loss tangent. This is one of the Maxwell-Wagner effects involving a series of homogeneous capacitors with parallel conduction. This gives (26)

$$\tan\delta = \frac{\sum \frac{d_i \rho_i}{1+\omega^2 \tau_i^2}}{\sum d_i \rho_i \frac{\omega \tau_i}{1+\omega^2 \tau_i^2}}$$

where

$$\tau_i = \epsilon_0 K_i \rho_i$$

and where

d_i = thickness of the layer
ρ_i = resistivity of the layer
K_i = dielectric constant of the layer
$\epsilon_0 = 8.8 \times 10^{-14}$ Farad-cm^{-1}

It is possible to make such a capacitor where the value of tan δ is nearly constant with frequency, choosing a large variety of materials, but as seen in the above equation, this effect will cease when $\omega \gg (\tau_{min})^{-1}$ and tan δ will be very small when $\omega > 100 \cdot (\tau_{min})^{-1}$.

Let us evaluate the possible range of τ_i for rock component. Most reported mineral resistivities are for ore minerals and little data is available for silicates. Reported values for quartz and micas are about 10^{12} ohm-cm or higher. For the major constituents of rocks, 10^7 ohm-cm to 10^{16} ohm-cm is the probable limiting range when dry. If the dielectric constant ranges from 5 to 10, the values of τ_i are:

$\tau_i = 10^{-5}$ sec. for $\rho_i = 10^7$ ohms-cm

$\tau_i = 10^4$ sec. for $\rho_i = 10^{10}$ ohms-cm

which is a wide range of relaxation times but the values are too low. A relatively favorable distribution of τ or β for a large range of values is not probable. This mechanism may explain part of the nearly frequency-independent loss tangent but cannot be the full explanation. At low temperature, say -50°C, the resistivities will be higher, shifting the frequency range of the favorable distribution function $G(\tau)$ toward longer times. In basalt AA, such a frequency independent loss tangent was observed at low temperature. It was lower but very constant for the frequency range observed.

IV.3. The Effect of Water

From these experiments, as well as from other investigations, it is clearly seen that water has a different influence on the dielectric properties of rocks, depending on its concentration. This indicates that more than one mechanism is involved. At very low concentration (0.1% by weight or less) water molecules must be captured primarily by various crystal imperfections and not by lattice defects inside the crystals. The crystallographic defects are too regular to give such a wide relaxation time distribution. However, microscopic imperfections especially at the surface, such as contacts, ruptures and surface vitreous regions or solid solution, where binding potentials to water with a range of values are likely, the trapped molecules would have varying freedoms of rotation under the influence of an applied electric field. This scattering in values of ease of rotation and therefore relaxation time, will result in a frequency-independent loss tangent.

At a critical concentration, the water has a drastic

influence on the dielectric properties of rocks. It is at this concentration where a relaxation maximum is observed. This indicates that a well defined mechanism is involved. The question arises as to whether it is a Maxwell-Wagner type of relaxation where the conductive phase is a thin layer of water, covering the grain particles, which has dissolved some foreign ions found on the crystal surfaces, or whether it is a molecular relaxation type. A rotation of a bonded polar water molecule which is impeded in its motion by the binding force on the more regular surfaces, or those of the second or third layer where irregularities of the surface are less pronounced may be important. A relative regularity is necessary to explain the small spread in relaxation times as opposed to the preceding cases where a frequency-independent loss tangent is found. As explained by Hasted (13) the details of this question are not easy to answer.

The parameters of the observed relaxation phenomena are $\tau_0 = 10^{-24\pm4}$ sec. and E = 0.9ev$\pm$0.1ev. For bond water on silica gel, $\tau_0 = 10^{-20}$ sec and E = 0.6ev was found by Hasted[13], A relaxation maximum due to a slight amount of water has been observed in quartz sand by Chelidge (see Parkhomenko (23), p.222 or Fig. G2) for 0.03% water content. In fact, a relaxation maximum around $10^{4\pm1}$ Hz has been observed in many rocks (16), (23), but no detailed data are given on water concentration in these cases.

Above the critical concentration, other phenomena appear. The I.P. effect and electrode polarization at very low frequency will not be discussed since references are abundant (see for example ref. 20). At very high frequency, above 10^6 Hz, it seems that no other effects appear and the dielectric properties show little dependence on the water concentration above that critical value. This is seen in Fig. C8 and C9 as well

in an experiment on quartz sand reported by Chelidge using 0.4% to 12% water content (see Fig. G2). For very large water concentrations, at high frequencies, the Maxwell-Wagner theory works quite well. The samples tested by Keller and Licastro which show a very large dispersion at low frequency in their dielectric constant (i.e. those which seem to have a large water content; this data is not given in detail in this literature) have in most cases a dielectric constant value of 10 to 30 at 10^7Hz.

IV.4. The Relaxation Peak in Powdered Rocks

All dry rock powders tested here, show a relaxation peak at low frequency. This relaxation is not an electrode effect, or a contact effect between different minerals, but is due only to the presence of a specific mineral in the rock as clearly shown in the mixture tests Fig. A16 and A17. We will see that both the Maxwell-Wagner effect and the presence of a relaxation peak in a particular mineral give rise to this absorption peak. For the cases investigated, basalt M and granite, the peak was due to the presence of the biotite mineral(and possibly hornblende in basalt M).

The dielectric constant of biotite varies widely and lies between 4.5 to 10, (3) and must have a large anisotropy. No resistivity data is available for biotite, but for muscovite it is 10^{14}-10^{16} ohms-cm and for phlogopite, about 10^{13}-10^{14} ohms-cm (23). The biotite may have a lower resistivity and at 100°C, 10^{10} ohms-cm is possible. If not so, it may have a dielectric absorption maximum at 100Hz of a value of 0.4 (such a value is observed in phlogopite but at a different frequency), then an equivalent AC resistivity of 10^{10} ohms-cm at 100Hz, 100°C.

Let us suppose for simplicity that both biotite and the powder sample have a dielectric constant of 4.5

In the case of conducting spheres embedded in a continuous dielectric medium under the influence of an alternating AC field (26)

$$\langle 1 \rangle \qquad \tan \delta = 3v \frac{\omega \tau}{1+\omega^2 \tau^2}$$

$$\langle 2 \rangle \qquad \tau = 3 \epsilon_0 K \rho_i$$

where

$\epsilon_0 = 8.84 \times 10^{-14}$ Farad-cm^{-1}

K = dielectric constant of the materials

ρ_i = resistivity of the inclusion in ohm-cm.

v = volume fraction of the inclusion

The condition of a "continuous" surrounding medium is not quite satisfied in this case, as well as the condition of spherical particles, but approximation is probably quite good in making estimates good to one order of magnitude. For 10% biotite inclusion, $\tau = 10^{-2}$ sec and tan δ max = 0.15 which is quite close to the observed values.

This order of magnitude calculation is adequate to show the plausibility of both the Maxwell-Wagner and the relaxation effect. In fact, it is not so important to know which mechanism is dominant for these particular samples, but it must be recognized that many powdered, dry rocks show such a loss maximum.

IV.5. The Relaxation in Pyroxenes

Both pyroxenes tested also exhibit a relaxation peak. These relaxation peaks are not due to a mineralogic impurity. Let us take the controversial case of augite

with a high impurity content. The microscopic observation shows that this impurity is no more than 10% and probably only a few percent. The packing factor of augite is not well known but is approximately 55%. Its high frequency dielectric constant as a powder is 4.3. Using the Lichtenecker formula (see Parkhomenko (23) or Volger (26)), which relates the effective dielectric constant of a mixture with the known value of the component concentration as well as the dielectric constant of the components.

$$K = \prod_{i=1}^{N} K_i^{v_i}$$

where

K = the effective dielectric constant of the mixture

K_i = the dielectric constant of the component i

v_i = the volume fraction of the component i

N = the number of components

At high frequency, the dielectric constant of the solid augite should be about 18.4. If its impurity content was 10% so that the impurity occupies about 5% of the total space, fifty per cent is occupied by the augite and forty-five per cent by the air (or vacuum). Let us, for simplicity, consider the case where the dielectric constant of the impurity is 1 at high frequency and 100 at low frequency and all the observed phenomena come from this impurity. At high frequency, the dielectric constant of solid augite is then 18.4, using the Lichtenecker formula.

At low frequency, the mixture will have:

$$18.4^{.50} \times 100^{.05} \times 1^{.45} = 5.4 = K(\text{mixt}).$$

If the impurity has a constant of 2000 instead of 100, K(mixt) = 7.6.

The relaxation comes then from the augite itself and its low frequency dielectric constant must lie around

100-200. The same is true for the hypersthene sample, where the impurity content was lower, about 2%.

Since it is in powder form (being inhomogeneous), the observed relaxation maximum may be due to a classical Maxwell-Wagner effect, but this is not so, as will be shown. The equation giving the frequency of the maximum of the imaginary dielectric constant K" of a system of conducting spheres of dielectric constant K_2 and conductivity , embedded in a continuous medium of dielectric constant K_1 is (21)

$$\langle 3 \rangle \qquad FHz = 1.8 \times 10^{12} \frac{1}{\rho(2K_1 + K_2)}$$

which is a more general equation than equation 2 . As we see, this frequency is dependent on both values of the dielectric constants. From the above discussion and looking at the mixture tests and comparing Fig. A15 to Fig. A14, we see that it is not the case. The frequency of maximum loss tangent is unchanged.

The only other possible relaxation mechanisms which are possible are related to crystal defects (2) or imperfections (26) or chemical impurities. The values of and E for hypersthene (see Table III) are too low to be due to some ionic or molecular jumps or rotations in the crystal.

IV.6. Behaviour at Low Frequency

In all cases of dry rocks, solid or powder, as well as dry minerals, the observed value of tan becomes larger as the frequency of the applied electric field decreases. This may be due to the DC resistivity, but

calculation shows that its contribution is insignificant. If there were no other relaxation mechanism than the one observed, the dielectric constant would show less dispersion at low frequency. However, in most cases, the dispersion increases and irreversible thermal changes in tan δ and in the dielectric constant are observed at low frequency.

These observations show clearly that this rise is related to a relaxation peak. This explains why the AC resistivity is so different from the DC resistivity. Looking at figure series A and B, we will remark that this slope is displaced along the frequency axis with temperature as if its activation energy was about 0.3 to 0.6 ev. Its maximum is not observed but at 300°C, looking at figure series A and B, 1-10 Hz is not an unreasonable value for the peak. From the relation $\nu_m \cdot \nu_{om} e^{-E/kT}$, this maximum will lie at about 10^{-3}Hz to 10^{-5}Hz at room temperature.

Wenden (28) shows that an anomalous current which has the character of a dielectric charging current and is a completely reversible phenomenon (Q charging = Q discharging) exists in quartz. Its relaxation time was found to be about 10^{-2}-10^{-3}Hz and the "static" dielectric constant of the quartz is around 13000, a quite high value.

The tan δ observed in our experiment, and the anomalous current observed by Wenden, may be two different manifestations of the same phenomenon. In fact, this is a Maxwell-Wagner type relaxation, but it is not necessarily of the classical type. The non-classical mechanism is a more general case; lattice defects acting as traps and charged accumulations at interfaces with their resulting diffusion current are also taken into account. Volger (26) discusses both effects and finds

for the classical theory case, that a large dispersion in dielectric constant and in loss tangent is found in polycrystalline semiconductors. He refers to some experimental cases where a value of 10^4 for the dielectric constant may be found.

IV.7. Differences Observed Between Powder and Solid Forms of the Same Material

The first observation made, when comparing the data for powder and solid samples, is the disappearance of the relaxation maximum in the case of solids.

Let us suppose that the relaxation maximum observed in powders is purely a Maxwell-Wagner effect. Looking to the equation <3> , it is seen that as the dielectric constant of the medium grows larger, the frequency of the maximum loss tangent shifts to a lower value. The condition of applicability of this equation is not well met, especially the condition of a loss-free surrounding medium (2), and the condition of homogeneity, although the approximation is acceptable. In addition, in solids, the loss due to the general Maxwell-Wagner effect (classical or not) and principally due to the DC conductivity is higher, also tending to hide the relaxation maximum. In the more conductive surrounding rock, the biotite tends to be "short circuited". At 100°C, the AC resistivity of solid basalt M and of solid granite is about $10^9 \Omega\text{-}cm$ and $10^{10} \Omega\text{-}cm$ (see Fig. D1, D2), and the evaluated AC resistivity of the biotite at 100Hz is about $10^{10} \Omega\text{-}cm$ (see p.33). This last comment holds also if the low value of AC resistivity of the biotite is due to a relaxation maximum.

Another observed difference between powders and solids is that they have a slightly different activation

energy derived from the DC resistivity-temperature data. This difference may be as high as 0.2 ev as observed in granite. There are 3 possible causes: an electrode effect due to a non-ohmic contact between powder grains and gold surfaces, an intergrain contact effect, or too short a measurement time for the resistivity of powder. The present investigation does not answer this question.

The absolute resistivity value is quite different by as much as five orders of magnitude between powders and solids of the same material. Very high resistivities for powders were expected (6). In powders the resistivity is so high that in AC investigation, other loss mechanisms will always dominate the DC conductivity effect loss. Extrapolation of the DC resistivity of powder basalt AA to 27°C gives about 10^{14} to 10^{15} ohms-cm (Fig. D1) which is in perfect agreement with the DC resistivity evaluated at room temperature with sample holder #1 which has a four-electrode configuration. This puts some confidence in the fact that electrode effects are not too large in the powder investigation.

IV.8. The Dielectric Constant Value

There are many different formulas available which may be used to calculate the dielectric constant of a mixture knowing the dielectric constant of each of its constituents.

Three of these are:

1) Lichtenecker's formula for a system of unordered mixture of components

$$K = \prod_{i=1}^{N} K_i^{v_i}$$

2) Odelevskii's formula

$$K = B + \sqrt{B^2 + K_1 K_2 / 2}$$

$$B = [(3v_1 - 1)K_1 + (3v_2 - 1)K_2]/4$$

3) Bottcher's formula for granular material

$$\frac{K - 1}{3K} = \frac{K_{material} - 1}{K_{material} + 2K} \; v_{material}$$

where K = observed dielectric constant of the mixture

K_i = dielectric constant of each component

v_i = volume fraction of each component

where $\sum_{i=1}^{N} v_i = 1$

N = total number of component types

The Powder Case

Knowing the dielectric constant of solid rock, the dielectric constant of the powder, and the known packing factor, the formulas have been checked for the applicability (see Table VI).

The Lichtenecker formula slightly underestimates the bulk dielectric constant of a powder, but gives the closest values for rocks with the exception of olivine.

The Solid Rock Case

Looking at Table V, we can see that the dielectric constant of granite is about the average of the dielectric constant of its constituents. Values given here come from the Handbook of Physical Constant (3) as well as from tables given by Parkhomenko (23).

Table IV

Mineralogic Analysis
of Basalt M

Count on 500 Grains

Mineral	%	K	Comments
Plagioclase	55	7.5	10% are zoned, 10% are altered into sericite
Pyroxene	1	10-20	
Biotite	16	5-10	
Hornblende	16	5-6	Exsolution of opaque mineral along one plane
Opaques	5		
Altered Pyroxenes	3		
Carbonates	1		Interstitial
Chlorites	1		
Apatite	1	11	Needle, high relief
*Basalt M		10.5	At 1.0 MHz

*The more exact name for basalt M is Porphyritic Diabase.

Table V

Mineralogic Analysis of Granite

Count on 500 Grains

Mineral	%	K	Comments
Plagioclase	42 ± 10	6-7	10% of them are altered to sericite
Quartz	25 ± 10	4.6	
Microcline	20 ± 10	6	
Biotite	7	5-10	
Muscovite	2 ± 1	5	
Myrmekite	2		90% oligoclase and 10% quartz
Apatite	1		
Opaques	1		
Na Amphibole	1		
Epidote	1		
Carbonate	traces		
Granite		6.5	At 1.0 MHz

Table VI

Calculated and Measured Values of the Dielectric Constant of Powders

Material	Packing factor	f	T	K_{solid}	K_{powder}	Lichtenecker	Odelevskii	Bottcher
Basalt M	.48	10MHz	27°C	10.1	3.2	3.04	3.81	3.83
		100Hz	27°C	15.00	3.64-4.0	3.66	5.09	5.08
		5KHz	230-245°C	33.90	5.11	5.40		
Granite	.53	10MHz	27°C	6.4	2.9	2.68	3.43	3.12
		100Hz	100°C	$9.0 \pm .5$	3.34	3.20	4.22	3.98
			285°C	20		4.88	7.40	7.50
Olivine	.55	1MHz	27°C	8.08	3.4	3.15	3.85	3.66
		100Hz	250°C	9.69	3.59	3.48	4.35	4.41

Note: The value of K at 10MHz was evaluated by extrapolation.

In the case of basalt M (see Table IV) the rock has a higher dielectric constant than each of its major constituents, which is quite surprising.

Mineralogical analysis shows that many of its crystals were altered, contain interstitial components, and exsolutions. All these must seriously effect the dielectric constant of the rock as well as its dielectric loss, and these irregular structures must also be the source of the high value of the frequency independent part of the tan δ .

IV.9. The Irreversible Thermal Effect

In all cases, a definite irreversible thermal effect is observed at low frequency at 150°C - 250°C. If the tan δ rise at low frequency is a foot hill of a relaxation peak, and this peak is due to some kind of reversible trapping of charge carriers by crystal imperfection or crystal lattice defects (the Wenden mechanism), the observed irreversibility effect may be explained by an irreversible change in the crystal imperfections. This irreversible thermal effect could also represent the contribution of tightly bonded water which is evaporated by the heating process.

In some cases, such as in plagioclase, in solid granite and in dunite, this effect is seen at all frequencies. In the case of dunite, this effect might be explained by the release of tightly-bonded water of small concentration which leads, as we have already seen for basalt AA, to a frequency independent loss tangent contribution.

The cases of plagioclase and solid granite, however, are harder to explain since the high frequency loss

tangent is higher after the heating cycle than before (Fig. A3 and B4) and is less frequency dependent for the case of plagioclase. Irreversible thermal effects are also found in DC conductivity, on solid samples and on powdered basalts.

Let us consider the conduction mechanism due to lattice defects, leading to ionic conduction. The temperature dependence of such a conductivity is

$$\sigma = \sigma_0 e^{-w/kT} \qquad w = (U+2u)/2$$

where U = activation energy related to the concentration of points defects (Schottky or Frenkel type).
u = activation energy related to the mobility of the charge carriers.

When heating such a conductor, more and more crystal defects appear and are exponentially dependent on the temperature. When cooling, this concentration may not have time to reach its equilibrium value (15). This may take, in fact, a very long time, longer than the experimental investigation time (22). In this case we get what is called a "frozen state". Here the conductivity relation to the temperature will be

$$\sigma = \sigma_0 e^{-u/kT}$$

having a smaller activation energy.

This may explain the case of basalt AA, but not the case of powder basalt M.

IV.10. Other Effects

Looking at Fig. A7, we can see for the dunite case a small hump at about 10^6Hz, which remains constant in position and in amplitude with temperature. This phenomenon has not been explained, but it could be an instrument effect.

V. CONCLUSION

The Maxwell-Wagner effect makes an important contribution to the dielectric properties of dry rocks, and explains most of their dielectric behaviour, at least macroscopically.

Some effects of the classical as well as the non-classical Maxwell-Wagner theory are:

(1) A rise of $\tan\delta$ and of the dielectric constant at very low frequency.

(2) A low value of AC resistivity at low frequency in comparison to the bulk DC resistivity.

(3) The existence in many cases of a relaxation maximum in powders or in rocks with large porosity value due to the presence of some minerals.

(4) Perhaps, a part of the low frequency (10Hz-10KHz) loss tangent which shows relatively little dependence on frequency but where the Gevers and du Pre relation seems to give a smaller value of γ.

Garton's mechanism is probably the main cause of the frequency independent part of the loss tangent at high frequency.

Both mechanisms predict that unaltered rocks with coarse grains will have a tendency to have a lower frequency independent loss tangent and slightly lower dielectric constant than their volcanic or fine grained counterparts of the same porosity.

The dielectric loss due to the bulk DC resistivity of powders is so small at all frequencies, except for periods of minutes or hours, it can be neglected.

When a powdered earth material is very slightly moistened, it exhibits a frequency independent increase in its loss tangent and a corresponding small increase in its dielectric constant depending on the amount of

water. At a critical value of moisture content, the dielectric properties change drastically. At low water contents, a relaxation maximum may appear, observed in quartz sand by Chelidge and in basalt in this study. The relaxation maximum observed by Keller and Licastro may be of a different nature.

Above the critical value, the Maxwell-Wagner theory explains most of the effects of water at high frequency, but another phenomenon, called the IP effect, appears at low frequency.

REFERENCES

1. R.G. Breckenridge.
   Low Frequency Dispersion in Ionic Crystals, Jour. of Chem. Phys., 16, 959 (1948).

2. R.G. Breckenridge.
   Relaxation Effects in Ionic Crystals, in Chap. 8 of "Imperfections in Nearly Perfect Crystals", National Research Council (1952) Wiley.

3. S.P. Clark, Jr.
   Handbook of Physical Constants, G.S.A. Memoir 97 (1966).

4. N. Cusack.
   The Electrical and Magnetic Properties of Solid, (1968) Wiley.

5. V.V. Daniel.
   Dielectric Relaxation (1967) Academic Press.

6. A.W. England, Gene Simmons, D. Strangway.
   Electrical Conductivity of the Moon, J.G.R., 73, 3219 (1968).

7. S. Evans.
   Dielectric Properties of Ice and Snow - A Review, Journ. of Glaciology, 5, 773 (1965).

8. R.M. Fuoss and J.G. Kirkwood.
   Dipole Moments in Polyvinyl Chloride-Diphenyl Systems, Journal of Amer. Chem. Soc., 63, 385 (1941).

9. H. Frohlich.
   Theory of Dielectrics (1949) Clarendon Press, Oxford, England.

10. C.G. Garton.
    The Distribution of Relaxation Times in Dielectrics, Trans. Faraday Society, 42A, 57 (1946).

11. M. Gevers and F.K. du Pre.
    Power Factor and Temperature Coefficient of Solid (Amorphous) Dielectrics, Trans. Faraday Society, 42A, 47 (1946).

12. M. Gevers and F.K. du Pre.
    A Remarkable Property of Technical Solid Dielectrics, Philips Tech. Rev., 9, 91,(1947).

13. J.B. Hasted.
The Dielectric Properties of Water, Progress in Dielectrics, 3, 103 (1961).

14. B.F. Howell and P.H. Licastro
Dielectric Behaviour of Rocks and Minerals, Am. Mineralogist, 46, 269 (1961).

15. A.F. Ioffe.
Physics of Semiconductors (1960) Academic Press.

16. G.V. Keller and P.H. Licastro.
Dielectric Constant and Electrical Resistivity of Natural-State Corps, U.S.G.S. Bull. 1052, 257 (1959).

17. J.V. Keymeulen and W. Dekeyser.
Dielectric Loss of Defects in Clay Minerals, Jour. of Chem. Phys., 27, 172 (1957).

18. W.D. Kingery.
Introduction to Ceramics (1960) Wiley.

19. C. Kittel.
Introduction to Solid State Physics, Third edition (1967) Wiley.

20. D.I. Marshall and T.R. Madden.
Induced Polarization, a Study of its Causes, Geophysics, 24, 790 (1959).

21. B.J. Meakins.
Mechanisms of Dielectric Absorption in Solids, Progress in Dielectrics, 3, 153,(1961).

22. N.F. Mott and R.W. Gurney.
Electronic Processes in Ionic Crystals (1948) Dover.

23. E.I. Parkhomenko.
Electrical Properties of Rocks (1967) Plenum Press.

24. J.H. Scott, R.D. Carroll and D.R. Cunningham.
Dielectric Constant and Electrical Conductivity, Measurements of Moist Rocks: A New Laboratory Method, J.G.R., 72, 5101 (1967).

25. M.R. Stuart.
Dielectric Constant of Quartz as a Function of Frequency and Temperature, Journal of Applied Phys., 26, 1399 (1955).

26. J. Volger.
Dielectric Properties of Solids in Relation to Imperfections, Progress in Semiconductors, 4, 205 (1960).

27. S.H. Ward, G.R. Jiracek and W.I. Linlor.
Electromagnetic Reflection from Plane-Layered Lunar Model, J.G.R., 73, 1355 (1968).

28. H.E. Wenden.
Ionic Diffusion and the Properties of Quartz, I. The Direct Current Resistivity, Am. Mineralogist, 42, 859 (1957).

Appendix A

COMPUTER OUTPUT

Some data are not shown on graphs, but are found in tables, series CO. In particular, the data for dunite, plagioclase and some of the low frequency data have not been included in graphs. Tables CO-1 to CO-5 give data on the packing factor or the ratio of the volume fraction of powder density to solid density for the powdered samples, while Tables CO-9, CO-10, CO-11 refer only to solid samples. The values of packing factor are known to $\pm$2% and for the hypersthene and augite to $\pm$5%.

Temperatures are given in the order in which they were measured. The maximum temperature shown in a table represents the maximum temperature which the sample underwent during that particular series. Exceptions are granite, which was heated to 340°C for a short time and augite, which was heated to 300°C. The case of solid basalt M is special, the temperatures are in chronological order but the first 10 were taken in one day and the remaining ones four days later. Between the two sets of measurements, the sample was stored with silica gel to keep it dry. A small discrepancy of temperature (less than 5-6°C) may exist between those given on graphs and the computer output which has exact values. Due to the uncertainties of measurement, this difference is of no serious consequence.

All dielectric values, given in tables series CO, where a zero or a negative value is given, mean that no measurement was made. There are a few unreasonable values, such as a sudden minimum in dielectric constant. These might be due to misreading during experimentation but checking the original data gives no reason to change them.

DIELECTRIC PROPERTIES
OF
BASALT AA

Table CO-1 52

K MEANS DIELECTRIC CONSTANT OF THE SAMPLE
D MEANS DIELECTRIC LOSS TANGENT OF THE SAMPLE

TEMP. IN DEGRES CENTIGRADE
FREQ. IN KILOHERTZ

DENSITY OF SOLID SAMPLE IS 3.05
PACKING FACTOR IS 48%

FREQ.* 0.05		0.10	0.20	0.50	1.00	2.00	5.00	10.0	20.0	50.0	100	200	500	1000	2000
TEMP.*	*														
27.0*	K=*-0.28	3.55	3.44	3.33	3.28	3.24	3.19	3.17	3.15	3.13	3.11	3.09	3.04	3.03	3.03
*	D=*0.0	0.077	0.063	0.044	0.037	0.027	0.021	0.017	0.015	0.011	0.011	0.011	0.013	0.012	0.012
100.0*	K=* 5.33	4.93	4.57	4.17	3.91	3.69	3.49	3.37	3.29	3.22	3.19	3.14	3.09	3.07	3.08
*	D=*0.145	0.153	0.149	0.138	0.128	0.115	0.077	0.067	0.050	0.037	0.025	0.021	0.018	0.016	0.013
146.0*	K=* 6.37	5.93	5.53	5.02	4.66	4.33	3.96	3.73	3.55	3.38	3.29	3.22	3.14	3.11	3.12
*	D=*0.155	0.152	0.151	0.155	0.158	0.149	0.133	0.121	0.098	0.072	0.052	0.041	0.033	0.025	0.018
195.0*	K=*-0.0	7.10	6.66	6.06	5.63	5.22	4.73	4.39	4.08	3.76	3.56	3.40	3.26	3.20	3.17
*	D=*0.0	0.165	0.149	0.157	0.163	0.165	0.160	0.157	0.142	0.126	0.102	0.094	0.060	0.044	0.038
252.0*	K=*-0.0	8.46	7.85	7.11	6.62	6.14	5.55	5.14	4.74	4.29	3.99	3.71	3.46	3.30	3.27
*	D=*0.0	0.239	0.188	0.168	0.165	0.161	0.164	0.168	0.161	0.153	0.135	0.124	0.100	0.075	0.060
297.0*	K=*-0.0	9.58	8.78	7.95	7.43	6.92	6.31	5.97	5.43	4.89	4.53	4.20	3.81	3.59	3.44
*	D=*0.0	0.325	0.251	0.192	0.174	0.161	0.160	0.164	0.164	0.165	0.156	0.155	0.139	0.111	0.094
195.0*	K=*-0.0	6.92	6.50	5.96	5.57	5.18	4.69	4.37	4.08	3.75	3.56	3.41	-0.0	-0.0	-0.0
*	D=*0.0	0.146	0.143	0.146	0.154	0.155	0.155	0.152	0.137	0.120	0.099	0.083	0.0	0.0	0.0
150.0*	K=*-0.0	6.02	5.62	5.09	3.14	4.39	4.00	3.76	3.57	3.39	3.23	3.22	-0.0	-0.0	-0.0
*	D=*0.0	0.145	0.146	0.150	0.155	0.149	0.133	0.122	0.099	0.074	0.055	0.042	0.0	0.0	0.0
105.0*	K=* 5.49	5.03	4.69	4.26	3.99	3.75	3.52	3.39	3.30	3.22	3.18	3.14	-0.0	-0.0	-0.0
*	D=*0.145	0.149	0.147	0.138	0.134	0.114	0.092	0.076	0.056	0.038	0.028	0.021	0.0	0.0	0.0

Table CO-2

DIELECTRIC PROPERTIES
OF
PLAGIOCLASE

K MEANS DIELECTRIC CONSTANT OF THE SAMPLE
D MEANS DIELECTRIC LOSS TANGENT OF THE SAMPLE

TEMP. IN DEGRES CENTIGRADE
FREQ. IN KILOHERTZ

DENSITY OF SOLID SAMPLE IS 2.70
PACKING FACTOR IS 57%

FREQ.*		0.05	0.10	0.20	0.50	1.00	2.00	5.00	10.0	20.0	50.0	100	200	500	1000	2000
TEMP.*	*															
27.0*	K=*-0.0	3.35	3.34	3.33	3.32	3.31	3.31	3.30	3.30	3.29	3.29	3.29	3.27	3.28	3.31	
*	D=*0.0	0.008	0.006	0.005	0.004	0.004	0.003	0.003	0.003	0.002	0.002	0.002	0.002	0.002	0.001	
98.0*	K=*-0.0	3.41	3.39	3.37	3.36	3.34	3.33	3.33	3.32	3.32	3.31	3.30	3.31	3.32	3.31	
*	D=*0.0	0.015	0.011	0.009	0.008	0.006	0.005	0.005	0.004	0.003	0.003	0.003	0.003	0.002	0.001	
152.0*	K=*-0.0	3.47	3.44	3.40	3.38	3.37	3.35	3.34	3.34	3.33	3.32	3.32	3.29	3.29	3.32	
*	D=*0.0	0.024	0.018	0.014	0.011	0.008	0.007	0.006	0.005	0.004	0.003	0.003	0.003	0.003	0.002	
195.0*	K=*-0.0	3.53	3.49	3.44	3.42	3.40	3.38	3.36	3.35	3.34	3.33	3.33	3.30	3.31	3.34	
*	D=*0.0	0.033	0.025	0.019	0.016	0.013	0.010	0.008	0.006	0.005	0.004	0.004	0.004	0.004	0.003	
245.0*	K=*-0.0	3.62	3.56	3.50	3.47	3.44	3.41	3.39	3.38	3.36	3.35	3.34	3.31	3.32	3.34	
*	D=*0.0	0.045	0.032	0.025	0.022	0.017	0.013	0.011	0.009	0.006	0.005	0.005	0.005	0.004	0.002	
300.0*	K=*-0.0	3.76	3.68	3.59	3.54	3.51	3.46	3.44	3.42	3.40	3.38	3.37	3.34	3.34	3.38	
*	D=*0.0	0.068	0.052	0.036	0.030	0.023	0.018	0.015	0.012	0.009	0.008	0.007	0.007	0.006	0.006	
350.0*	K=*-0.0	4.08	3.91	3.74	3.66	3.60	3.52	3.49	3.46	3.40	3.42	3.40	-0.0	-0.0	-0.0	
*	D=*0.0	0.143	0.104	0.068	0.054	0.040	0.028	0.023	0.018	0.014	0.011	0.010	0.0	0.0	0.0	
195.0*	K=*-0.0	3.56	3.54	3.50	3.48	3.46	3.44	3.42	3.41	3.39	3.38	3.37	-0.0	3.33	-0.0	
*	D=*0.0	0.021	0.017	0.015	0.014	0.012	0.010	0.009	0.008	0.007	0.007	0.007	0.0	0.007	0.0	
100.0*	K=*-0.0	3.49	3.47	3.45	3.45	3.43	3.41	3.40	3.39	3.37	3.36	3.34	-0.0	-0.0	-0.0	
*	D=*0.0	0.011	0.009	0.008	0.008	0.007	0.007	0.007	0.007	0.007	0.007	0.007	0.0	0.0	0.0	

Table CO-3

DIELECTRIC PROPERTIES
OF
HYPERSTENE

K MEANS DIELECTRIC CONSTANT OF THE SAMPLE
D MEANS DIELECTRIC LOSS TANGENT OF THE SAMPLE

TEMP. IN DEGRES CENTIGRADE
FREQ. IN KILOHERTZ

DENSITY OF SOLID SAMPLE IS 3.40
PACKING FACTOR IS 49%

TEMP.*	FREQ.*	0.05	0.10	0.20	0.50	1.00	2.00	5.00	10.0	20.0	50.0	100	200	500	1000	2000
27.0*	K=*	-0.0	3.27	3.24	3.21	3.19	3.17	3.15	3.15	3.14	3.14	3.14	3.13	3.11	3.12	3.15
*	D=*	0.0	0.028	0.021	0.015	0.012	0.009	0.007	0.005	0.004	0.002	0.001	0.001	0.001	0.001	0.001
100.0*	K=*	3.82	3.68	3.55	3.40	3.34	3.28	3.23	3.20	3.19	3.17	3.16	3.15	3.13	3.13	3.16
*	D=*	0.073	0.073	0.067	0.052	0.043	0.032	0.022	0.017	0.012	0.008	0.005	0.004	0.004	0.003	0.001
150.0*	K=*	4.12	4.05	3.91	3.68	3.55	3.44	3.33	3.28	3.24	3.21	3.19	3.18	3.15	3.15	3.17
*	D=*	0.052	0.061	0.070	0.072	0.070	0.058	0.042	0.033	0.024	0.016	0.010	0.008	0.007	0.006	0.003
195.0*	K=*	4.37	4.28	4.19	4.01	3.87	3.71	3.52	3.41	3.34	3.27	3.24	3.21	3.17	3.17	3.19
*	D=*	0.041	0.047	0.055	0.068	0.077	0.078	0.068	0.057	0.043	0.028	0.019	0.013	0.011	0.007	0.006
250.0*	K=*	4.56	4.49	4.39	4.24	4.12	3.97	3.76	3.61	3.48	3.36	3.30	3.26	3.21	3.20	3.22
*	D=*	0.050	0.046	0.048	0.057	0.067	0.076	0.081	0.077	0.065	0.045	0.033	0.025	0.017	0.012	0.006
300.0*	K=*	4.68	4.60	4.50	4.37	4.27	4.16	3.97	3.81	3.66	3.48	3.39	3.32	3.24	3.22	3.23
*	D=*	0.058	0.053	0.049	0.049	0.056	0.068	0.075	0.081	0.078	0.063	0.048	0.037	0.027	0.018	0.015
350.0*	K=*	4.86	4.71	4.61	4.47	4.38	4.29	4.14	4.01	3.86	3.64	3.51	3.42	3.30	3.26	3.27
*	D=*	0.100	0.077	0.062	0.051	0.051	0.056	0.063	0.073	0.077	0.074	0.062	0.052	0.038	0.027	0.022
245.0*	K=*	-0.0	4.34	4.27	4.16	4.07	3.94	3.73	3.59	3.47	3.35	3.30	3.25	-0.0	-0.0	-0.0
*	D=*	0.0	0.036	0.039	0.048	0.059	0.069	0.075	0.074	0.063	0.045	0.033	0.023	0.0	0.0	0.0
200.0*	K=*	-0.0	4.23	4.16	4.00	3.87	3.72	3.16	3.40	3.33	3.26	3.23	3.20	-0.0	-0.0	-0.0
*	D=*	0.0	0.037	0.046	0.060	0.072	0.076	0.067	0.057	0.042	0.022	0.019	0.014	0.0	0.0	0.0
150.0*	K=*	-0.0	4.05	3.92	3.70	3.57	3.44	3.32	3.27	3.23	3.21	3.18	3.16	-0.0	-0.0	-0.0
*	D=*	0.0	0.054	0.066	0.073	0.072	0.060	0.043	0.033	0.023	0.014	0.009	0.006	0.0	0.0	0.0
100.0*	K=*	3.87	3.73	3.57	3.40	3.33	3.27	3.18	3.20	3.17	3.16	3.15	3.15	-0.0	-0.0	-0.0
*	D=*	0.066	0.072	0.070	0.055	0.045	0.032	0.022	0.016	0.011	0.007	0.005	0.004	0.0	0.0	0.0

DIELECTRIC PROPERTIES OF DUNITE

Table CO-4

K MEANS DIELECTRIC CONSTANT OF THE SAMPLE
D MEANS DIELECTRIC LOSS TANGENT OF THE SAMPLE

TEMP. IN DEGRES CENTIGRADE
FREQ. IN KILOHERTZ

DENSITY OF SOLID SAMPLE IS 3.32
PACKING FACTOR IS 55%

TEMP.* FREQ.*		0.05	0.10	0.20	0.50	1.00	2.00	5.00	10.0	20.0	50.0	100	200	500	1000	2000
27.0*	K=*	3.46	3.47	3.47	3.46	3.45	3.45	3.45	3.44	3.44	3.44	3.43	3.42	3.40	3.40	3.43
*	K=*	0.0100	0.0058	0.0047	0.0035	0.0030	0.0025	0.0023	0.0023	0.0022	0.0024	0.0025	0.0028	0.0032	0.0027	0.0029
102.0*	K=*	-0.0	3.50	3.49	3.48	3.48	3.47	3.46	3.46	3.45	3.45	3.45	3.44	3.42	3.43	3.46
*	K=*	0.0	0.0090	0.0070	0.0050	0.0041	0.0032	0.0026	0.0024	0.0021	0.0017	0.0015	0.0016	0.0027	0.0033	0.0030
152.0*	K=*	-0.0	3.53	3.52	3.50	3.49	3.48	3.48	3.47	3.47	3.46	3.46	3.46	3.43	3.44	3.47
*	K=*	0.0	0.0135	0.0104	0.0075	0.0062	0.0047	0.0036	0.0031	0.0025	0.0018	0.0015	0.0016	0.0024	0.0022	0.0018
205.0*	K=*	-0.0	3.55	3.54	3.51	3.50	3.49	3.48	3.48	3.48	3.47	3.47	3.47	3.44	3.45	3.48
*	K=*	0.0	0.0220	0.0144	0.0090	0.0072	0.0052	0.0040	0.0033	0.0026	0.0021	0.0016	0.0014	0.0035	0.0047	0.0070
255.0*	K=*	-0.0	3.59	3.56	3.53	3.52	3.52	3.50	3.50	3.49	3.49	3.49	3.48	3.46	3.47	3.50
*	K=*	0.0	0.0560	0.0326	0.0170	0.0113	0.0074	0.0050	0.0040	0.0032	0.0020	0.0019	0.0017	0.0024	0.0020	0.0
310.0*	K=*	-0.0	3.73	3.63	3.56	3.54	3.52	3.50	3.49	3.48	3.48	3.48	3.47	3.44	3.45	-0.0
*	K=*	0.0	0.2054	0.1128	0.0500	0.0320	0.0182	0.0100	0.0072	0.0050	0.0029	0.0027	0.0024	0.0029	0.0022	0.0
200.0*	K=*	-0.0	3.49	3.48	3.47	3.46	3.46	3.45	3.45	3.45	3.44	3.44	3.44	3.41	3.42	-0.0
*	K=*	0.0	0.0195	0.0106	0.0070	0.0050	0.0036	0.0028	0.0024	0.0020	0.0011	0.0011	0.0010	0.0018	0.0016	0.0
150.0*	K=*	-0.0	3.45	3.45	3.44	3.44	3.43	3.43	3.43	3.42	3.42	3.42	3.42	3.40	3.40	-0.0
*	K=*	0.0	0.0065	0.0045	0.0032	0.0026	0.0021	0.0018	0.0015	0.0013	0.0010	0.0008	0.0008	0.0017	0.0017	0.0
100.0*	K=*	-0.0	3.43	3.43	3.42	3.42	3.41	3.41	3.41	3.40	3.40	3.40	3.40	3.37	3.38	-0.0
*	K=*	0.0	0.0040	0.0028	0.0021	0.0018	0.0014	0.0011	0.0010	0.0008	0.0006	0.0005	0.0007	0.0018	0.0024	0.0

DIELECTRIC PROPERTIES
OF
BASALT M

Table CO-5 56

K MEANS DIELECTRIC CONSTANT OF THE SAMPLE
D MEANS DIELECTRIC LOSS TANGENT OF THE SAMPLE

TEMP. IN DEGRES CENTIGRADE
FREQ. IN KILOHERTZ

DENSITY OF SOLID SAMPLE IS 2.95
PACKING FACTOR IS 48%

FREQ.* 0.05		0.10	0.20	0.50	1.00	2.00	5.00	10.0	20.0	50.0	100	200	500	1000	2000
TEMP.*															
27.0*	K=*-0.0	3.64	3.57	3.50	3.46	3.42	3.37	3.35	3.32	3.29	3.27	3.25	3.20	3.18	3.19
*	D=*0.0	0.047	0.036	0.030	0.027	0.023	0.020	0.019	0.017	0.015	0.015	0.015	0.015	0.015	0.014
103.0*	K=* 4.81	4.58	4.28	3.99	3.83	3.71	3.59	3.53	3.48	3.42	3.38	3.35	3.29	3.27	3.27
*	D=*0.107	0.117	0.108	0.097	0.082	0.065	0.048	0.041	0.031	0.025	0.022	0.021	0.019	0.018	0.017
153.0*	K=* 5.47	5.29	5.06	4.73	4.47	4.22	3.93	3.78	3.66	3.55	3.49	3.44	3.35	3.32	3.32
*	D=*0.090	0.094	0.101	0.111	0.120	0.113	0.098	0.082	0.064	0.050	0.035	0.032	0.027	0.023	0.022
203.0*	K=* 6.15	5.89	5.64	5.35	5.13	4.88	4.53	4.27	4.01	3.78	3.65	3.55	3.43	3.39	3.38
*	D=*0.100	0.091	0.090	0.092	0.101	0.106	0.119	0.123	0.108	0.090	0.067	0.058	0.044	0.035	0.030
245.0*	K=* 6.72	6.41	6.17	5.85	5.63	5.40	5.11	4.86	4.60	4.23	3.98	3.78	3.59	3.49	3.44
*	D=*0.140	0.118	0.103	0.093	0.094	0.095	0.105	0.115	0.120	0.123	0.106	0.099	0.075	0.056	0.047
303.0*	K=*-0.0	7.35	6.88	6.42	6.14	5.89	5.57	5.36	5.12	4.77	4.49	4.19	3.85	3.67	3.56
*	D=*0.0	0.197	0.156	0.123	0.107	0.098	0.096	0.101	0.105	0.118	0.123	0.130	0.111	0.089	0.072
200.0*	K=* 6.09	5.88	5.64	5.35	5.14	4.89	4.55	4.28	4.03	3.78	3.64	3.53	3.42	3.38	3.34
*	D=*0.091	0.087	0.088	0.090	0.099	0.104	0.118	0.123	0.111	0.089	0.070	0.060	0.045	0.035	0.031
155.0*	K=* 5.61	5.37	5.11	4.79	4.54	4.27	3.96	3.78	3.64	3.53	3.46	3.40	3.33	3.30	3.30
*	D=*0.075	0.089	0.094	0.105	0.117	0.115	0.103	0.089	0.070	0.050	0.040	0.033	0.027	0.023	0.020
103.0*	K=*-0.0	4.87	4.43	4.07	3.87	3.71	3.58	3.51	3.45	3.39	3.36	3.32	3.28	3.26	3.26
*	D=*0.0	0.108	0.100	0.105	0.097	0.075	0.055	0.045	0.035	0.027	0.022	0.020	0.018	0.017	0.016

Table CO-6

DIELECTRIC PROPERTIES
OF
GRANITE

K MEANS DIELECTRIC CONSTANT OF THE SAMPLE
D MEANS DIELECTRIC LOSS TANGENT OF THE SAMPLE

TEMP. IN DEGREES CENTIGRADE
FREQ. IN KILOHERTZ

DENSITY OF SOLID SAMPLE IS 2.71
PACKING FACTOR IS 53%

FREQ.*		0.05	0.10	0.20	0.50	1.00	2.00	5.00	10.0	20.0	50.0	100	200	500	1000	2000
TEMP.*	*															
27.0*	K=*-0.0	3.10	3.08	3.05	3.06	3.02	2.99	2.98	2.97	2.96	2.95	2.94	2.90	2.91	2.93	
*	D=*0.0	0.022	0.017	0.015	0.013	0.011	0.010	0.009	0.007	0.006	0.004	0.004	0.004	0.003	0.002	
100.0*	K=*-0.0	3.36	3.30	3.22	3.17	3.13	3.08	3.06	3.03	3.00	2.99	2.98	2.94	2.94	2.96	
*	D=*0.0	0.033	0.032	0.030	0.029	0.025	0.021	0.018	0.015	0.011	0.009	0.008	0.007	0.006	0.005	
150.0*	K=*-0.0	3.49	3.45	3.39	3.33	3.27	3.21	3.16	3.07	3.07	3.04	3.02	2.98	2.98	2.99	
*	D=*0.0	0.034	0.034	0.030	0.032	0.032	0.031	0.030	0.028	0.021	0.015	0.014	0.012	0.009	0.008	
200.0*	K=*-0.0	3.62	3.56	3.49	3.44	3.41	3.34	3.29	3.23	3.17	3.12	3.08	3.02	3.01	3.02	
*	D=*0.0	0.042	0.035	0.029	0.029	0.028	0.030	0.032	0.032	0.030	0.026	0.023	0.020	0.016	0.012	
250.0*	K=*-0.0	3.78	3.69	3.59	3.55	3.46	3.40	3.40	3.35	3.29	3.24	3.15	3.10	3.06	3.05	
*	D=*0.0	0.054	0.045	0.037	0.034	0.030	0.027	0.028	0.029	0.030	0.029	0.030	0.030	0.025	0.022	
305.0*	K=*-0.0	3.95	3.84	3.71	3.64	3.57	3.50	3.45	3.41	3.36	3.31	3.27	3.19	3.14	3.12	
*	D=*0.0	0.083	0.066	0.050	0.044	0.038	0.032	0.030	0.028	0.027	0.027	0.031	0.033	0.031	0.027	
250.0*	K=*-0.0	-0.0	3.61	3.54	3.49	3.45	3.39	3.36	3.32	3.27	3.22	3.17	3.10	3.07	3.06	
*	D=*0.0	0.0	0.038	0.031	0.030	0.026	0.024	0.024	0.025	0.026	0.027	0.029	0.030	0.027	0.022	
200.0*	K=*-0.0	3.55	3.50	3.44	3.40	3.33	3.32	3.28	3.24	3.18	3.13	3.09	3.05	3.02	3.03	
*	D=*0.0	0.030	0.027	0.025	0.024	0.023	0.025	0.027	0.028	0.026	0.025	0.025	0.022	0.017	0.016	
150.0*	K=*-0.0	3.41	3.39	3.34	3.31	3.27	3.21	3.16	3.12	3.08	3.04	3.02	2.98	2.98	2.98	
*	D=*0.0	0.022	0.023	0.024	0.025	0.026	0.027	0.027	0.025	0.024	0.017	0.015	0.013	0.011	0.010	
100.0*	K=*-0.0	3.32	3.28	3.22	3.18	3.14	3.09	3.06	3.04	3.01	3.00	2.98	2.96	2.95	2.97	
*	D=*0.0	0.026	0.027	0.027	0.027	0.024	0.021	0.018	0.015	0.012	0.011	0.009	0.009	0.007	0.007	

Table CO-7

DIELECTRIC PROPERTIES
OF
AUGITE

K MEANS DIELECTRIC CONSTANT OF THE SAMPLE
D MEANS DIELECTRIC LOSS TANGENT OF THE SAMPLE

TEMP. IN DEGRES CENTIGRADE
FREQ. IN KILOHERTZ

DENSITY OF SOLID SAMPLE IS 3.25
PACKING FACTOR IS 51%

FREQ.*		0.05	0.10	0.20	0.50	1.00	2.00	5.00	10.0	20.0	50.0	100	200	500	1000	2000
TEMP.*	*															
27.0*	K=*	12.66	12.46	11.96	10.54	8.60	7.19	5.95	5.47	5.14	4.82	4.66	4.54	4.41	4.35	4.35
*	D=*	0.055	0.091	0.152	0.274	0.338	0.331	0.258	0.205	0.150	0.104	0.078	0.064	0.045	0.034	0.028
100.0*	K=*	12.91	12.73	12.63	12.46	12.34	12.16	11.43	10.30	8.69	6.89	5.90	6.92	4.89	4.68	4.58
*	D=*	0.048	0.037	0.033	0.038	0.052	0.082	0.162	0.254	0.327	0.348	0.268	0.219	0.148	0.103	0.080
155.0*	K=*	13.54	13.22	12.97	12.70	12.54	12.42	12.23	12.02	11.59	10.09	8.48	7.02	5.71	5.22	4.93
*	D=*	0.111	0.078	0.060	0.041	0.033	0.036	0.055	0.087	0.144	0.256	0.327	0.353	0.275	0.199	0.152
200.0*	K=*	-0.0	14.47	13.91	13.27	12.90	12.73	12.49	12.34	12.20	11.82	11.22	10.13	8.06	8.02	5.72
*	D=*	0.0	0.188	0.144	0.091	0.051	0.041	0.039	0.045	0.059	0.103	0.167	0.263	0.368	0.317	0.261
250.0*	K=*	-0.0	17.06	15.91	14.68	13.85	13.51	13.17	12.99	12.82	12.58	12.31	11.91	10.56	8.96	7.43
*	D=*	0.0	0.415	0.289	0.173	0.099	0.070	0.049	0.045	0.046	0.060	0.086	0.139	0.239	0.309	0.333
150.0*	K=*	14.42	13.88	13.46	13.00	12.77	12.61	12.37	12.15	11.71	10.23	8.56	7.07	5.71	5.22	4.93
*	D=*	0.160	0.120	0.084	0.067	0.046	0.045	0.059	0.090	0.145	0.256	0.333	0.362	0.294	0.203	0.156

Table CO-8

DIELECTRIC PROPERTIES
OF
DIABASE P

K MEANS DIELECTRIC CONSTANT OF THE SAMPLE
D MEANS DIELECTRIC LOSS TANGENT OF THE SAMPLE

TEMP. IN DEGRES CENTIGRADE
FREQ. IN KILOHERTZ

DENSITY OF SOLID SAMPLE IS 2.90
PACKING FACTOR IS 50%

FREQ.* 0.05		0.10	0.20	0.50	1.00	2.00	5.00	10.0	20.0	50.0	100	200	500	1000	2000
TEMP.*	*														
27.0*	K=*-0.0	3.58	3.55	3.52	3.50	3.48	3.47	3.46	3.45	3.44	3.43	3.43	3.40	3.40	3.43
*	D=*0.0	0.024	0.017	0.013	0.010	0.008	0.007	0.006	0.006	0.006	0.005	0.005	0.007	0.007	0.008
100.0*	K=* 4.32	4.12	3.96	3.79	3.70	3.64	3.58	3.55	3.53	3.50	3.48	3.47	3.46	3.45	3.47
*	D=*0.107	0.110	0.081	0.059	0.048	0.036	0.025	0.019	0.015	0.011	0.009	0.008	0.008	0.008	0.007
150.0*	K=*-0.0	4.85	4.56	4.22	4.04	3.89	3.74	3.66	3.61	3.55	3.53	3.50	3.47	3.46	3.48
*	D=*0.0	0.155	0.128	0.107	0.096	0.078	0.056	0.044	0.032	0.022	0.012	0.014	0.012	0.010	0.008
200.0*	K=* 6.22	5.77	5.36	4.84	4.55	4.31	4.02	3.87	3.76	3.65	3.59	3.54	3.50	3.49	3.50
*	D=*0.165	0.162	0.156	0.143	0.136	0.117	0.095	0.080	0.062	0.042	0.032	0.025	0.018	0.015	0.012
265.0*	K=* 7.71	7.17	6.67	5.96	5.53	5.13	4.65	4.38	4.15	3.90	3.77	3.67	3.59	3.55	3.55
*	D=*0.155	0.166	0.168	0.169	0.169	0.159	0.143	0.132	0.114	0.086	0.066	0.054	0.038	0.027	0.022
315.0*	K=* 9.39	8.80	8.21	7.37	6.83	6.30	5.61	5.21	4.85	4.41	4.17	3.97	3.71	3.65	3.61
*	D=*0.190	0.177	0.172	0.173	0.182	0.180	0.173	0.170	0.154	0.134	0.116	0.102	0.075	0.055	0.042
375.0*	K=*-0.0	10.27	9.42	8.35	7.71	7.11	6.31	5.81	5.36	4.81	4.50	4.23	3.92	3.77	3.69
*	D=*0.0	0.275	0.235	0.198	0.198	0.192	0.184	0.185	0.174	0.159	0.143	0.130	0.102	0.077	0.062
260.0*	K=* 7.61	7.13	6.60	5.89	5.47	5.08	4.60	4.34	4.11	3.86	3.73	3.64	-0.0	-0.0	-0.0
*	D=*0.177	0.165	0.161	0.165	0.168	0.158	0.141	0.130	0.111	0.084	0.066	0.054	0.0	0.0	0.0
150.0*	K=*-0.0	4.83	-0.0	-0.0	4.02	-0.0	-0.0	3.62	-0.0	3.50	3.48	3.45	3.44	3.43	-0.28
*	D=*0.0	0.145	0.0	0.0	0.102	0.0	0.0	0.045	0.0	0.021	0.016	0.014	0.011	0.009	7.483

K MEANS DIELECTRIC CONSTANT OF THE SAMPLE
D MEANS DIELECTRIC LOSS TANGENT OF THE SAMPLE

TEMP. IN DEGRES CENTIGRADE
FREQ. IN KILOHERTZ

DENSITY OF SOLID SAMPLE IS 2.95

TEMP.	FREQ.	0.05	0.10	0.20	0.50	1.00	2.00	5.00	10.0	20.0	50.0	100	200	500	1000	2000
27.0	K=	27.23	24.23	21.67	19.47	18.03	16.83	15.54	14.78	14.06	13.27	12.76	12.31	11.71	11.32	10.91
	D=	0.356	0.287	0.270	0.202	0.198	0.162	0.154	0.129	0.110	0.093	0.088	0.087	0.081	0.069	0.071
103.0	K=	0.0	74.42	58.60	43.29	36.09	30.40	25.30	22.48	20.22	18.02	16.69	15.58	14.27	13.41	12.76
	D=	0.0	0.706	0.660	0.567	0.534	0.450	0.366	0.316	0.257	0.209	0.176	0.171	0.148	0.127	0.118
162.0	K=	0.0	0.0	89.85	75.42	62.00	48.32	35.07	29.62	25.27	21.38	19.16	17.37	15.56	14.40	13.55
	D=	0.0	0.0	1.041	0.753	0.734	0.669	0.593	0.519	0.418	0.323	0.271	0.244	0.195	0.164	0.144
235.0	K=	0.0	0.0	0.0	80.83	56.24	56.45	38.43	31.05	25.32	20.52	19.70	16.45	14.86	13.86	13.08
	D=	0.0	0.0	0.0	1.019	0.921	0.780	0.747	0.689	0.560	0.419	0.307	0.277	0.210	0.169	0.144
330.0	K=	0.0	0.0	0.0	0.0	0.0	98.05	70.23	59.12	45.42	30.70	25.30	20.32	16.72	14.88	13.61
	D=	0.0	0.0	0.0	0.0	0.0	1.017	0.838	0.796	0.748	0.732	0.615	0.563	0.412	0.307	0.238
508.0	K=	0.0	0.0	0.0	0.0	0.0	0.0	0.0	0.0	0.0	0.0	0.0	0.0	0.0	27.14	0.0
	D=	0.0	0.0	0.0	0.0	0.0	0.0	0.0	0.0	0.0	0.0	0.0	0.0	0.0	0.827	0.0
324.0	K=	0.0	0.0	0.0	0.0	0.0	0.0	0.0	0.0	0.0	0.0	25.92	0.0	0.0	14.89	0.0
	D=	0.0	0.0	0.0	0.0	0.0	0.0	0.0	0.0	0.0	0.0	0.699	0.0	0.0	0.336	0.0
230.0	K=	0.0	0.0	0.0	61.09	33.25	48.32	33.90	28.34	23.09	18.66	16.63	15.02	13.57	12.83	12.13
	D=	0.0	0.0	0.0	1.605	1.528	1.013	0.866	0.744	0.600	0.458	0.337	0.282	0.189	0.146	0.098
166.0	K=	0.0	0.0	49.98	34.40	28.75	23.53	19.92	17.04	15.53	14.22	13.48	12.87	12.24	11.82	11.51
	D=	0.0	0.0	1.017	0.854	0.715	0.562	0.392	0.319	0.237	0.169	0.132	0.112	0.087	0.070	0.068
100.0	K=	0.0	26.82	22.66	19.04	17.21	15.82	14.32	13.89	13.30	12.72	12.33	12.05	11.54	11.33	11.05
	D=	0.0	0.642	0.499	0.348	0.272	0.212	0.156	0.129	0.101	0.078	0.066	0.060	0.054	0.044	0.042
27.0	K=	0.0	18.46	0.0	0.0	14.57	0.0	0.0	12.55	0.0	0.0	11.51	0.0	0.0	0.0	0.0
	D=	0.0	0.269	0.0	0.0	0.148	0.0	0.0	0.085	0.0	0.0	0.045	0.0	0.0	0.0	0.0
240.0	K=	0.0	0.0	0.0	0.0	0.0	48.39	33.92	27.79	22.46	18.06	16.14	14.49	0.0	12.42	0.0
	D=	0.0	0.0	0.0	0.0	0.0	0.928	0.801	0.714	0.576	0.426	0.296	0.270	0.0	0.143	0.0
100.0	K=	0.0	0.0	22.42	0.0	16.87	0.0	0.0	13.23	0.0	0.0	11.94	0.0	0.0	0.0	0.0
	D=	0.0	0.0	0.480	0.0	0.304	0.0	0.0	0.141	0.0	0.0	0.067	0.0	0.0	0.0	0.0
30.0	K=	0.0	15.00	14.26	13.47	13.93	13.50	13.03	11.77	11.53	11.30	11.08	10.91	10.65	10.52	10.40

DIELECTRIC PROPERTIES
OF
GRANITE

Table CO-10

K MEANS DIELECTRIC CONSTANT OF THE SAMPLE
D MEANS DIELECTRIC LOSS TANGENT OF THE SAMPLE

TEMP. IN DEGRES CENTIGRADE
FREQ. IN KILOHERTZ

DENSITY OF SOLID SAMPLE IS 2.71

TEMP.	FREQ.	0.05	0.10	0.20	0.50	1.00	2.00	5.00	10.0	20.0	50.0	100	200	500	1000	2000
32.0	K=	7.37	7.23	7.08	6.94	6.85	0.0	0.0	0.0	0.0	0.0	0.0	0.0	6.41	0.0	0.0
	D=	0.058	0.038	0.034	0.034	0.028	0.0	0.0	0.0	0.0	0.0	0.0	0.0	0.011	0.0	0.0
97.0	K=	9.30	8.59	8.17	7.73	7.49	7.28	7.06	6.94	6.84	6.76	6.67	6.61	6.58	6.52	0.0
	D=	0.100	0.121	0.097	0.087	0.075	0.061	0.047	0.040	0.027	0.024	0.020	0.020	0.019	0.016	0.0
180.0	K=	13.75	12.40	11.34	10.25	9.63	9.00	8.34	7.95	7.62	7.26	7.08	6.89	6.76	6.64	6.55
	D=	0.276	0.255	0.217	0.179	0.164	0.141	0.124	0.111	0.089	0.074	0.059	0.052	0.040	0.032	0.030
285.0	K=	0.0	19.44	17.24	14.65	12.99	11.83	10.73	10.08	9.50	8.82	8.33	7.90	7.38	7.08	6.83
	D=	0.0	0.504	0.413	0.328	0.270	0.222	0.180	0.160	0.138	0.126	0.117	0.112	0.097	0.077	0.064
400.0	K=	0.0	0.0	28.61	22.65	19.57	16.63	14.02	12.56	11.40	10.91	10.11	9.27	8.41	8.01	7.55
	D=	0.0	0.0	1.026	0.713	0.552	0.454	0.359	0.306	0.234	0.178	0.155	0.130	0.130	0.121	0.108
102.0	K=	0.0	9.65	9.14	8.62	8.26	7.95	7.62	7.41	7.25	7.09	6.97	6.78	6.58	6.49	0.0
	D=	0.0	0.132	0.111	0.099	0.091	0.080	0.069	0.063	0.049	0.040	0.031	0.033	0.035	0.029	0.0

DIELECTRIC PROPERTIES
OF
DUNITE

Table CO-11

K MEANS DIELECTRIC CONSTANT OF THE SAMPLE
D MEANS DIELECTRIC LOSS TANGENT OF THE SAMPLE

TEMP. IN DEGRES CENTIGRADE
FREQ. IN KILOHERTZ

DENSITY OF SOLID SAMPLE IS 3.32

TEMP.* FREQ.*		0.05	0.10	0.20	0.50	1.00	2.00	5.00	10.0	20.0	50.0	100	200	500	1000	2000
27.0*	K=*	0.0	8.38	8.35	8.26	8.23	0.0	0.0	8.17	0.0	0.0	8.11	8.08	8.08	8.08	0.0
*	D=*	0.0	0.012	0.007	0.007	0.007	0.0	0.0	0.005	0.0	0.0	0.006	0.007	0.009	0.007	0.0
290.0*	K=*	0.0	0.0	0.0	0.0	0.0	0.0	9.59	9.45	9.24	9.00	8.88	8.72	0.0	0.0	0.0
*	D=*	0.0	0.0	0.0	0.0	0.0	0.0	0.335	0.132	0.095	0.060	0.048	0.036	0.0	0.0	0.0
250.0*	K=*	0.0	9.69	9.30	0.0	8.78	0.0	0.0	8.53	0.0	0.0	8.44	0.0	0.0	8.32	0.0
*	D=*	0.0	0.207	0.128	0.0	0.057	0.0	0.0	0.016	0.0	0.0	0.007	0.0	0.0	0.007	0.0
185.0*	K=*	0.0	8.82	8.64	0.0	8.47	0.0	0.0	8.38	0.0	0.0	8.32	0.0	0.0	0.0	0.0
*	D=*	0.0	0.041	0.010	0.0	0.015	0.0	0.0	0.008	0.0	0.0	0.004	0.0	0.0	0.0	0.0
105.0*	K=*	0.0	0.0	8.32	0.0	8.26	0.0	0.0	8.20	0.0	0.0	8.20	0.0	0.0	0.0	0.0
*	D=*	0.0	0.0	0.004	0.0	0.004	0.0	0.0	0.003	0.0	0.0	0.003	0.0	0.0	0.0	0.0

Appendix B - GRAPHS
Explanation and List

There are seven series of graphs: A,B,C,D,E,F and G which are summarized here.

The A Series

The graphs are presented in the order in which they were measured. Two or three consecutive graphs related to the same material were measured at the same time.

The horizontal axis is the logarithm of frequency given as fHz. Most graphs in this series do not have the experimental points but these can be obtained from the related computer outputs. Additional frequencies were investigated near the maximum in the loss tangent curve. In general, at a given temperature, the curve showing data taken while heating coincides with that taken at the same temperature while cooling. Where discrepancies occur at some frequency, this is shown by dashed lines. An exception to this is Figure A17, which is explained later.

In the detailed explanation below, the letter (S) or (D) follows the figure number indicating if a smoothed (S) curve is drawn or if the line joins the experimental points (D), revealing the fine structure.

All of these samples were dried, as described in Section 2 of Chapter II.

Fig. A1 (D)
Basalt AA : Dielectric constant, dry powdered sample in vacuum.

Fig. A2 (S)
Basalt AA : Loss tangent, dry powdered sample in vacuum, dashed lines on cooling.

Fig. A3 (D)

Plagioclase : Loss tangent, dry powdered sample at 100°C in vacuum.

$\overline{\mathrm{I}}$ are data points taken before heating to 350°.

$\underline{\mathrm{I}}$ are data points taken after heating to 350°.

Fig. A4 (D)

Hypersthene : Dielectric constant, dry powdered sample in vacuum, dashed lines on cooling.

Fig. A5 (S)

Hypersthene : Loss tangent, dry powdered sample in vacuum.

All data taken during heating to 350°C.

Fig. A6 (S)

Hypersthene : Loss tangent, dry powdered sample in vacuum.

All data taken on cooling from 350°C.

Fig. A7 (D)

Dunite : Loss tangent, dry powdered sample in vacuum.

$\overline{\mathrm{I}}$ are data points taken at 100°C before heating to 310°C.

$\underline{\mathrm{I}}$ are data points taken at 100°C after heating to 310°C.

Δ are data points taken at 200°C after heating to 310°C.

Fig. A8 (D)

Basalt M : Dielectric constant, dry powdered sample in vacuum.

Fig. A9 (S)

Basalt M : Loss tangent, dry powdered sample in vacuum, dashed lines on cooling.

Fig. A10 (D)

Granite : Dielectric constant, dry powdered sample in vacuum, dashed lines on cooling.

Fig. A11 (D)

Granite : Loss tangent, dry powdered sample in vacuum.

All data here are taken while heating to 340°C.

Fig. A12 (D)

Granite : Loss tangent, dry powdered sample in vacuum.

All data here are taken on cooling from 340°C.

Fig. A13 (D)

Augite : Dielectric constant, dry powdered sample in vacuum, dashed lines on cooling.

Fig. A14 (S)

Augite : Loss tangent, dry powdered sample in vacuum, dashed lines on cooling.

(The loss tangent maximum at 250°C is an interpolation between experimental points at 1MHz and 2 MHz).

Fig. A15 (D)

Loss tangent of 10% by weight augite in plagioclase. The unbroken curve shows the loss tangent of pure plagioclase at 27°C before heating process in vacuum.

Fig. A16 (D)

Loss tangent: Mixture test.

(1) The upper unbroken curve shows the loss tangent of powdered granite in vacuum, at 200°C after heating to 340°C.

(2) The middle curve with experimental points shows the loss tangent of a mixture of 1.4% biotite by weight in powdered plagioclase, in vacuum. This biotite was obtained from the same sample of granite with the help of the Frantz magnetic separator. It is interesting to note

that the double hump structure of the curve found in granite is repeated in this mixture. The biotite was fairly pure, containing about 2% of mixed impurities. It was also very black. These values are taken at 200°C after heating to 340°C.

(3) The lower unbroken curve shows the loss tangent of powdered plagioclase in vacuum alone at 200°C after heating to 350°C.

Fig. A17

Loss tangent : Mixture test

(1) The unbroken curve shows the loss tangent of dry powdered basalt M in vacuum at 200°C after heating to 303°C, reduced scales (1/10).

(2) Δ are the experimental points for dry olivine in vacuum at 200°C after heating to 310°C.

(3) ϕ are the experimental points for a mixture of 1.5% biotite by weight in powdered olivine at 200°C after heating to 300°C. The biotite came from the same basalt M sample. The separation was also made with the help of the Frantz magnetic separator. Observation with a high power microscope revealed later that about 40% of this "biotite" sample was hornblende.

(4) The dashed curve represents approximately the contribution of this "biotite".

Fig. A18 (D)

Diabase P : Dielectric constant, dry powdered sample in vacuum.

Fig. A19 (S)

Diabase P : Loss tangent, dry powdered sample in vacuum.

The B Series

These curves summarize the data taken on solid samples. General comments for the A series also apply to the B series.

Fig. B1 (D)

Basalt M : Dielectric constant, dry solid sample in vacuum

The curves for 230°C, 166°C, 100°C are data after a second heating. The basalt M has been heated twice up to 150°C and once up to 230°C, in vacuum, then a measurement series was taken up to 508°C (see computer output table CO-9) and cooled. During the cooling process, some measurements were taken. Among those shown on this graph are: one series at 230°C, one series at 166°C and one series at 100°C. The experiment ended, the basalt sample was taken off and kept with dry silica gel for four days. On the fifth day, another measurement series was taken up to 240°C, then cooled down to 30°C. At this temperature, one series of measurements was taken and is shown on the graph (on the 27°C row).

Fig. B2 (D)

Basalt M : Loss tangent, dry solid sample in vacuum. Same comments as those in B1 (D).

Fig. B3 (D)

Granite : Dielectric constant, dry solid sample in vacuum.

Dotted curve represents the dielectric properties of granite at 102°C, after heating to 400°C. This granite has been heated before up to 150°C (see the experimental procedure).

Fig. B4 (D)

Granite : Loss tangent, dry solid sample in vacuum.
Same comments as those in B3 (D).

The C Series

These curves summarize an investigation of the effect of small water content at low temperature using basalt AA in powder form.

No data points are shown (with the exception of Fig. C7) but the curves are within the range of most probable values. The frequencies used are: 300Hz, 1KHz, 3KHz, 100KHz, 300KHz and 1MHz and occasionally 100Hz and 3MHz. Dry, 0.01%, 0.03% (not 0.05%), 0.1%, 0.2%, 0.5%, 1% and 2% dry weight basis are the only concentrations of distilled water investigated and are known to about $\pm$10% of their value.

Large uncertainties occur at 10KHz for low values of loss tangent, $\pm$20%, but are well known for high values. The same applies for 100KHz but in this case, large uncertainties occur at high values of loss tangent and are known to about $\pm$5% in the worst case (i.e. if $\tan\delta > 0.07$).

Fig. C1

Dry powdered basalt AA : Dielectric constant.

Fig. C2

Dry powdered basalt AA : Loss tangent.

Fig. C3

Powdered basalt AA with 0.1% H_2O dry weight basis: Dielectric constant.

Fig. C4

Powdered basalt AA with 0.1% H_2O dry weight basis: Loss tangent.

Fig. C5

Powdered basalt AA with 0.2% H_2O dry weight basis: Loss tangent.

Fig. C6

Powdered basalt AA with 0.5% H_2O dry weight basis: Dielectric constant.

Fig. C7

Powdered basalt AA with 0.5% H_2O dry weight basis: Loss tangent.

Fig. C8

Basalt AA : Dielectric constant at 1MHz.

This graph shows the effect of distilled water concentration on the dielectric constant of the powdered basalt AA.

Fig. C9

Basalt AA : Loss tangent at 1MHz

This graph shows the effect of distilled water concentration on the loss tangent of the powdered basalt AA.

The D Series

Resistivity data are shown on these four graphs. The vertical scale is logarithmic and shows the value of R, the resistance across the sample, NOT the resistivity. To obtain the resistivity values in ohm-cm, multiply the given values by 250 ± 10 for powder (or add 2.4 $\log_{10}$ scale), and multiply the given values by 40 ± 2 for solid samples (or add 1.6 on a $\log_{10}$ scale). The thick oblique straight line, starting at a $\log_{10}$ resistance of 7.75 at $\frac{1000}{T} = 1.3$, is the contribution of the ceramic feed-thru as a parallel resistor in both solid and powder investigations.

○ refers to the DC resistance of powder

□ refers to the DC resistance of solid

● refers to the AC resistance of powder at 50-100 Hz

△ refers to the AC resistance of solid at the lowest frequency investigated at this given temperature (see the computer output).

The size of points represents the uncertainty of the measurement.

Fig. D1

Basalts : M refers to basalt M
AA refers to basalt AA

Fig. D2

Granite : Q refers to quartz sand

Fig. D3

Dunite

Fig. D4

Plagioclase

The E Series

Various data are presented in this series.

Fig. E1

Relaxation maximum

This curve shows ν_m vs. $\frac{1000}{T}$ where ν_m is the frequency of the maximum loss tangent for various samples.

Fig. E2

Ohm's Law Test for solid basalt M

This graph shows, in log-log scale, the relation of the electric current which passes through the sample versus potential difference across the sample. It represents "proof" of an ohmic contact between the sample and the platinum electrode and between mineral grains. Ohm's Law holds for all temperatures investigated. Departure from the 45° slope would mean a non-ohmic behaviour.

This 45° slope holds also for dunite and granite for potential difference of 1v to 10v. Due to

their high impedance, current values at lower voltages were too difficult to investigate.

Fig. E3

Basalt M at 200°C

This is an Ohm's Law test for powdered basalt M, in a high electric field only, 15v/cm to 250v/cm, and shows a non-ohmic relation between V and I. This curve is typical for all powdered rocks or minerals investigated.

V is the potential difference across the sample.

I is the electric current through the sample in amperes.

Fig. E4

Basalt AA : 0.5% H_2O

This shows the relation between ν_m and $\frac{1000}{T}$, where ν_m is the frequency of maximum loss tangent, for basalt sand with 0.5% H_2O (dry weight basis). This is derived from curve C7.

Fig. E5

This shows the Gever and du Pre value of τ_o in sec. (in $\log_{10}$ scale) as a function of frequency for various materials. The uncertainty of $\log_{10} \tau_o$ value is ± 2. τ_o is in seconds.

Fig. E6

These points are Gever and du Pre values of $\log_{10} \tau_o$ vs. $\frac{1000}{T}$ for basalt AA from 27°C to -50°C. τ_o is in seconds.

Fig. E7

Gever and du Pre values of $\log_{10} \tau_o$ vs. T from 27°C to 250°C for four powder samples. $\log_{10} \tau_o$ is known to ± 2. τ_o is in seconds.

The F Series

These curves include the data from the C curves with additional data. Their purpose is to show clearly the effect of small water content on dielectric properties of basalt AA. Per cent H_2O is given on a dry weight basis. These curves are highly smoothed.

Fig. F1
Basalt AA : Dielectric constant at 27°C.

Fig. F2
Basalt AA : Loss tangent at 27°C.

Fig. F3
Basalt AA : Loss tangent at 0°C.

Fig. F4
Basalt AA : Dielectric constant at -45°C.

Fig. F5
Basalt AA : Loss tangent at -45°C.

The G Series

Fig. G1
Fig. 2(a), 2(b) and 3 of the reference (5).
Fig. 2(a) The real part of ϵ^* as a function of $\log \omega t$ according to the Debye equations (2.21) and (2.22) for a dielectric with $\epsilon_s = 8, \epsilon_\infty = 2$.
Fig. 2(b) The imaginary part of ϵ^* for the same dielectric.
Fig. 3. The loss tangent for the dielectric illustrated in Fig. 2(a) and (b).

Fig. G2
Fig. 92 of the reference (23).
Frequency dependence for the dielectric constant (a) and the resistivity (b) of a quartz sand. Water content in percent: (1) 12, (2) 0.4, (3) 0.03, (4) air dried with P_2O_5.

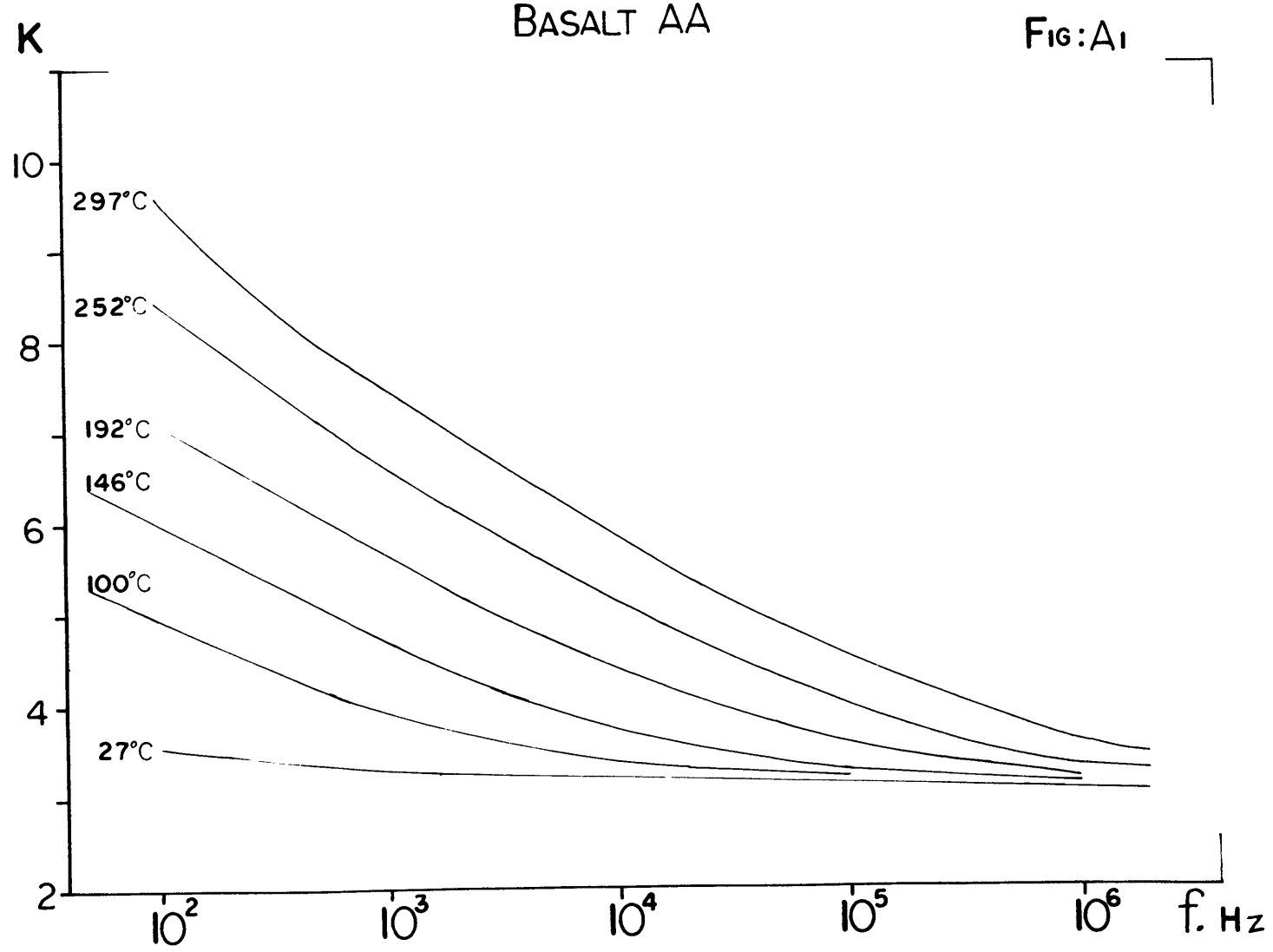
BASALT AA
FIG: A1
K
10
8
6
4
2
297°C
252°C
192°C
146°C
100°C
27°C
10^2
10^3
10^4
10^5
10^6
f. Hz

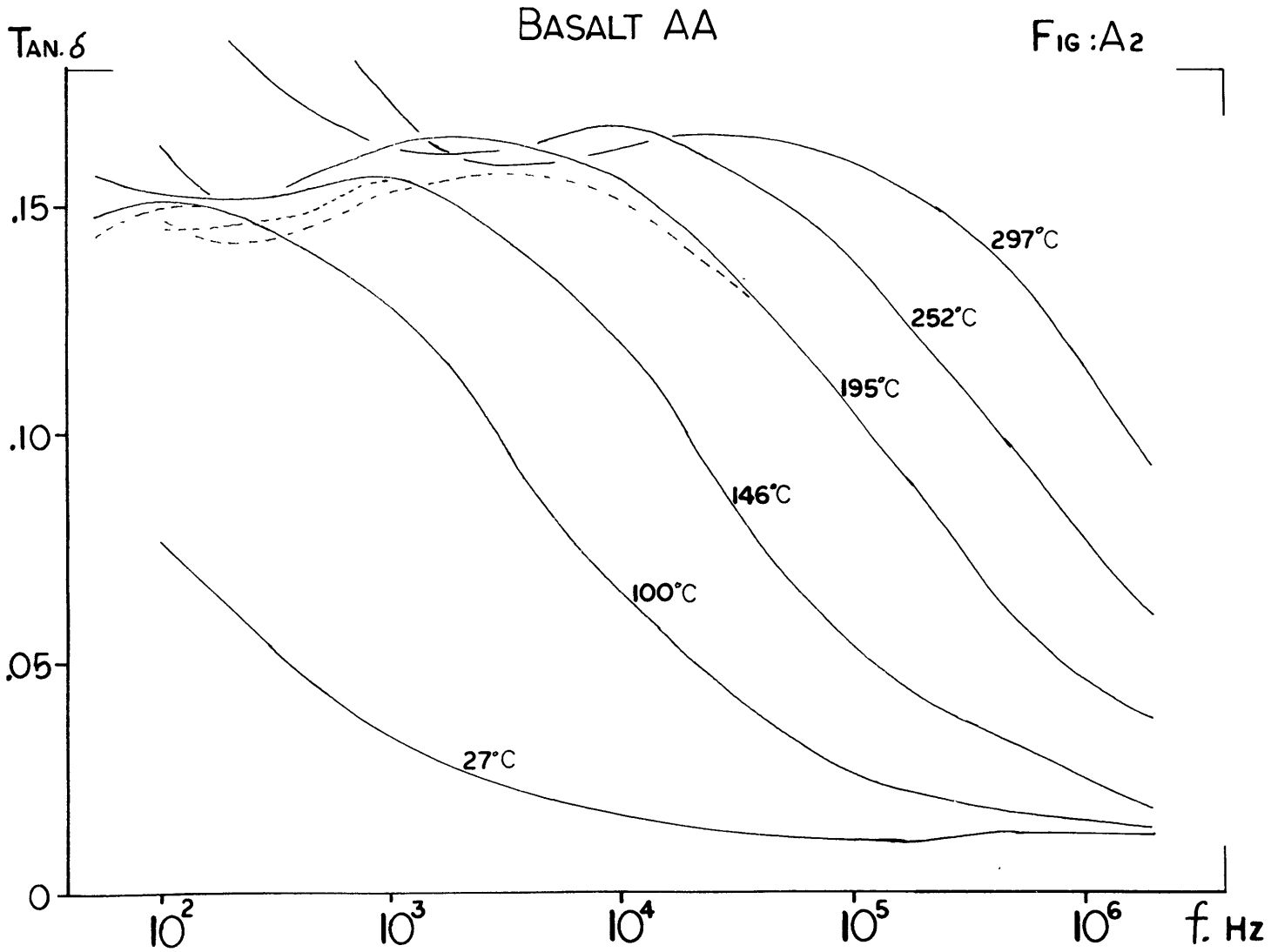
BASALT AA
FIG : A2
TAN. δ
.15
.10
.05
0
297°C
252°C
195°C
146°C
100°C
27°C
10^2
10^3
10^4
10^5
10^6
f. Hz

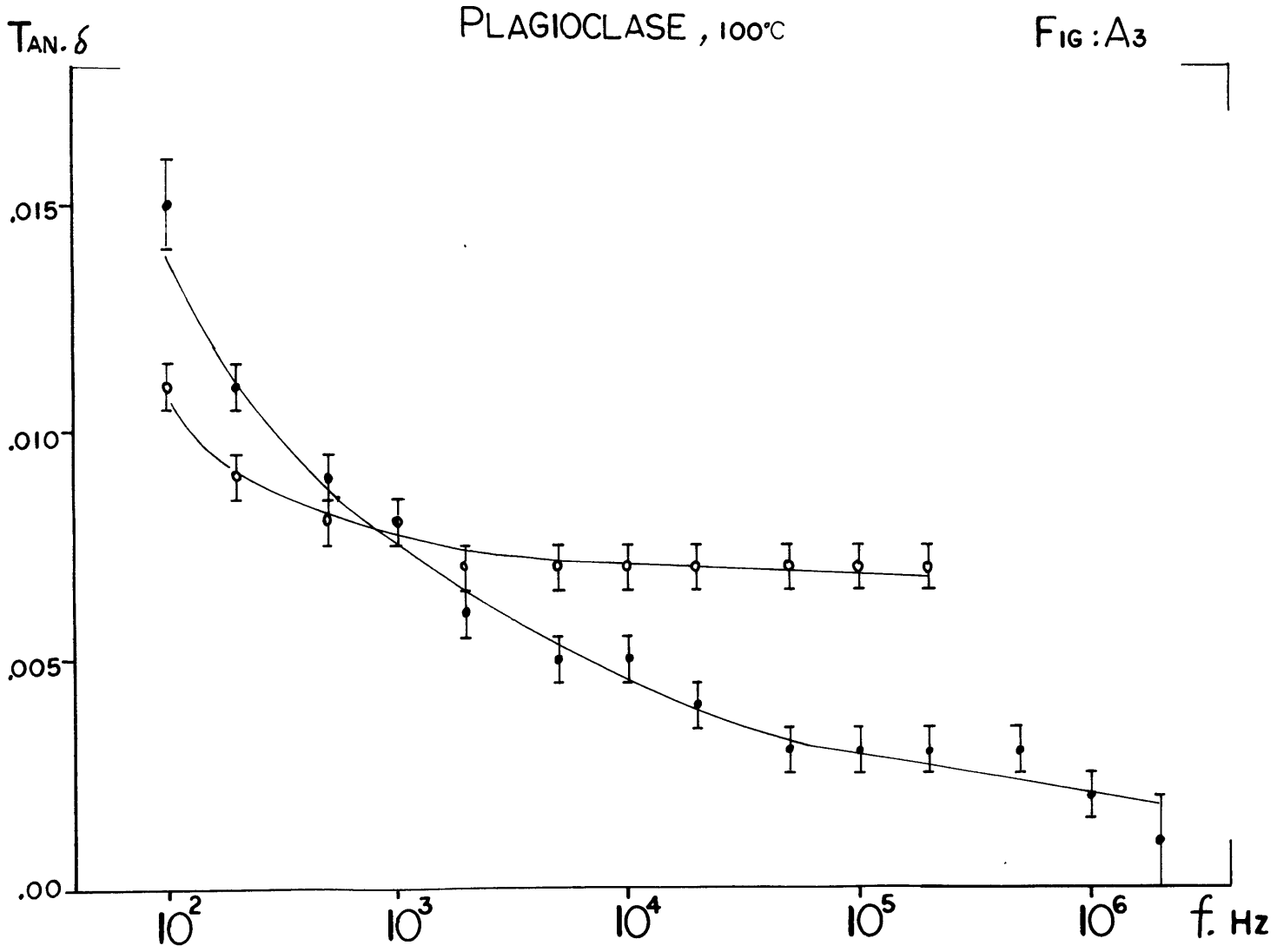
TAN. δ
PLAGIOCLASE , 100°C
FIG : A3
.015
.010
.005
.00
10^2
10^3
10^4
10^5
10^6
f. Hz

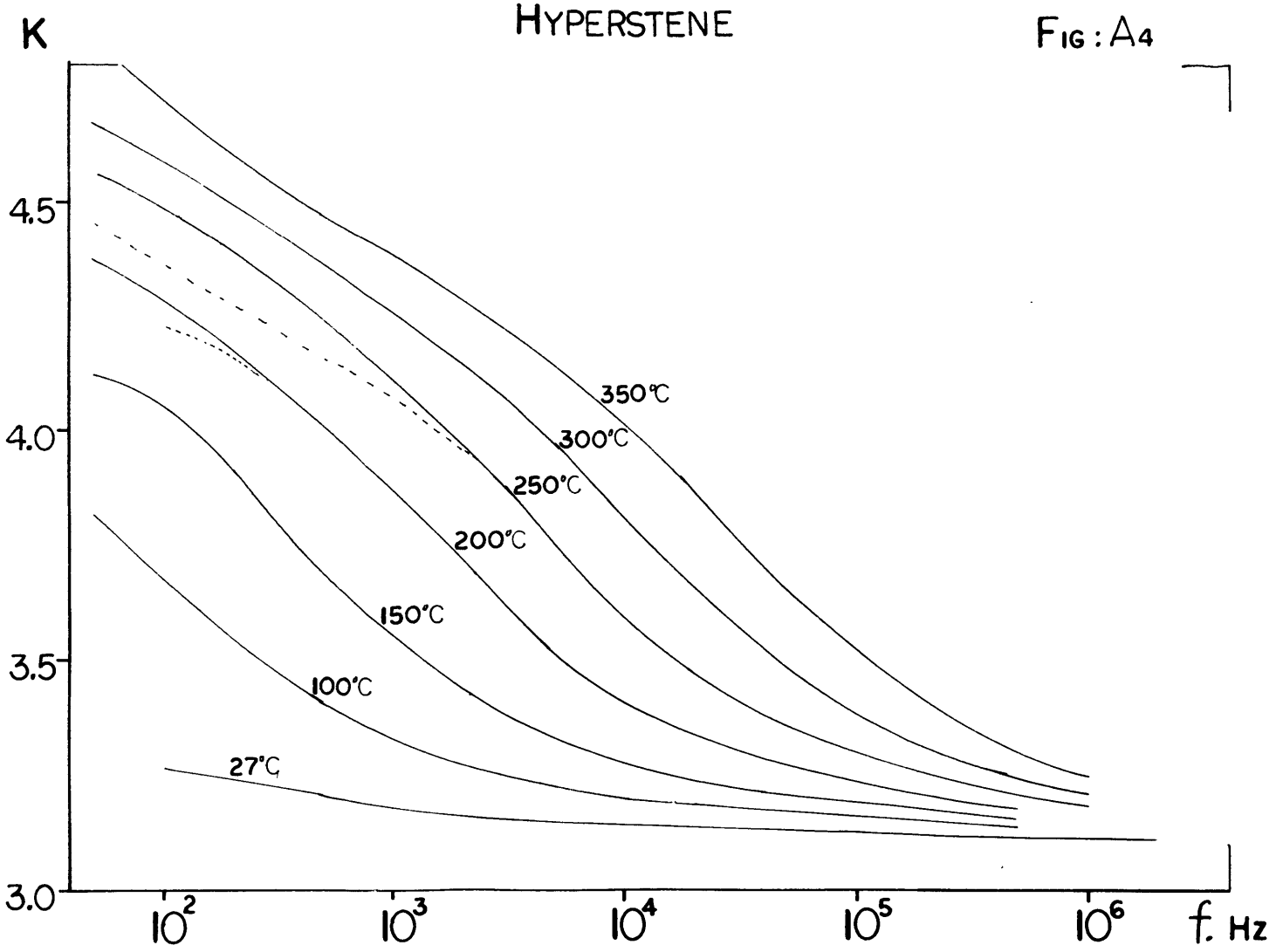
HYPERSTENE
FIG : A4
K
4.5
4.0
3.5
3.0
350°C
300°C
250°C
200°C
150°C
100°C
27°C
10^2
10^3
10^4
10^5
10^6
f. Hz

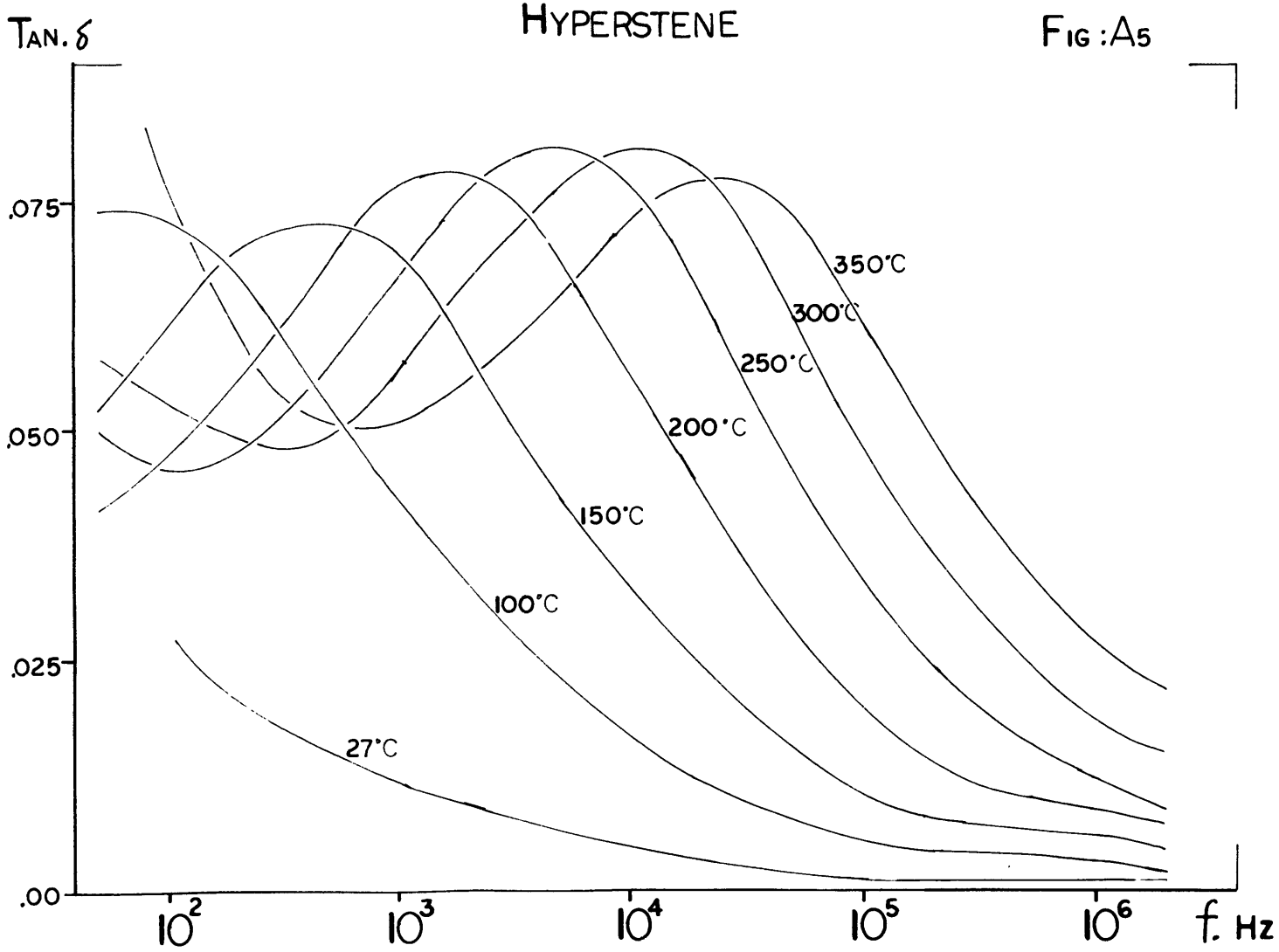
TAN. δ
HYPERSTENE
FIG : A5
.075
.050
.025
.00
350°C
300°C
250°C
200°C
150°C
100°C
27°C
10^2
10^3
10^4
10^5
10^6
f. Hz

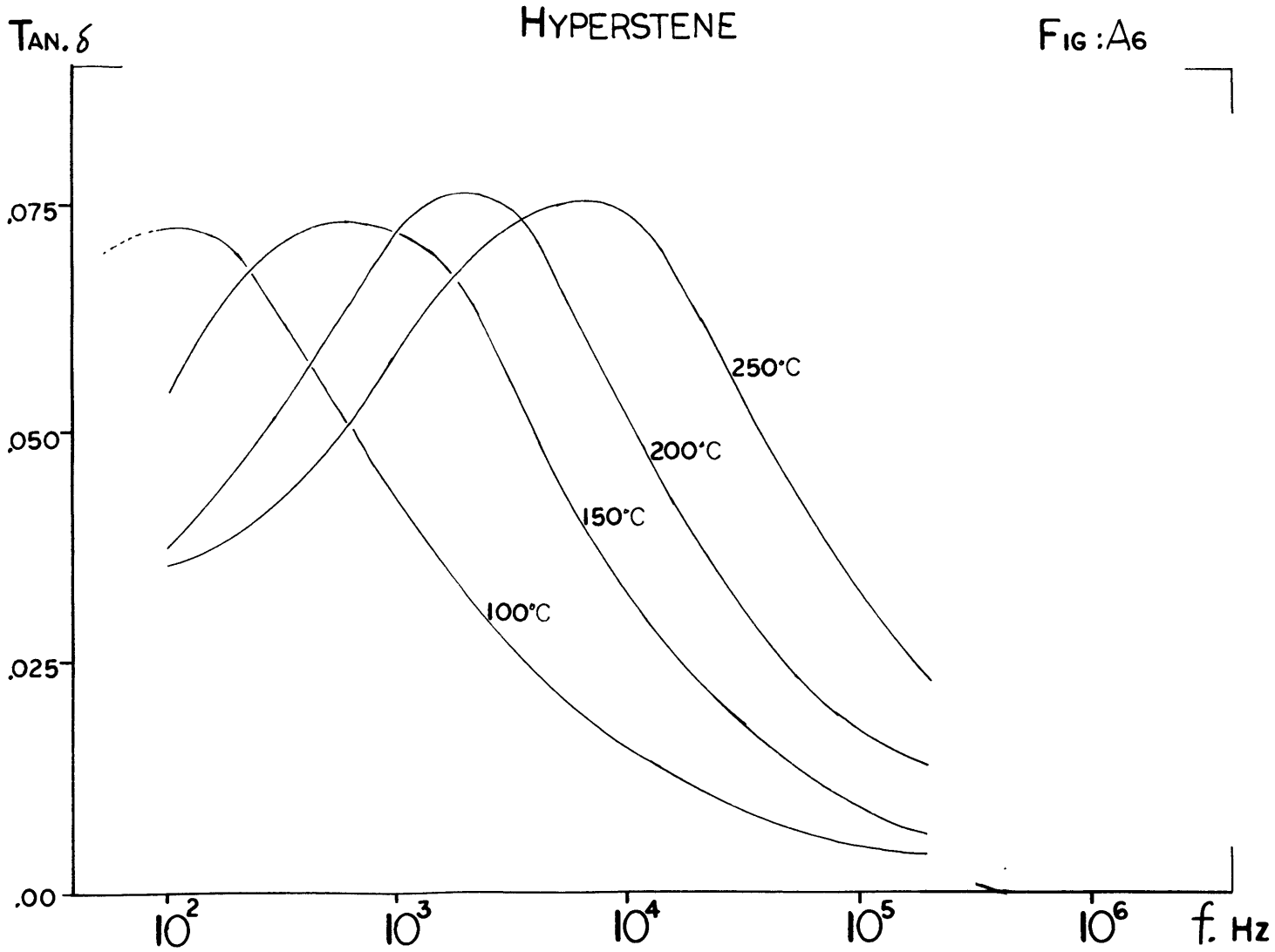
TAN. δ
HYPERSTENE
FIG : A6
.075
.050
.025
.00
250°C
200°C
150°C
100°C
10^2
10^3
10^4
10^5
10^6
f. Hz

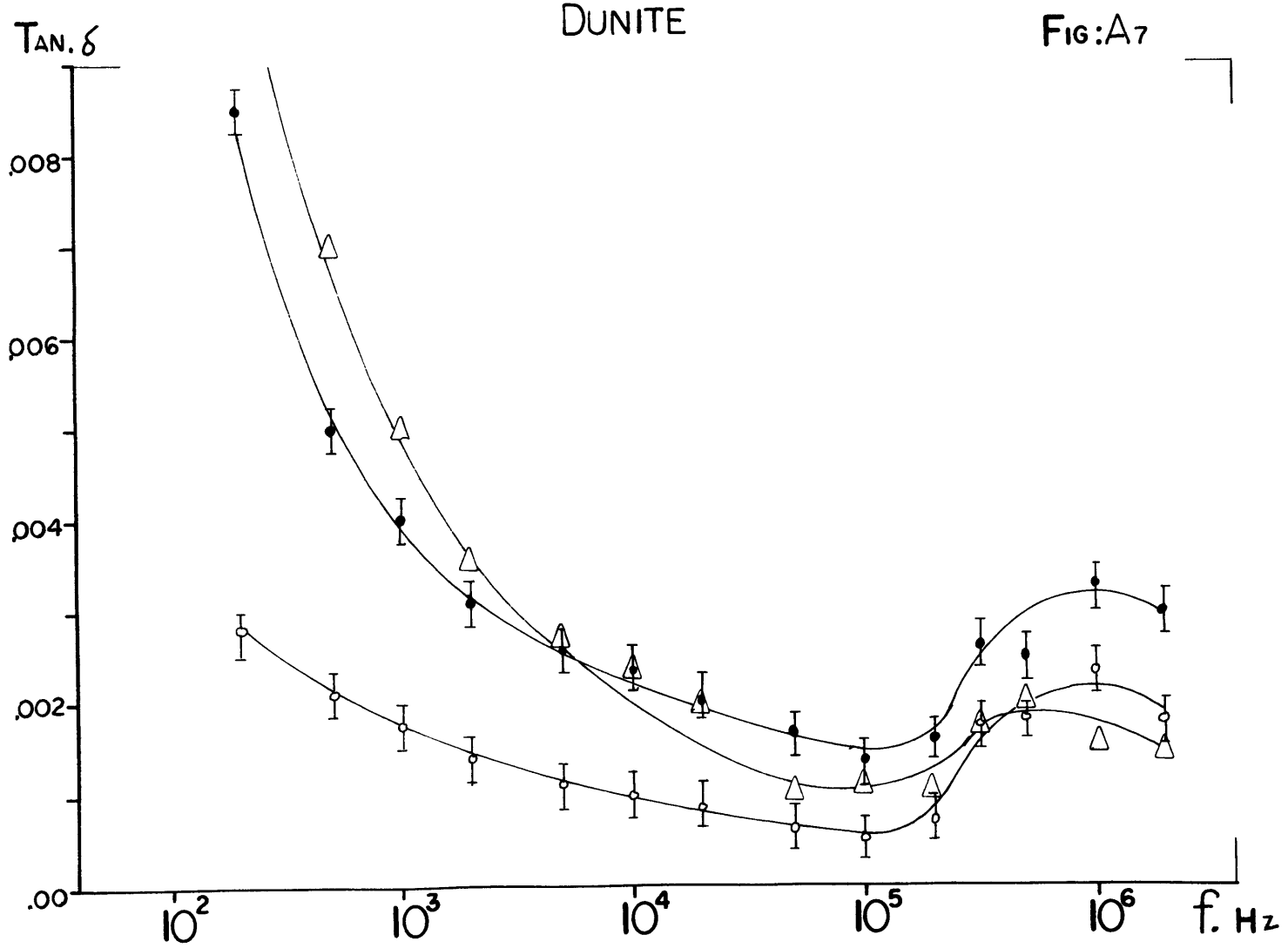
TAN. δ
DUNITE
FIG: A7
.008
.006
.004
.002
.00
10^2
10^3
10^4
10^5
10^6
f. Hz

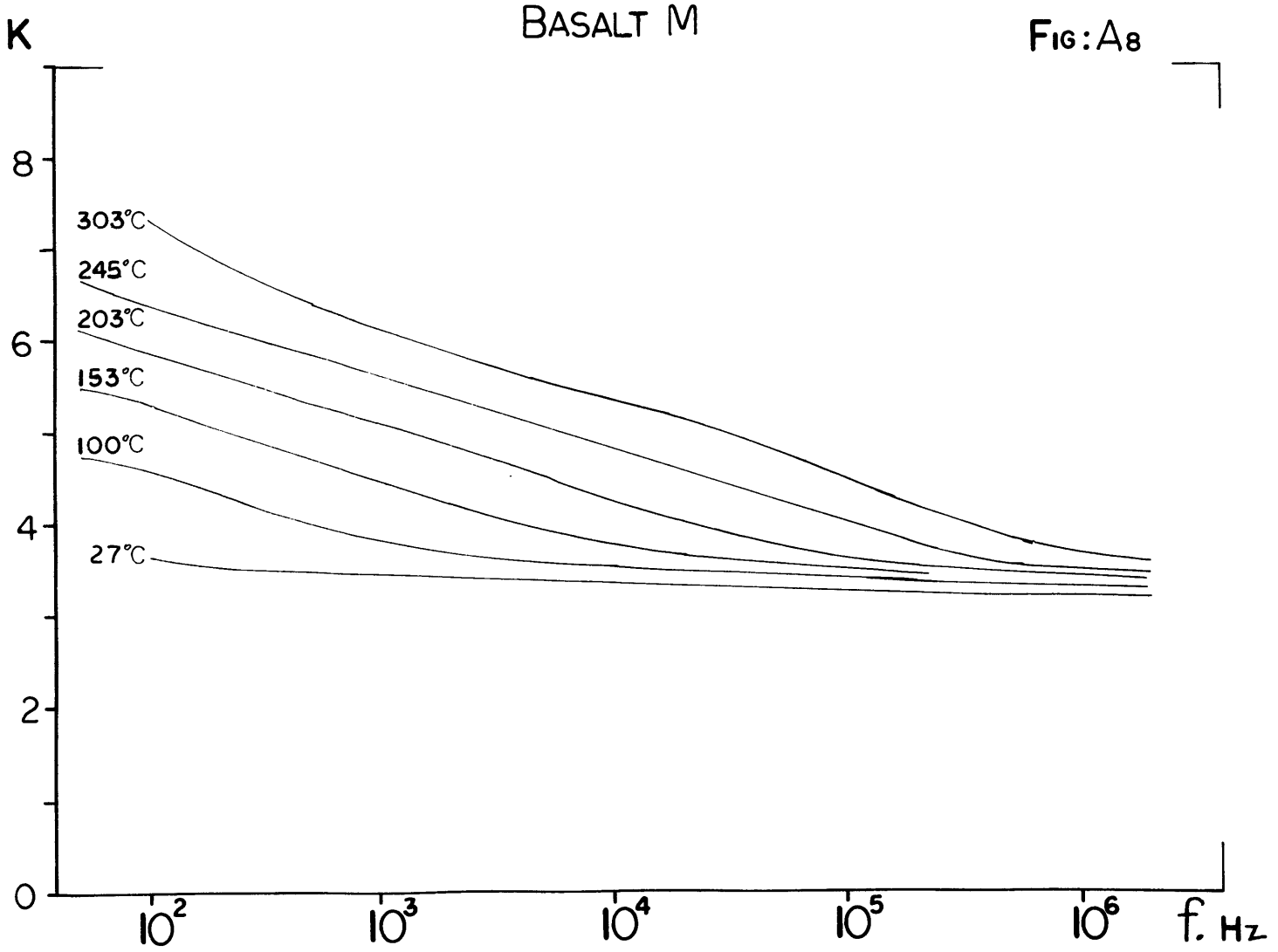
BASALT M
FIG: A8
K
8
6
4
2
0
303°C
245°C
203°C
153°C
100°C
27°C
10^2
10^3
10^4
10^5
10^6
f. Hz

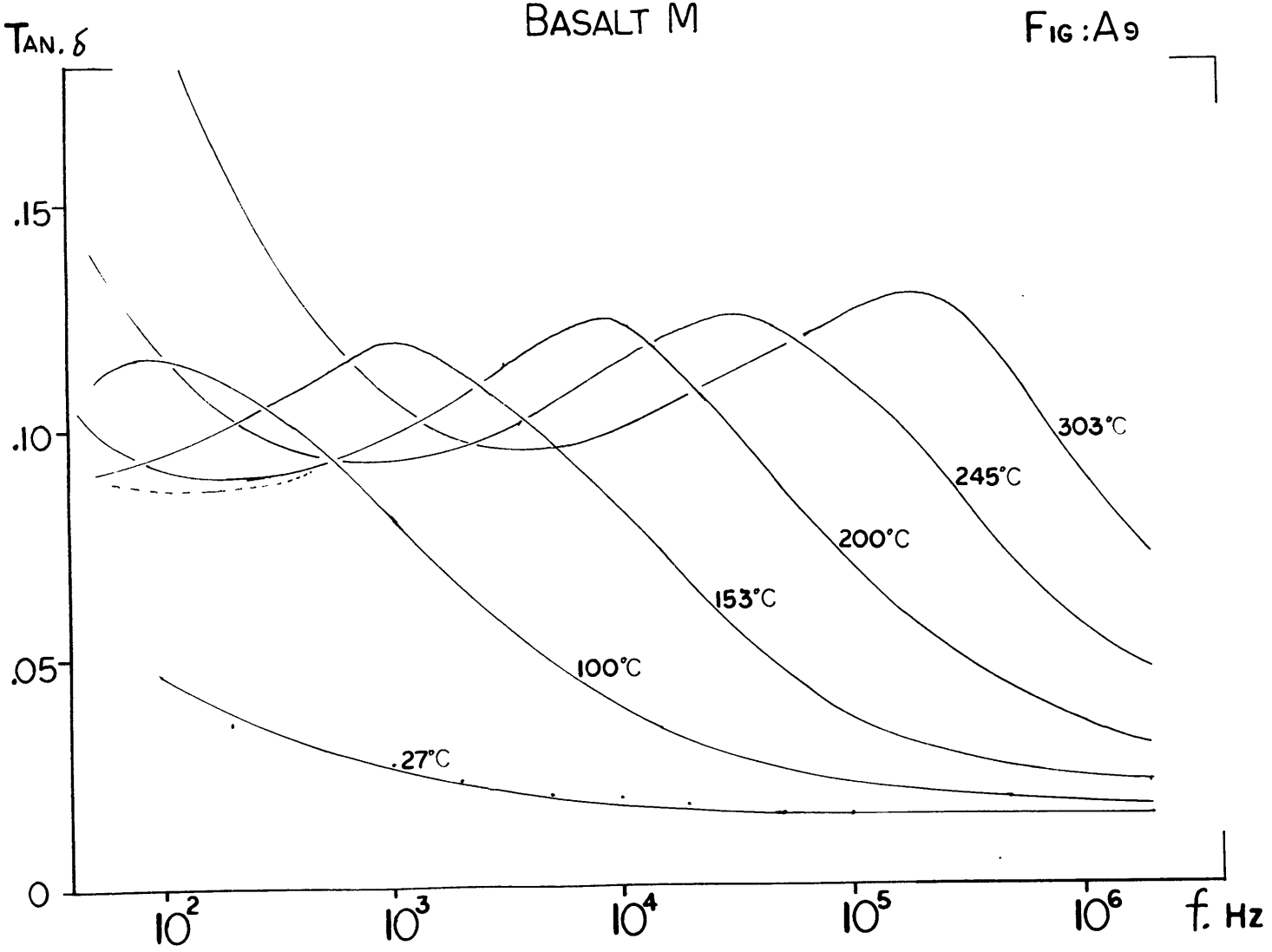
BASALT M
FIG : A9
TAN. δ
.15
.10
.05
0
303°C
245°C
200°C
153°C
100°C
27°C
10^2
10^3
10^4
10^5
10^6
f. Hz

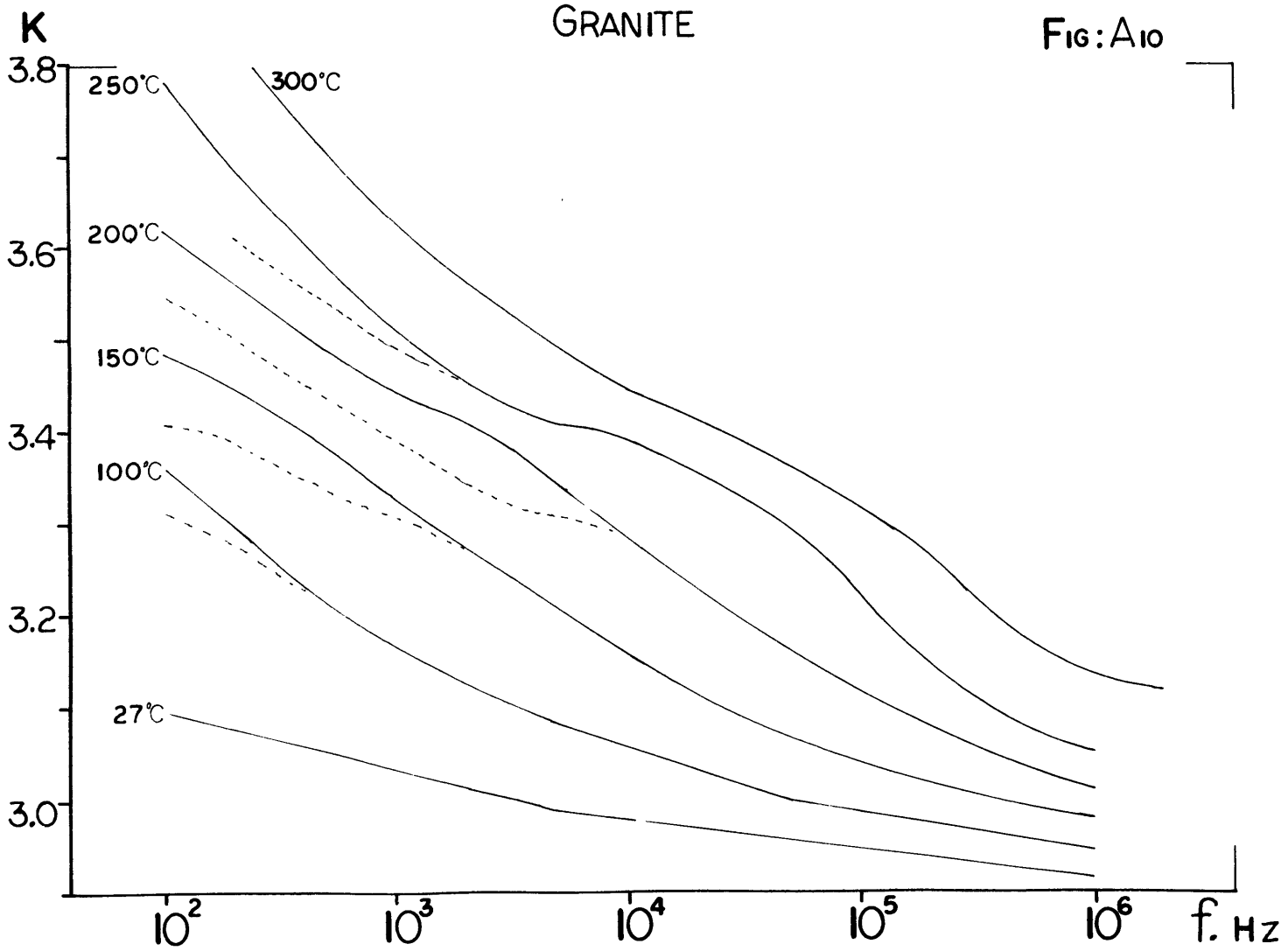
K
GRANITE
FIG: A10
3.8
3.6
3.4
3.2
3.0
250°C
300°C
200°C
150°C
100°C
27°C
10^2
10^3
10^4
10^5
10^6
f. Hz

GRANITE

FIG: A11

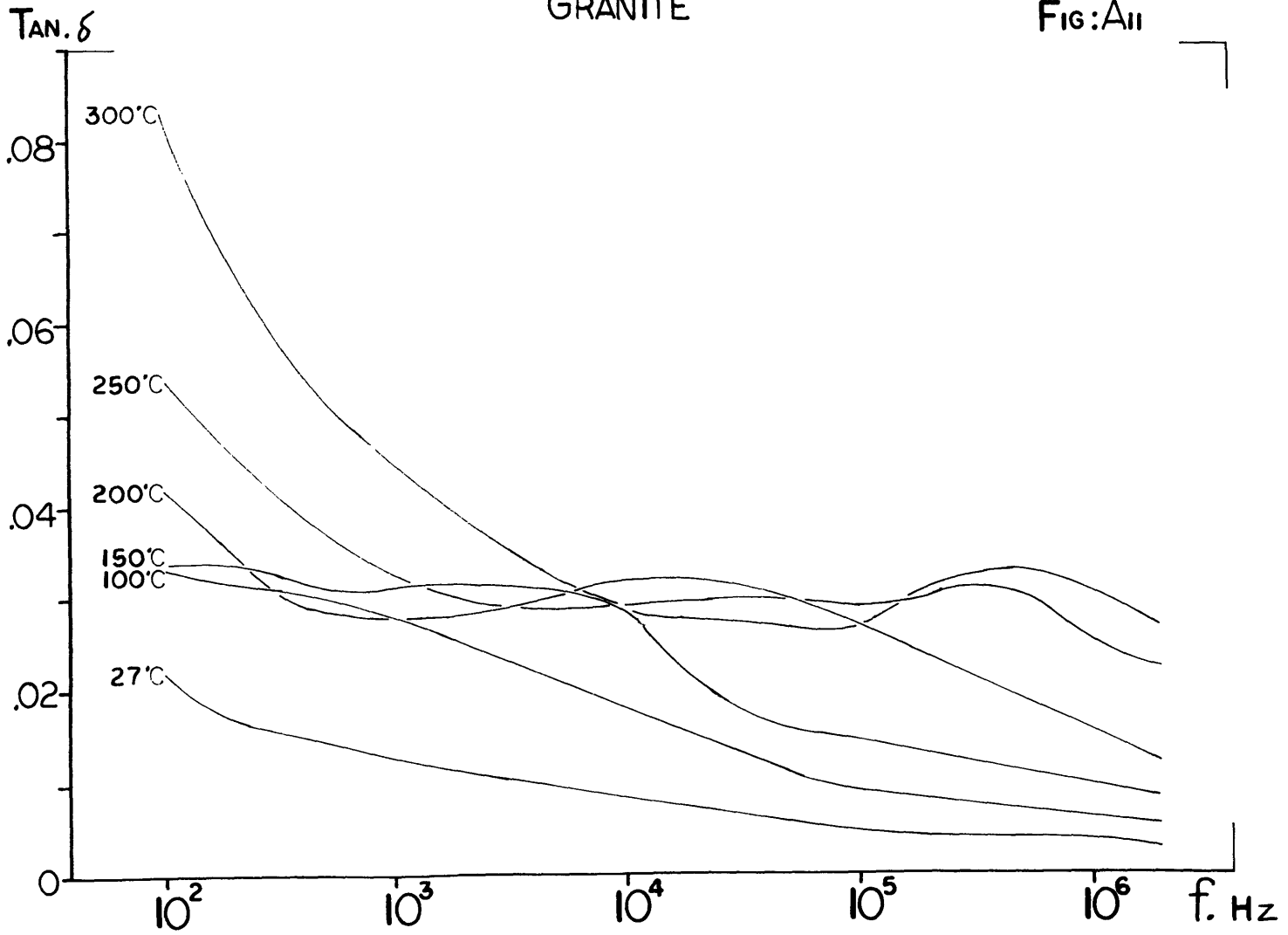

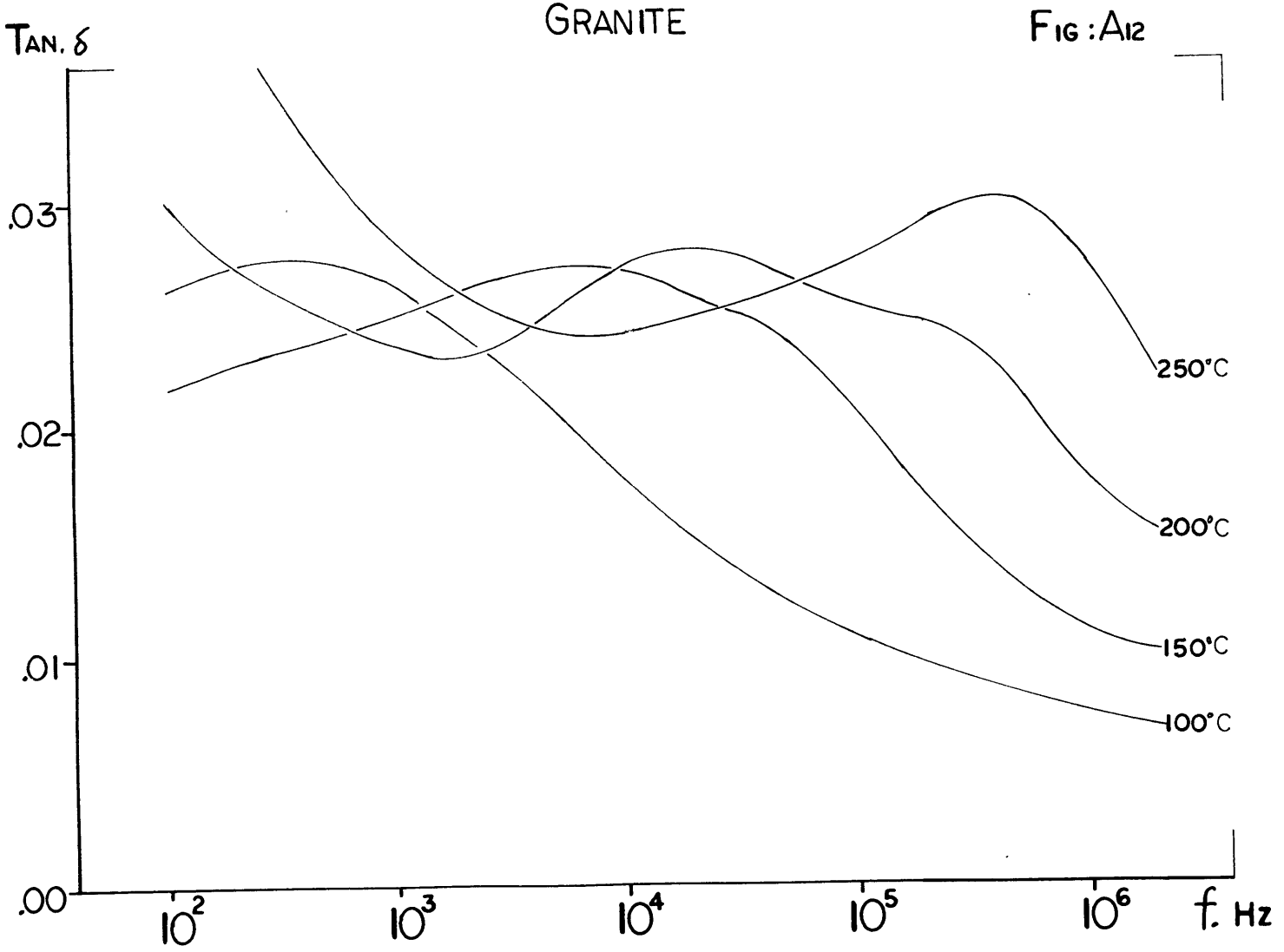
GRANITE
FIG : A12
TAN. δ
.03
.02
.01
.00
250°C
200°C
150°C
100°C
10^2
10^3
10^4
10^5
10^6
f. Hz

AUGITE

FIG : A13

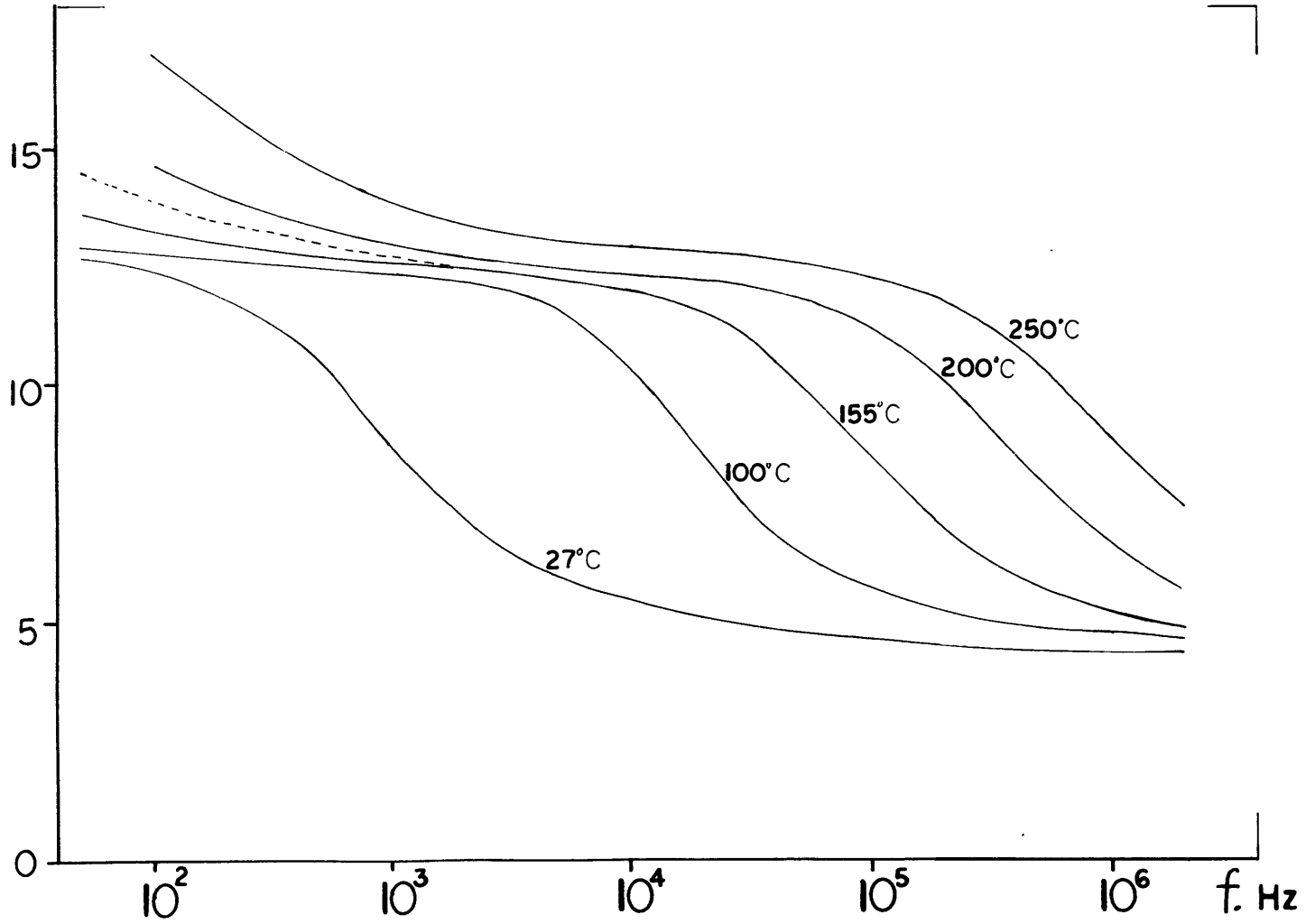

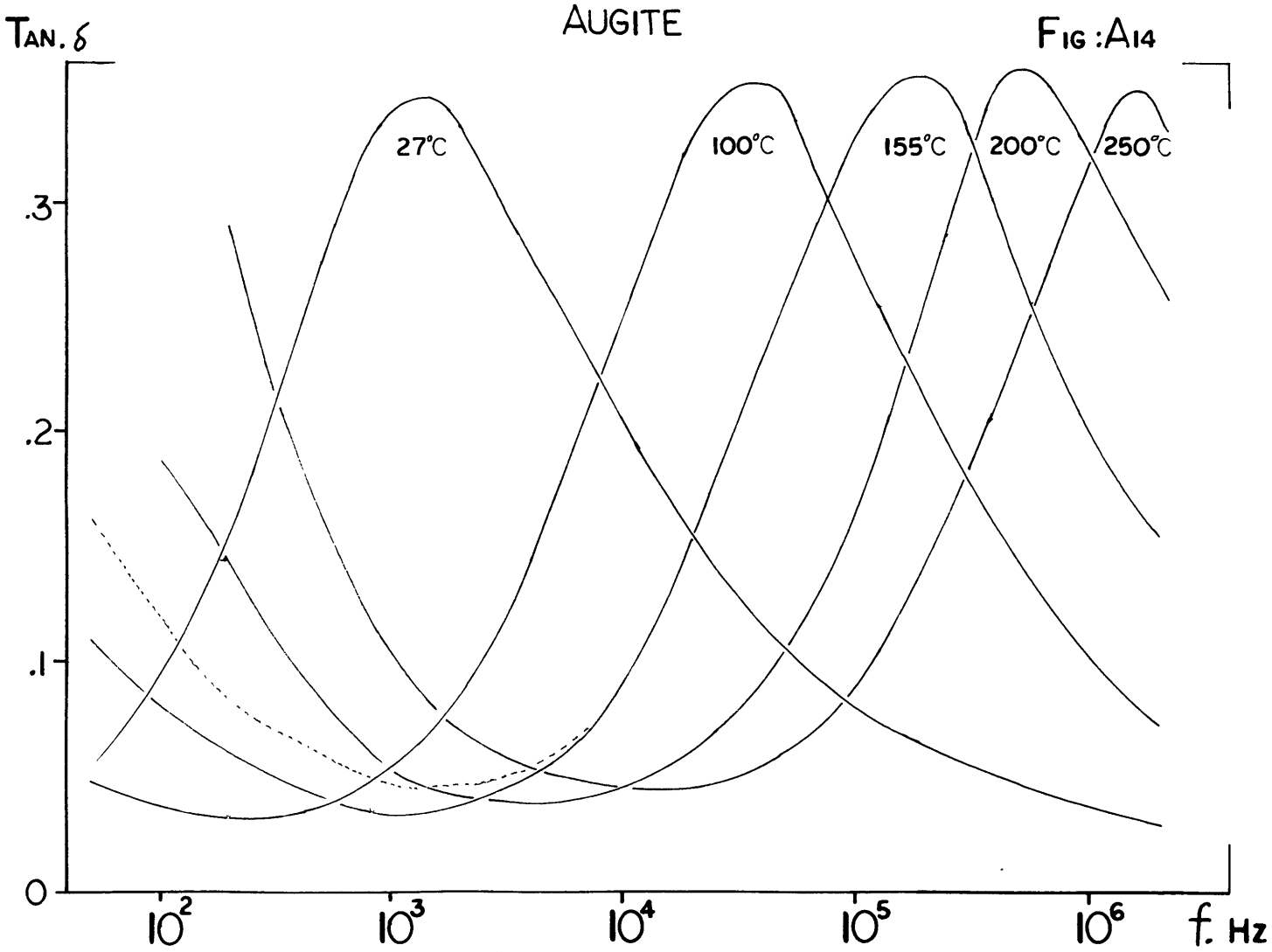
TAN. δ
AUGITE
FIG : A14
27°C
100°C
155°C
200°C
250°C
.3
.2
.1
0
10²
10³
10⁴
10⁵
10⁶
f. Hz

MIXTURE TEST

FIG: A15

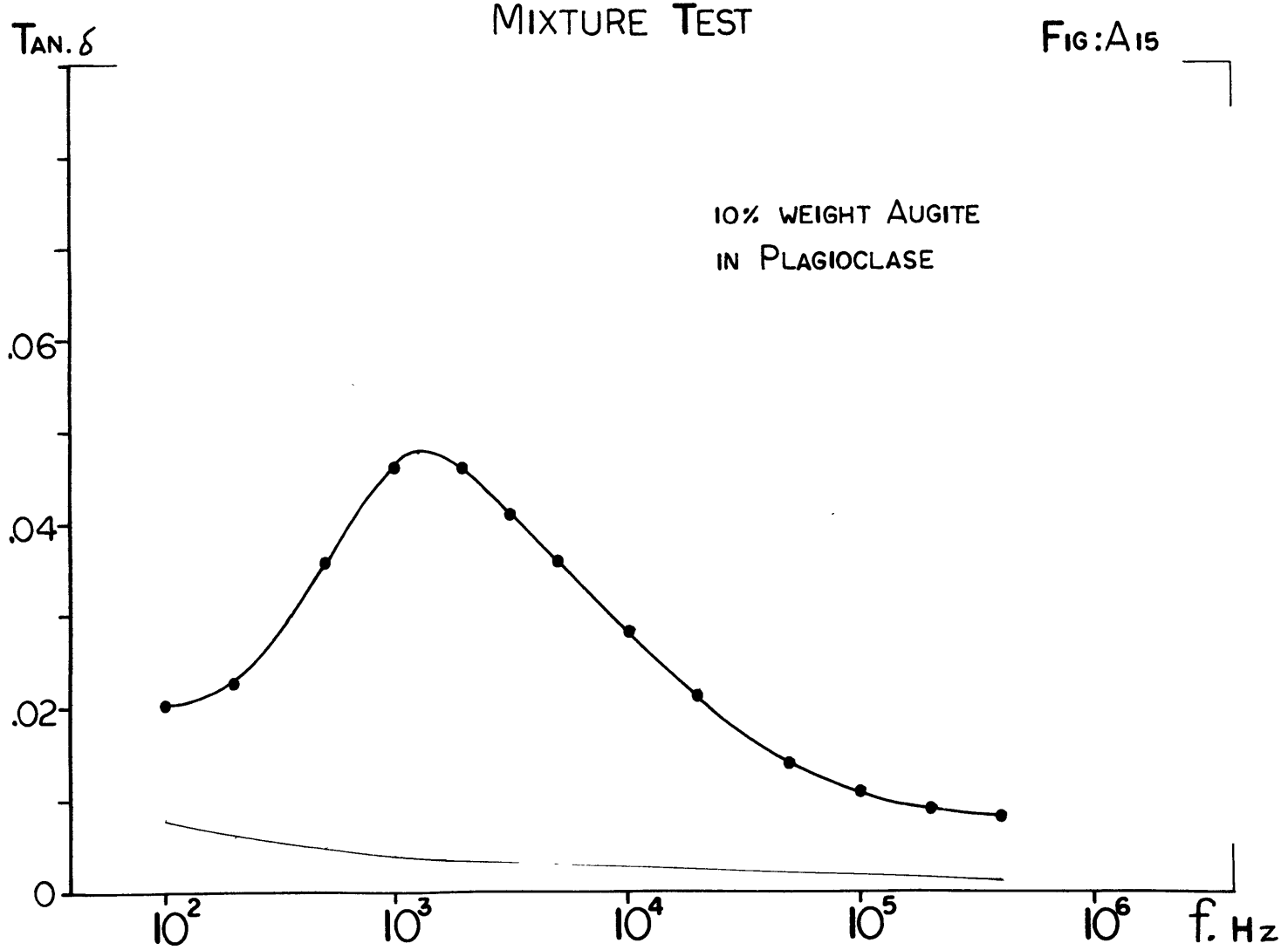

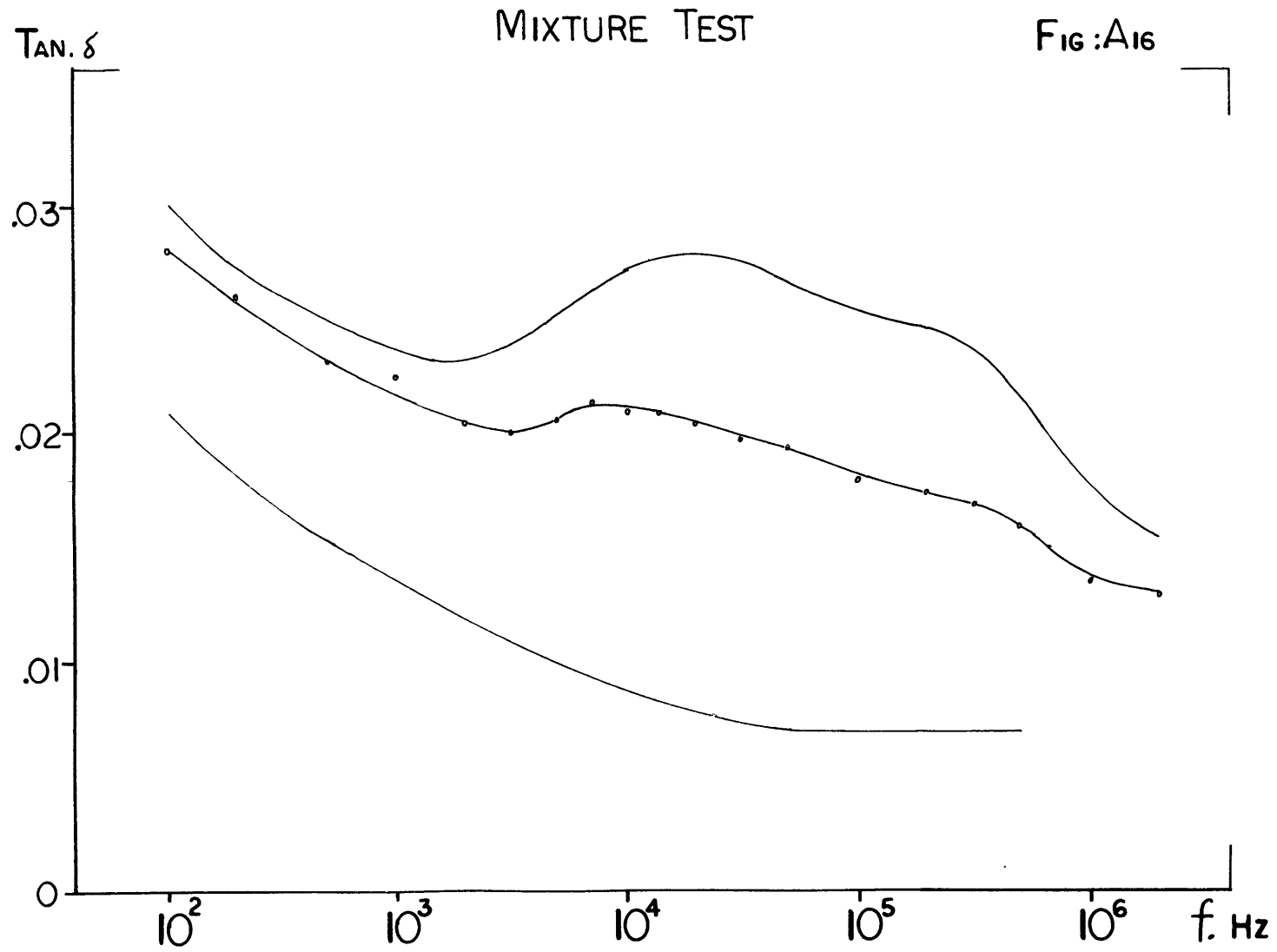
MIXTURE TEST
FIG : A16
TAN. δ
.03
.02
.01
0
10^2
10^3
10^4
10^5
10^6
f. Hz

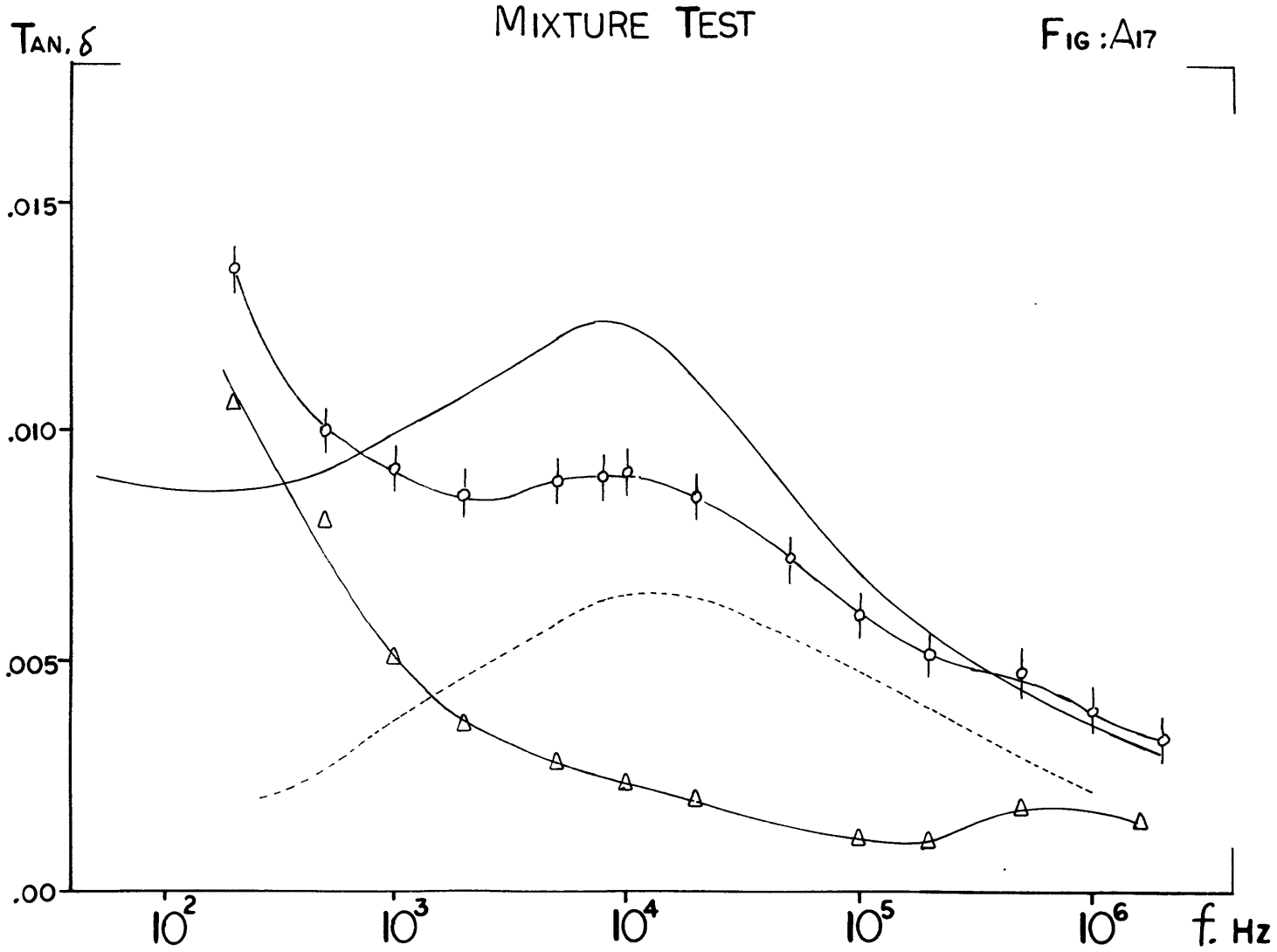
MIXTURE TEST
FIG : A17
TAN. δ
.015
.010
.005
.00
10^2
10^3
10^4
10^5
10^6
f. Hz

DIABASE P

FIG:A18

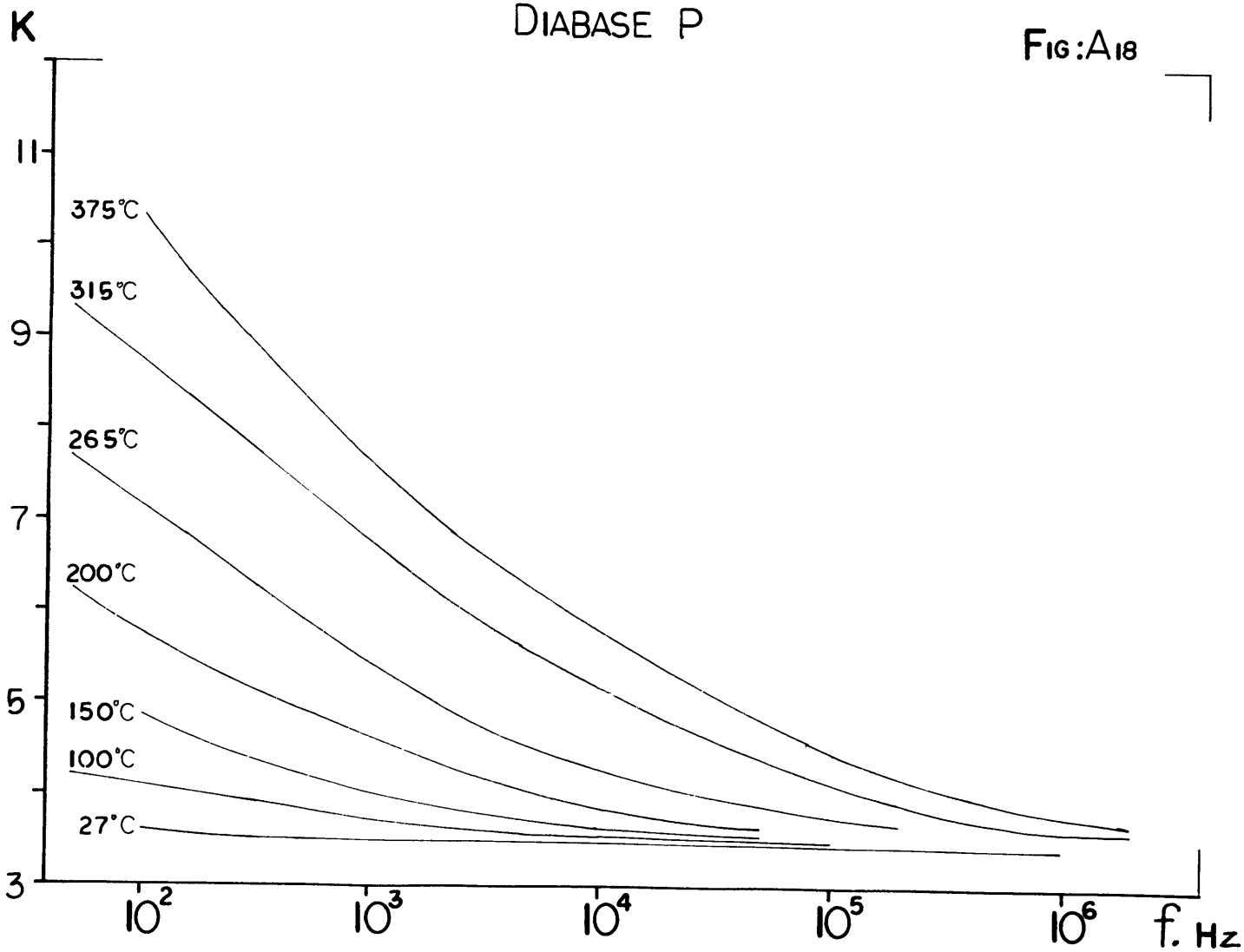

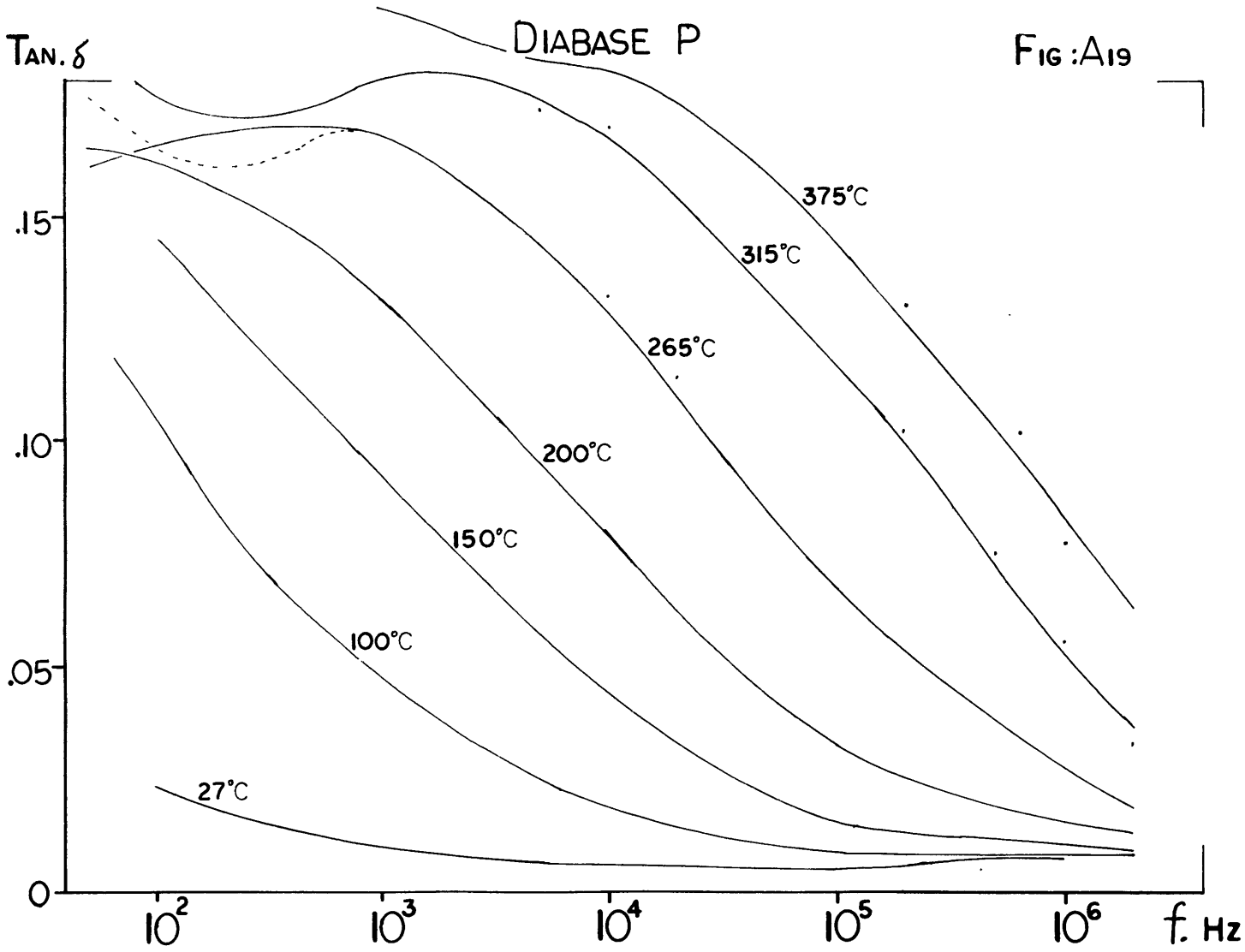
DIABASE P
TAN. δ
.15
.10
.05
0
375°C
315°C
265°C
200°C
150°C
100°C
27°C
10^2
10^3
10^4
10^5
10^6
f. Hz

FIG: A19

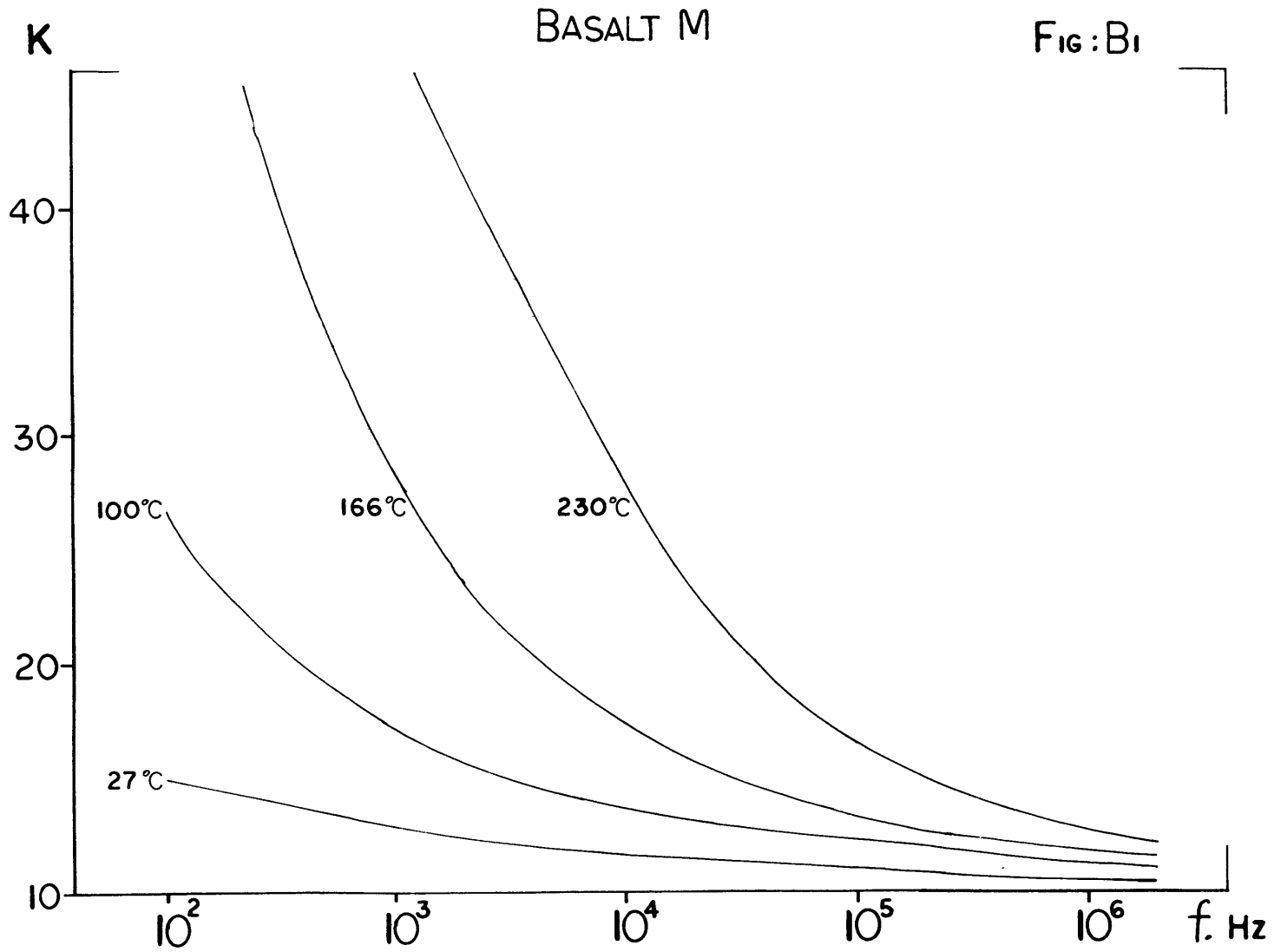
BASALT M
FIG : B1
K
40
30
20
10
100°C
166°C
230°C
27°C
10^2
10^3
10^4
10^5
10^6
f. Hz

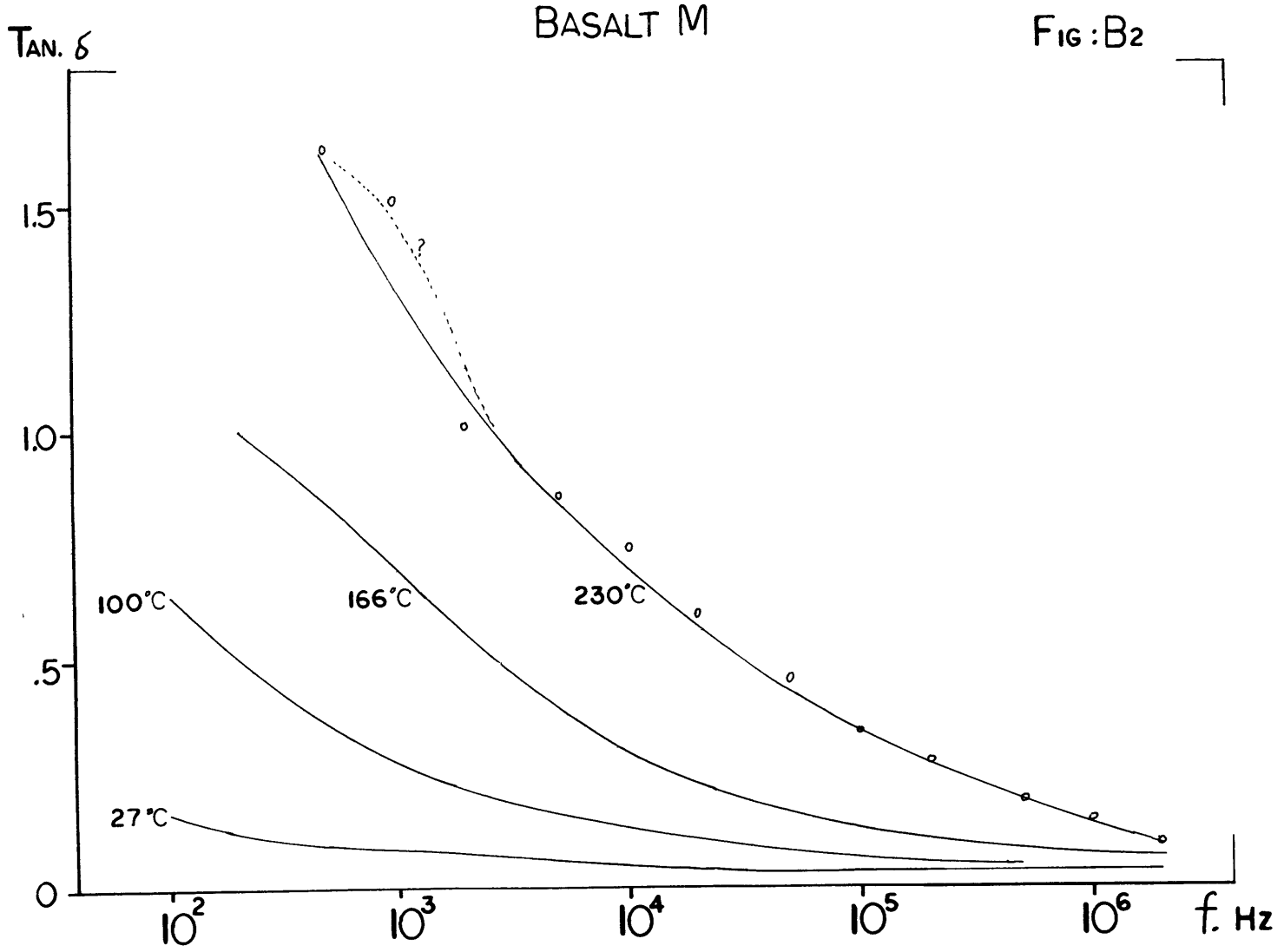
BASALT M
FIG : B2
TAN. δ
1.5
1.0
.5
0
100°C
166°C
230°C
27°C
10^2
10^3
10^4
10^5
10^6
f. Hz

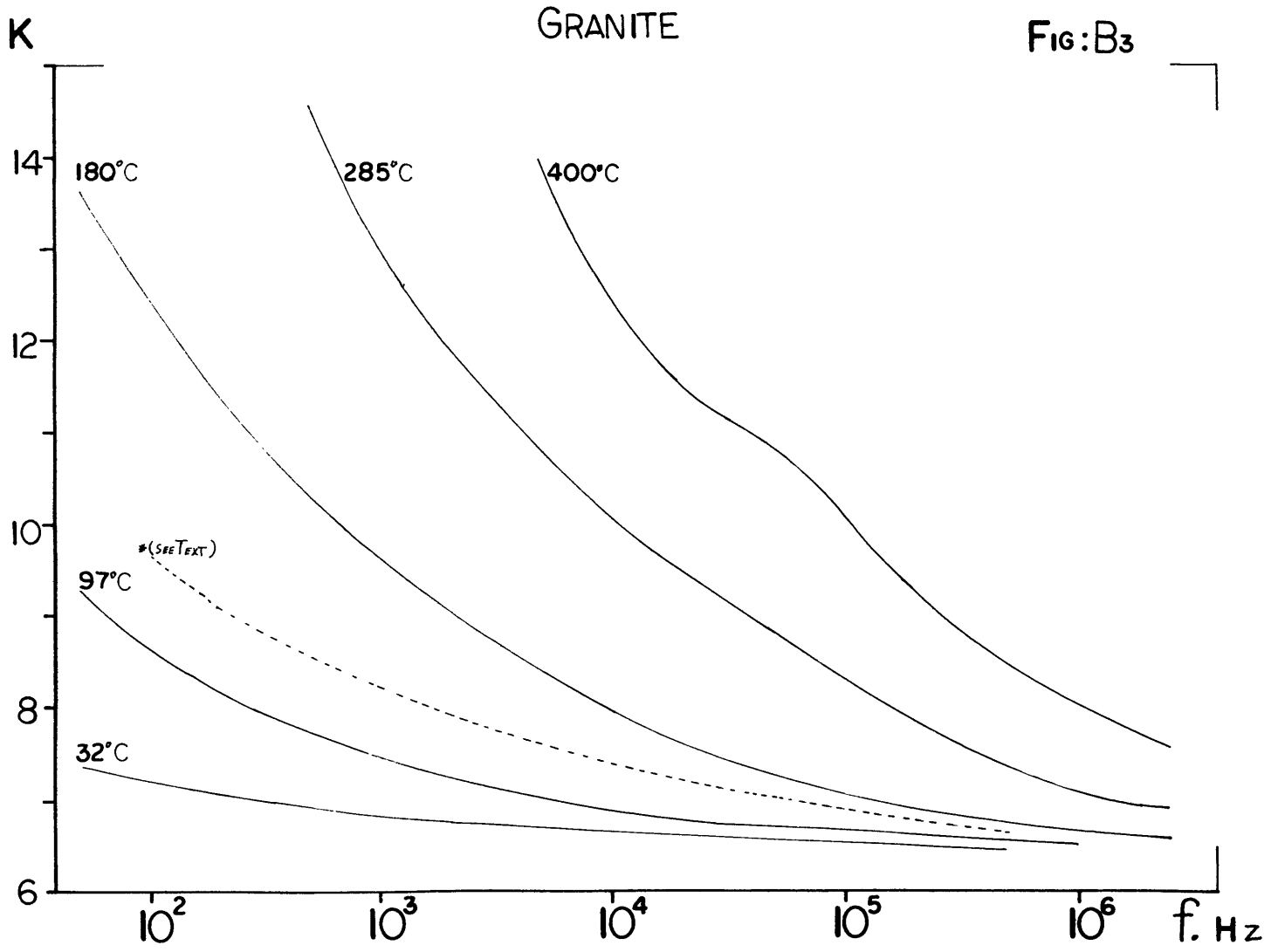
K
GRANITE
FIG: B3
14
12
10
8
6
180°C
285°C
400°C
*(SEE TEXT)
97°C
32°C
10^2
10^3
10^4
10^5
10^6
f. Hz

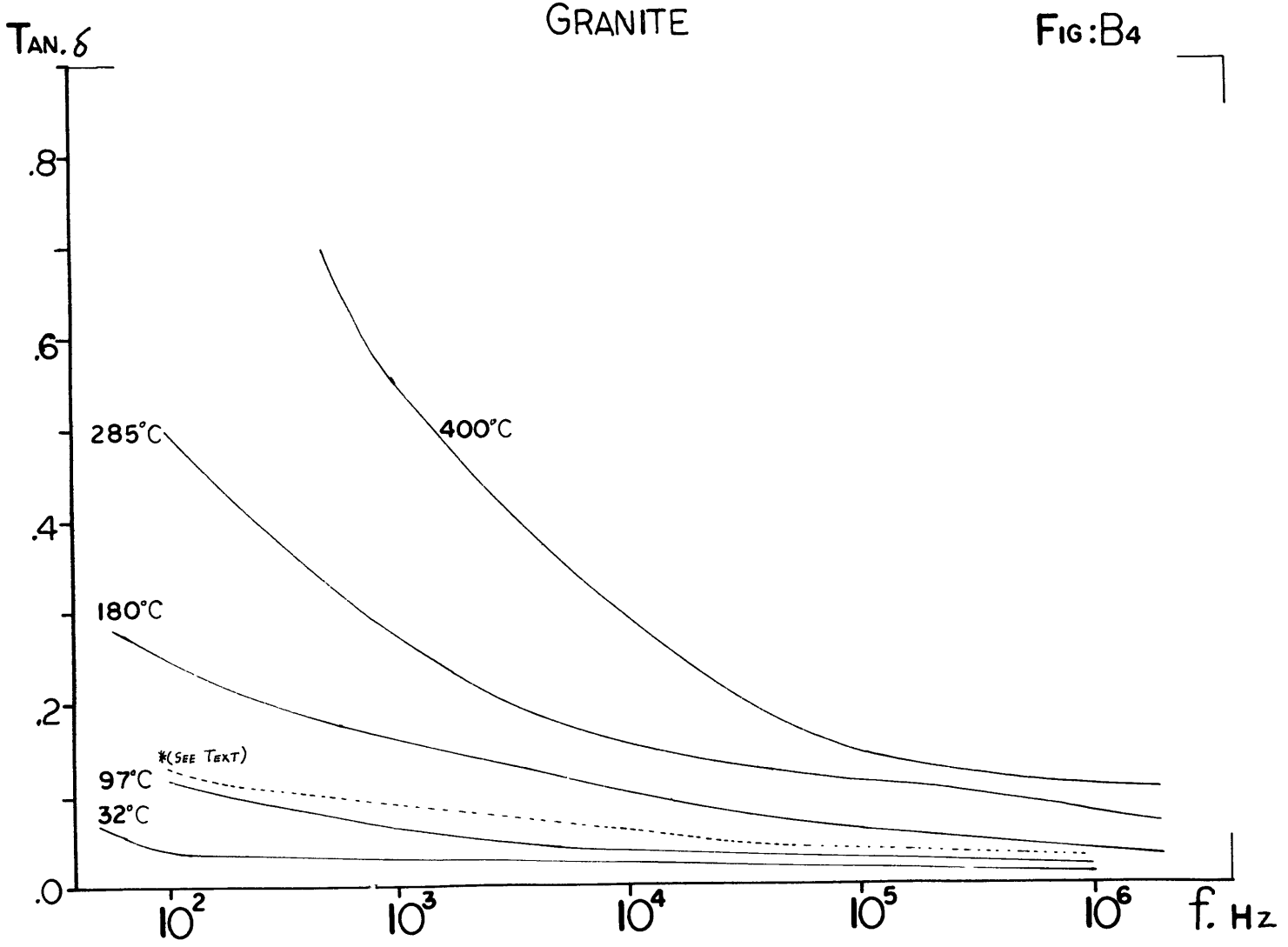
GRANITE
FIG: B4
TAN. δ
.8
.6
.4
.2
.0
285°C
400°C
180°C
*(SEE TEXT)
97°C
32°C
10²
10³
10⁴
10⁵
10⁶
f. Hz

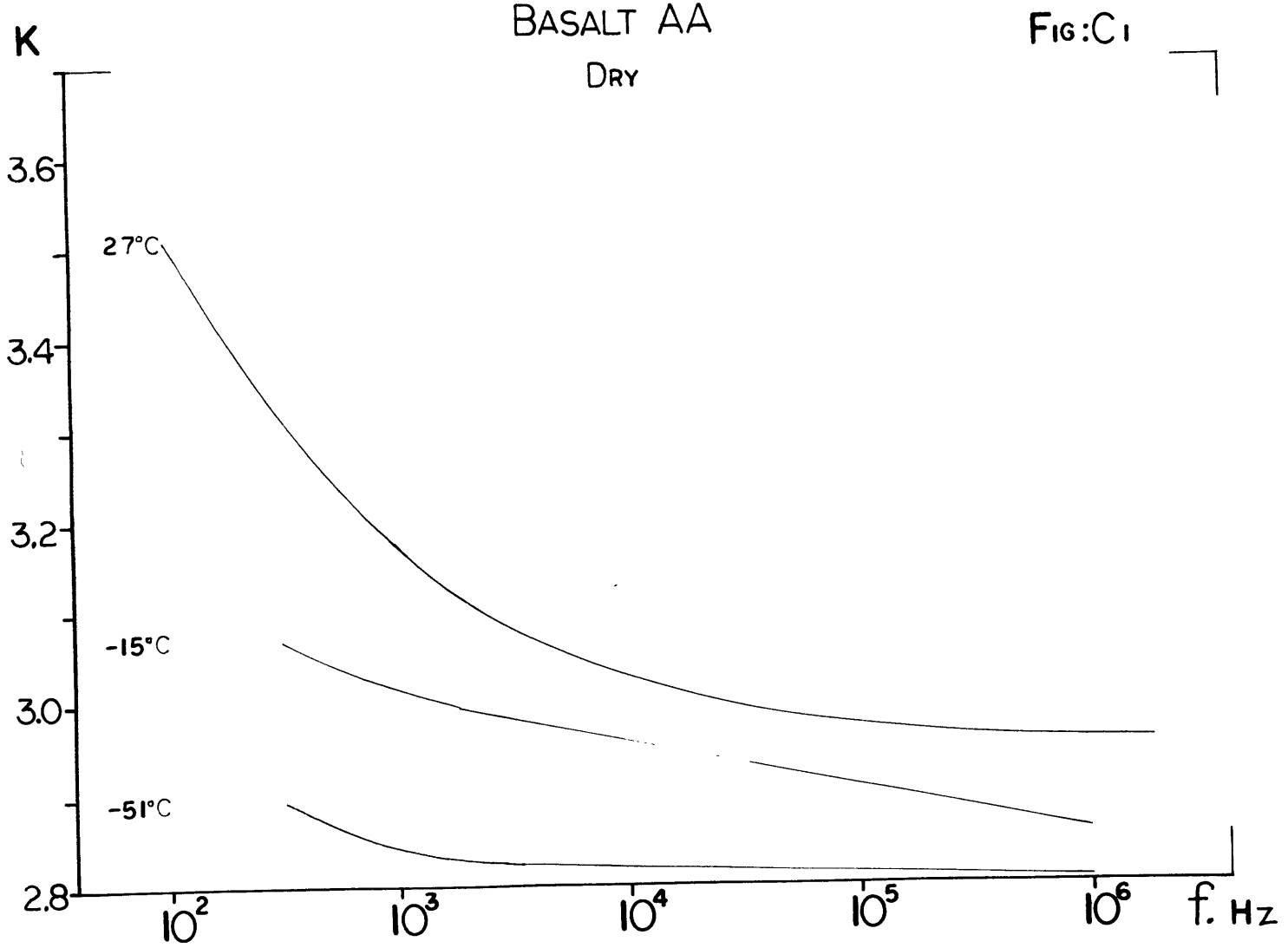
BASALT AA
DRY
FIG:C1
K
3.6
3.4
3.2
3.0
2.8
27°C
-15°C
-51°C
10^2
10^3
10^4
10^5
10^6
f. Hz

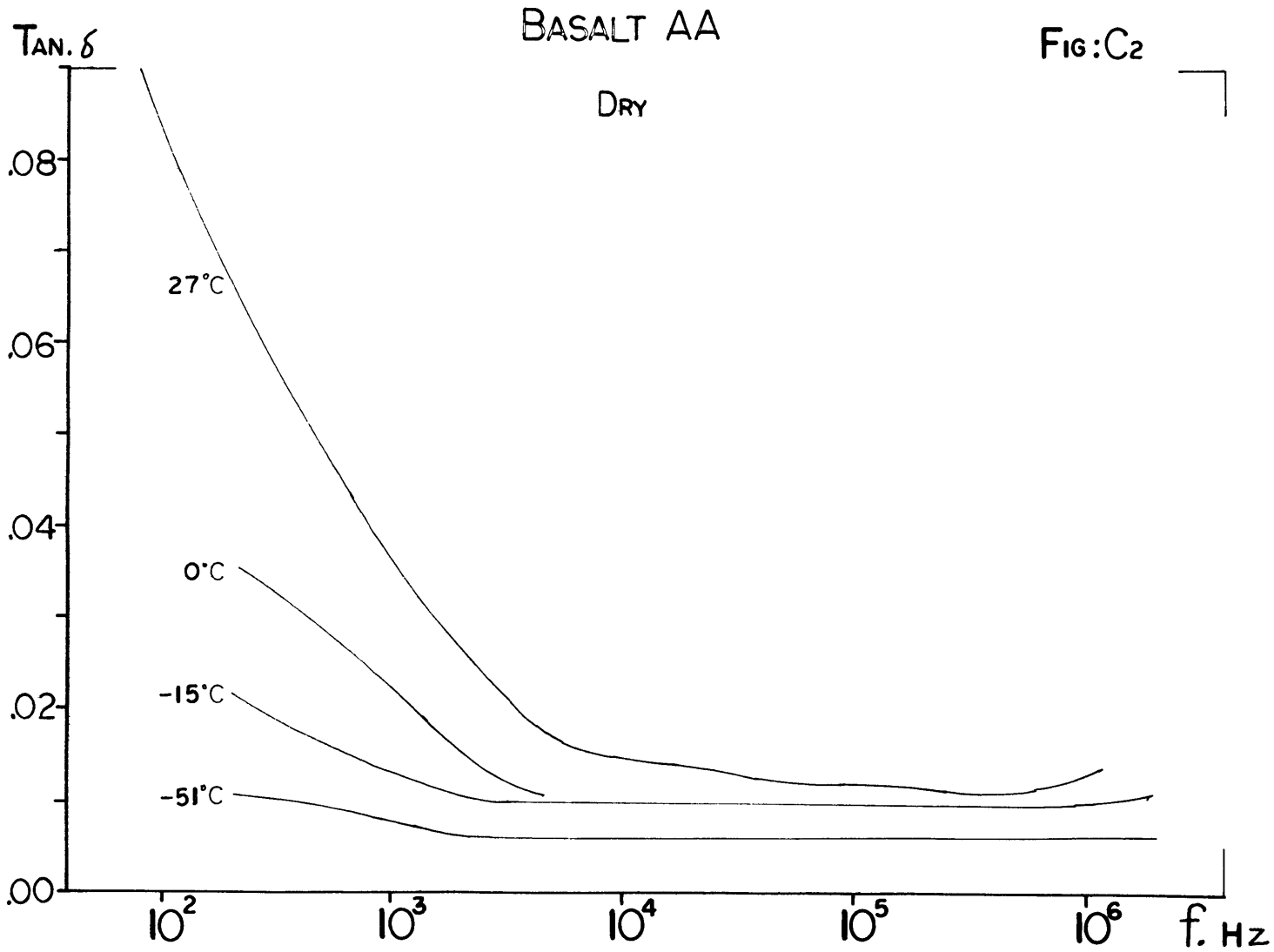
BASALT AA
DRY
FIG: C2
TAN. δ
.08
.06
.04
.02
.00
27°C
0°C
-15°C
-51°C
10^2
10^3
10^4
10^5
10^6
f. Hz

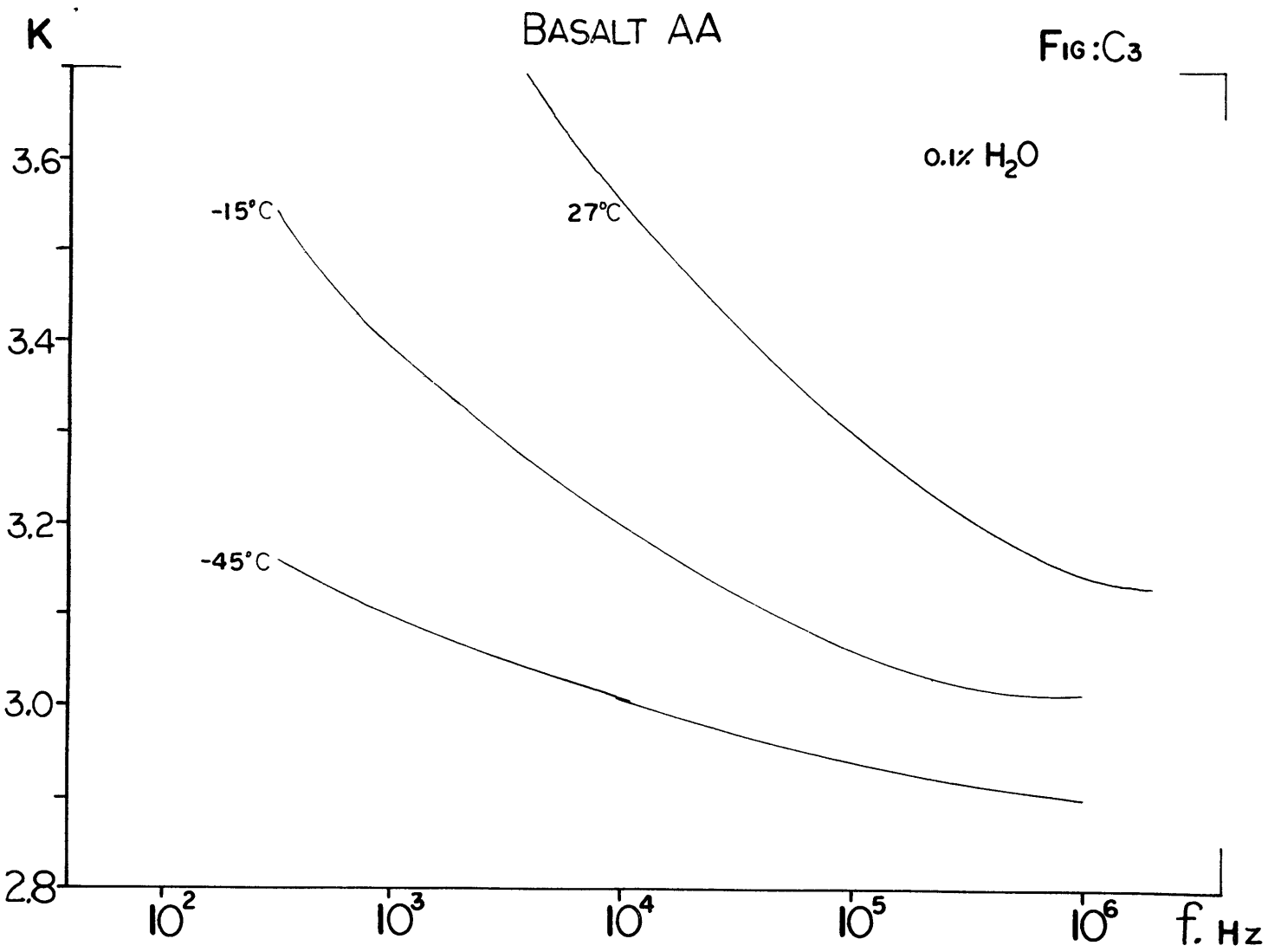
K
BASALT AA
FIG:C3
0.1% H_2O
-15°C
27°C
-45°C
3.6
3.4
3.2
3.0
2.8
10^2
10^3
10^4
10^5
10^6
f. Hz

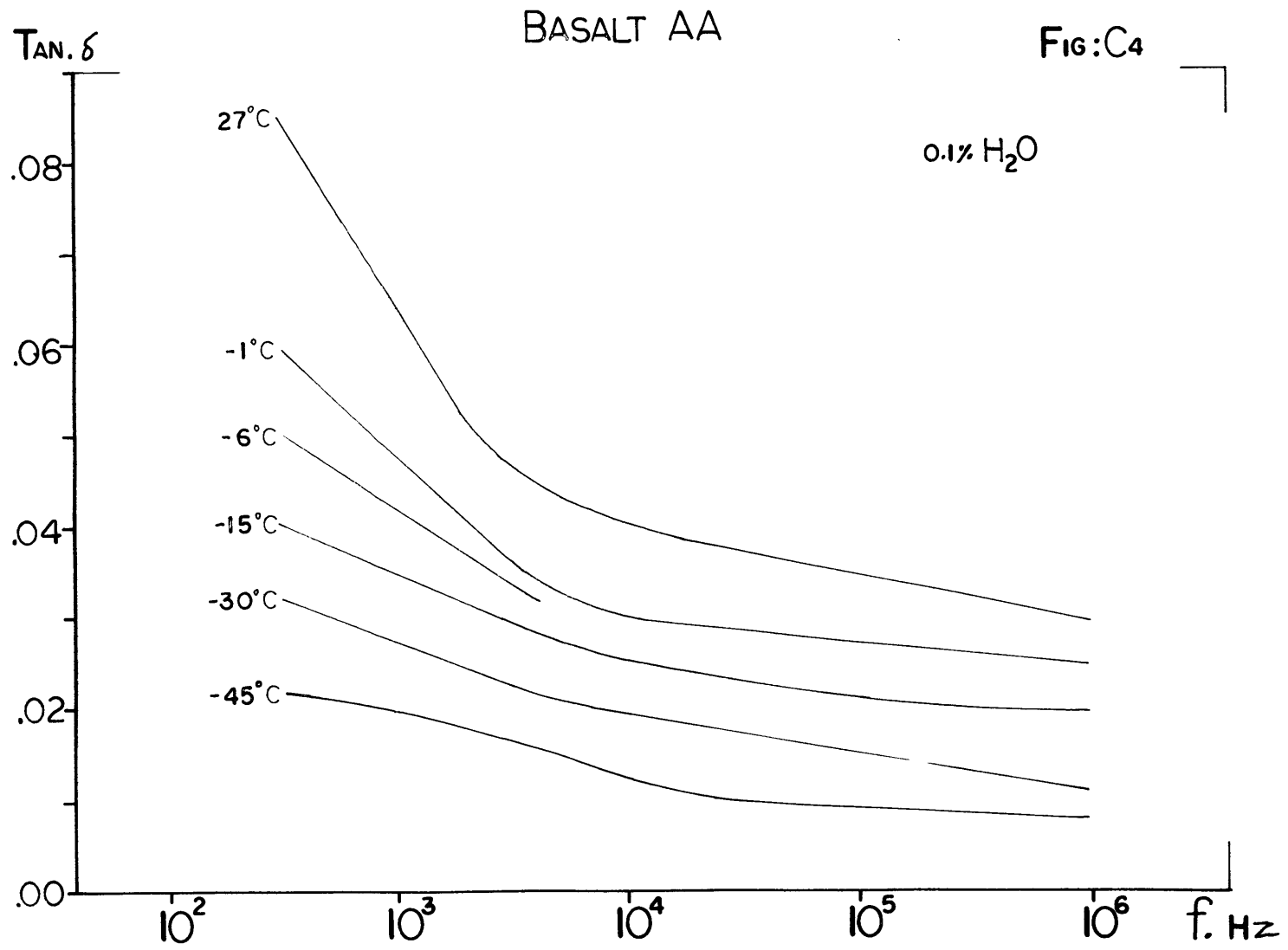
BASALT AA
FIG: C4
TAN. δ
0.1% H_2O
27°C
-1°C
-6°C
-15°C
-30°C
-45°C
.08
.06
.04
.02
.00
10^2
10^3
10^4
10^5
10^6
f. Hz

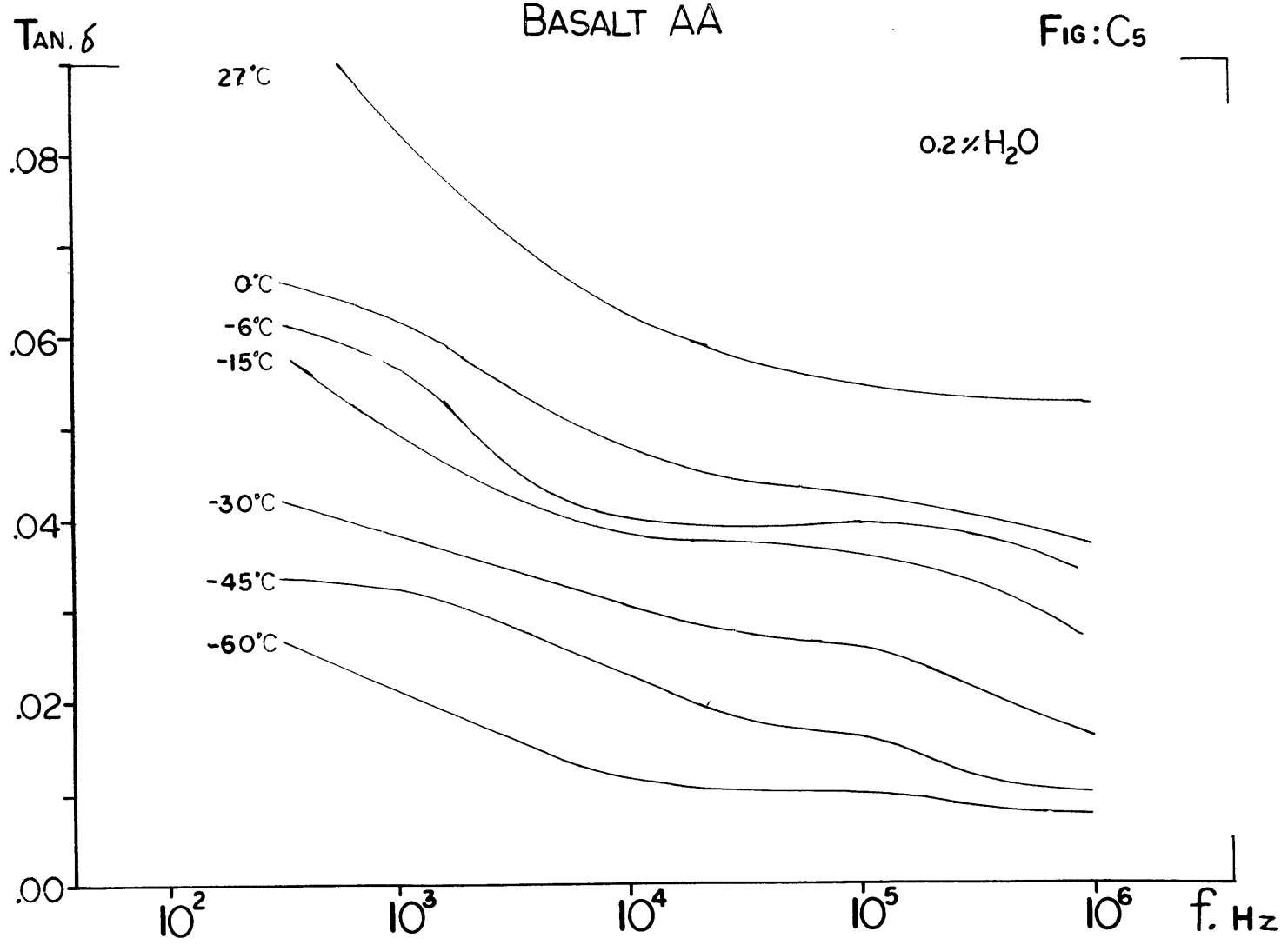
BASALT AA
FIG: C5
TAN. δ
27°C
0.2% H_2O
0°C
-6°C
-15°C
-30°C
-45°C
-60°C
.08
.06
.04
.02
.00
10^2
10^3
10^4
10^5
10^6
f. Hz

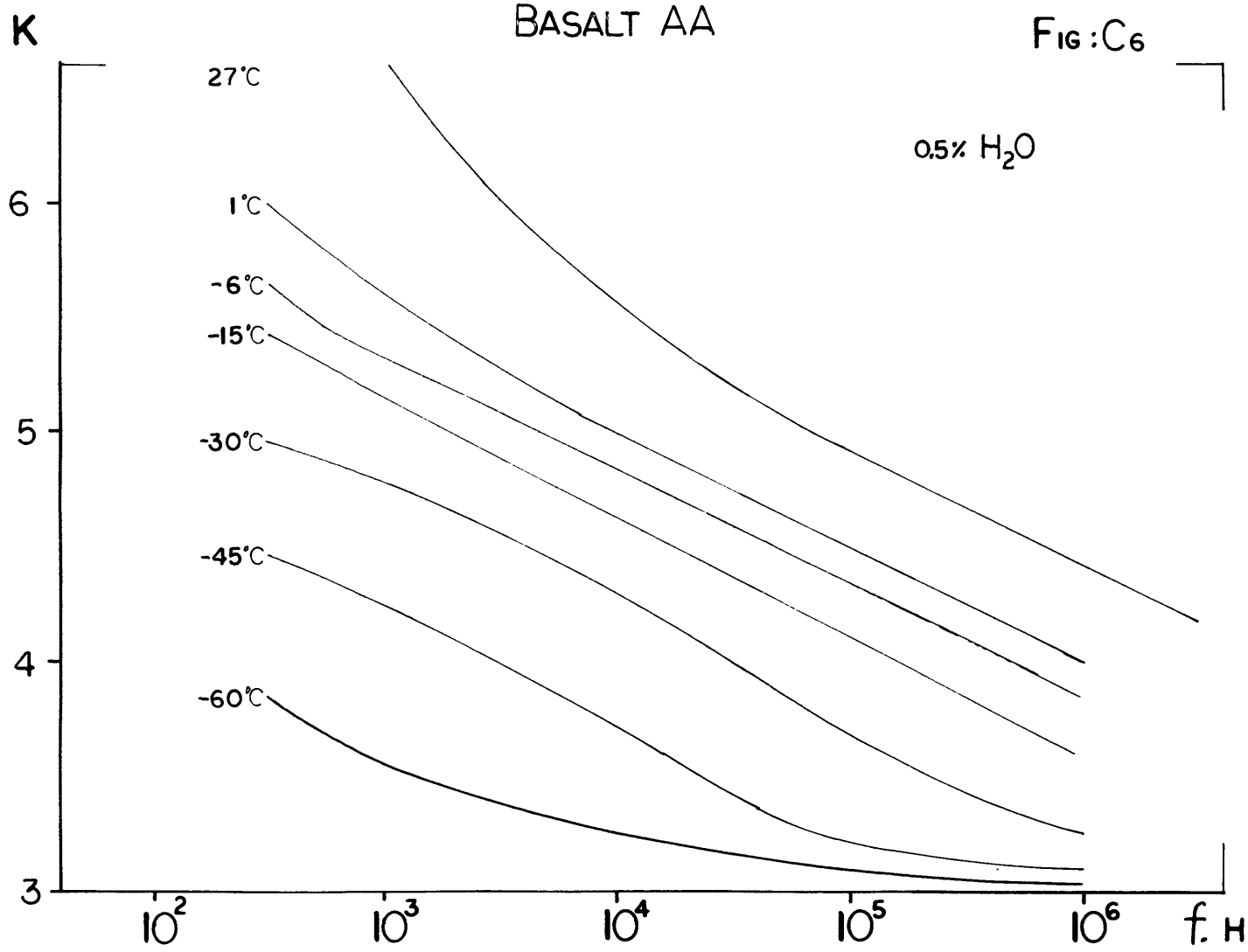
K
BASALT AA
FIG : C6
27°C
0.5% H2O
1°C
-6°C
-15°C
-30°C
-45°C
-60°C
6
5
4
3
10^2
10^3
10^4
10^5
10^6
f. Hz

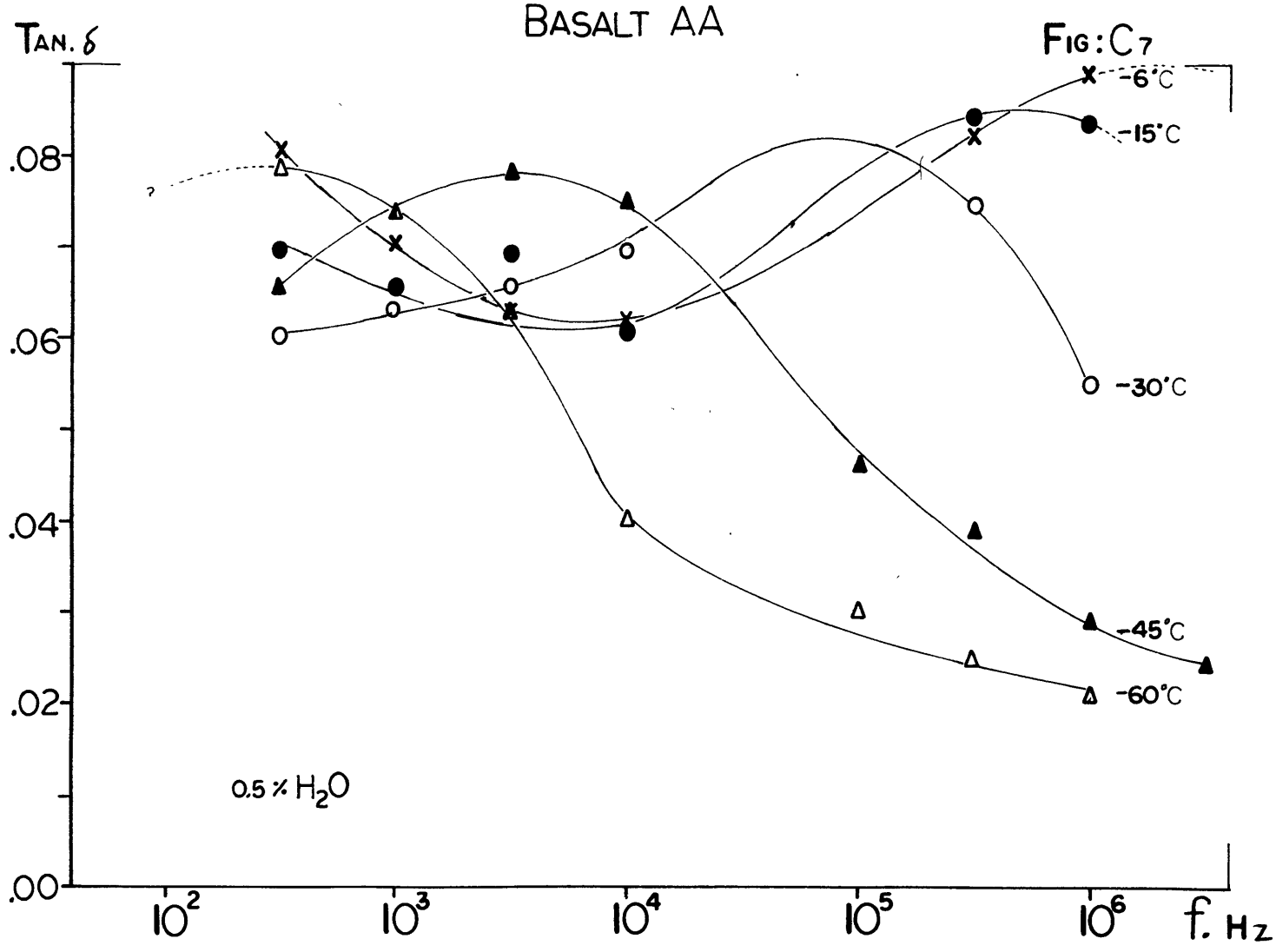
BASALT AA
FIG: C7
TAN. δ
.08
.06
.04
.02
.00
-6°C
-15°C
-30°C
-45°C
-60°C
0.5 % H2O
10^2
10^3
10^4
10^5
10^6
f. Hz

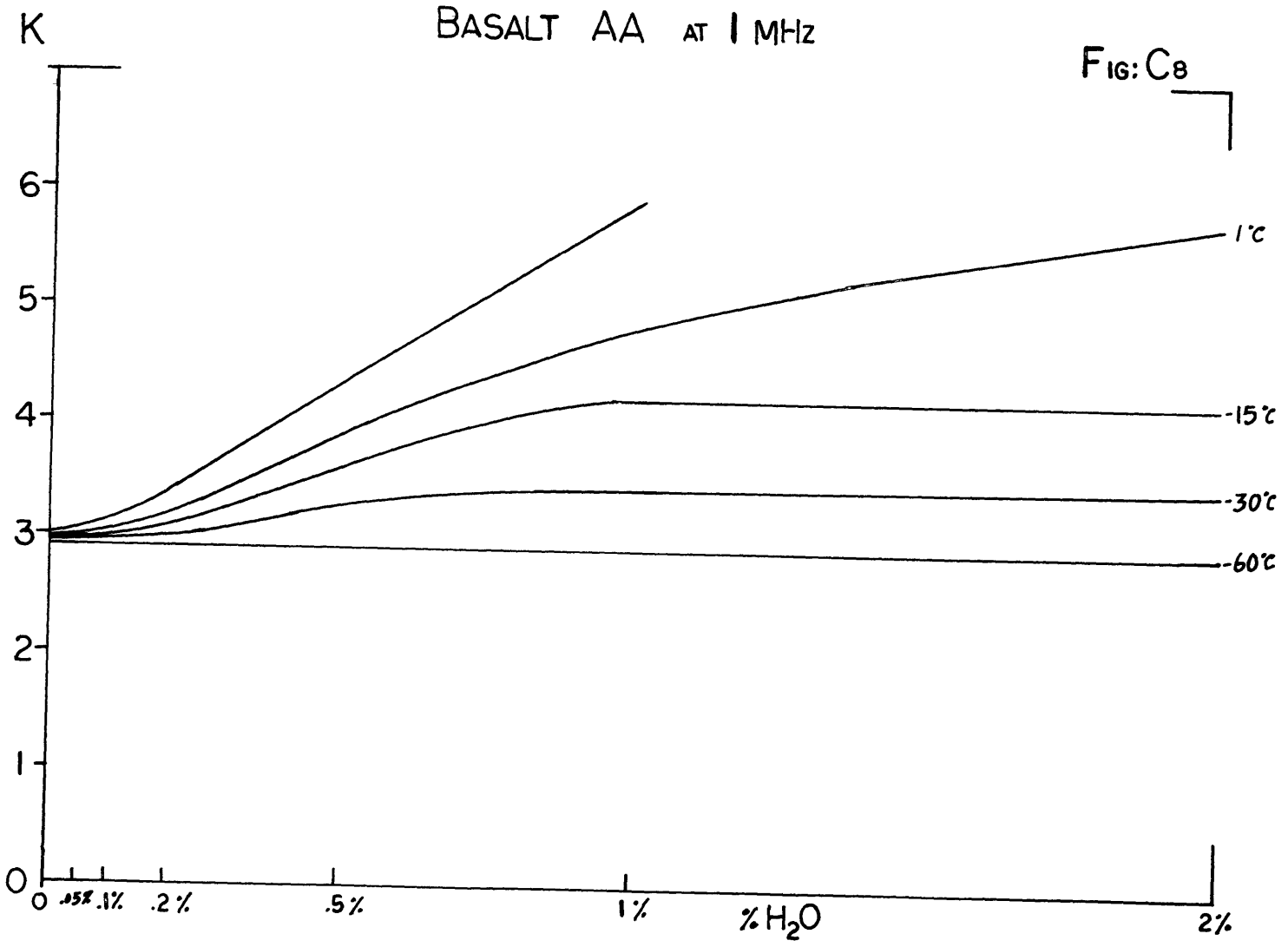
K
BASALT AA AT 1 MHz
FIG: C8
6
5
4
3
2
1
0
1°C
-15°C
-30°C
-60°C
0
.05%
.1%
.2%
.5%
1%
2%
% H_2O

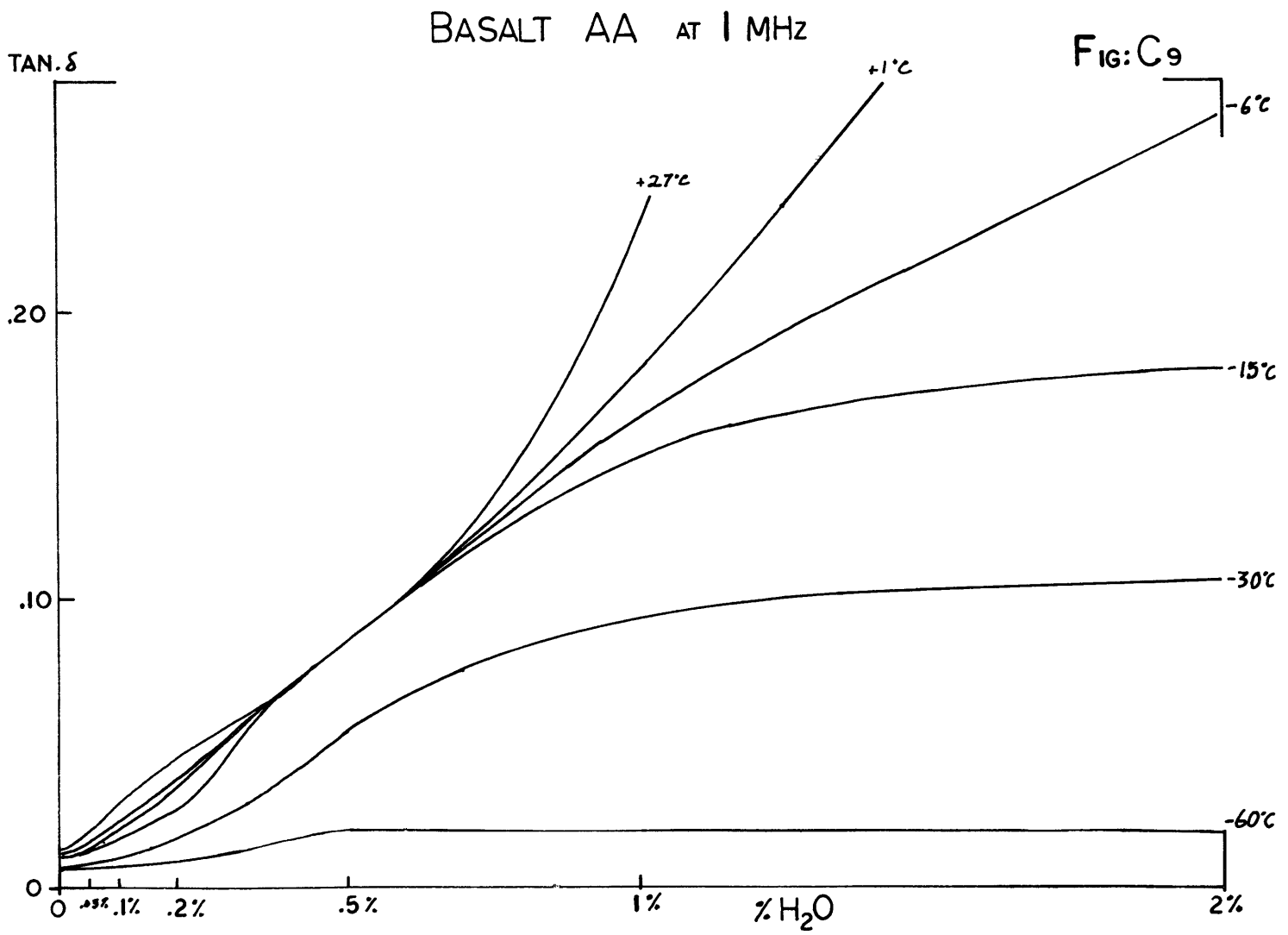
BASALT AA AT 1 MHz
FIG: C9
TAN. δ
.20
.10
0
+1°C
+27°C
-6°C
-15°C
-30°C
-60°C
0
.05%
.1%
.2%
.5%
1%
2%
% H2O

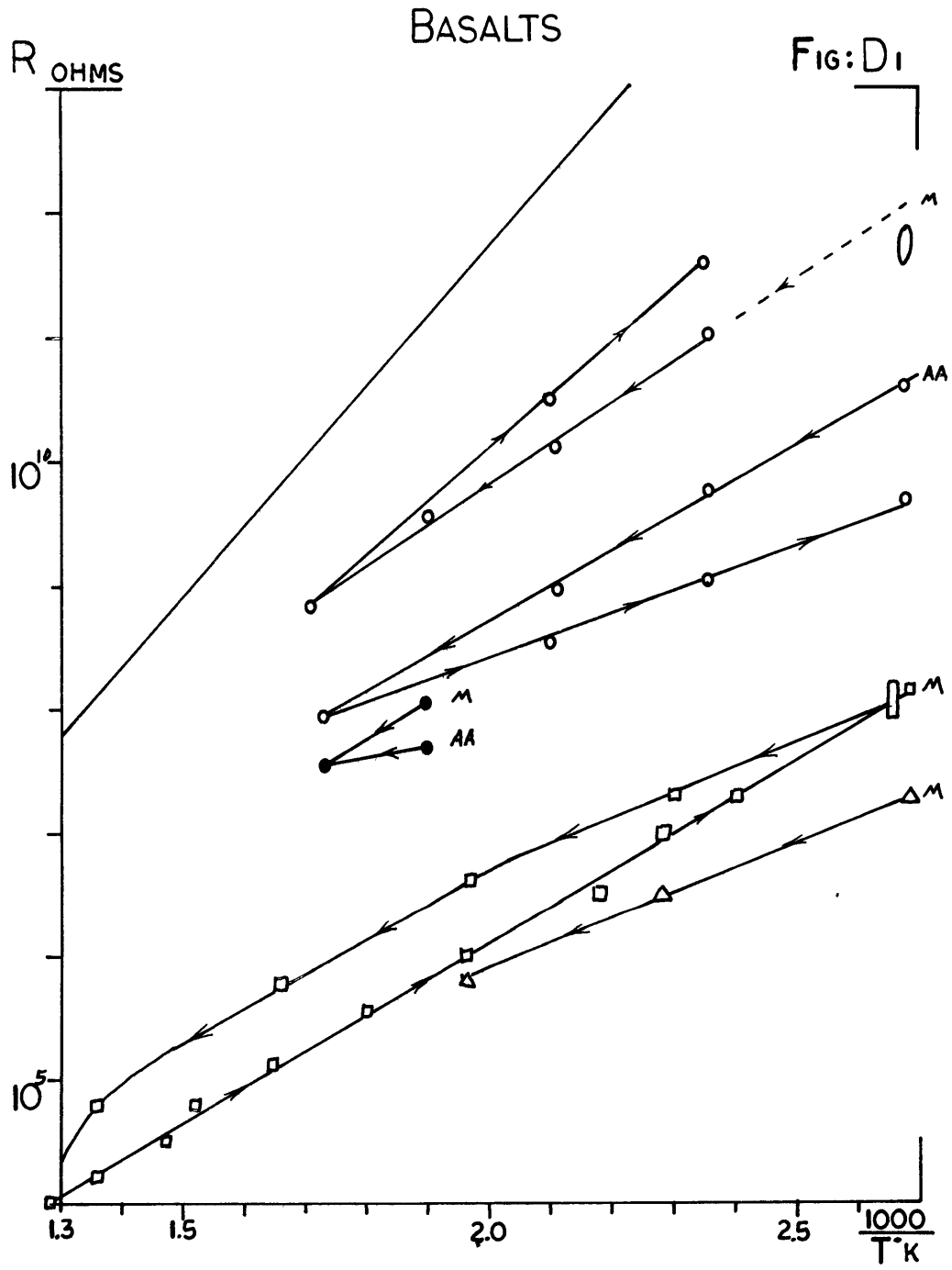
BASALTS
FIG: D1
R OHMS
10^{10}
10^{5}
M
AA
M
AA
M
M
1.3
1.5
2.0
2.5
1000
T°K

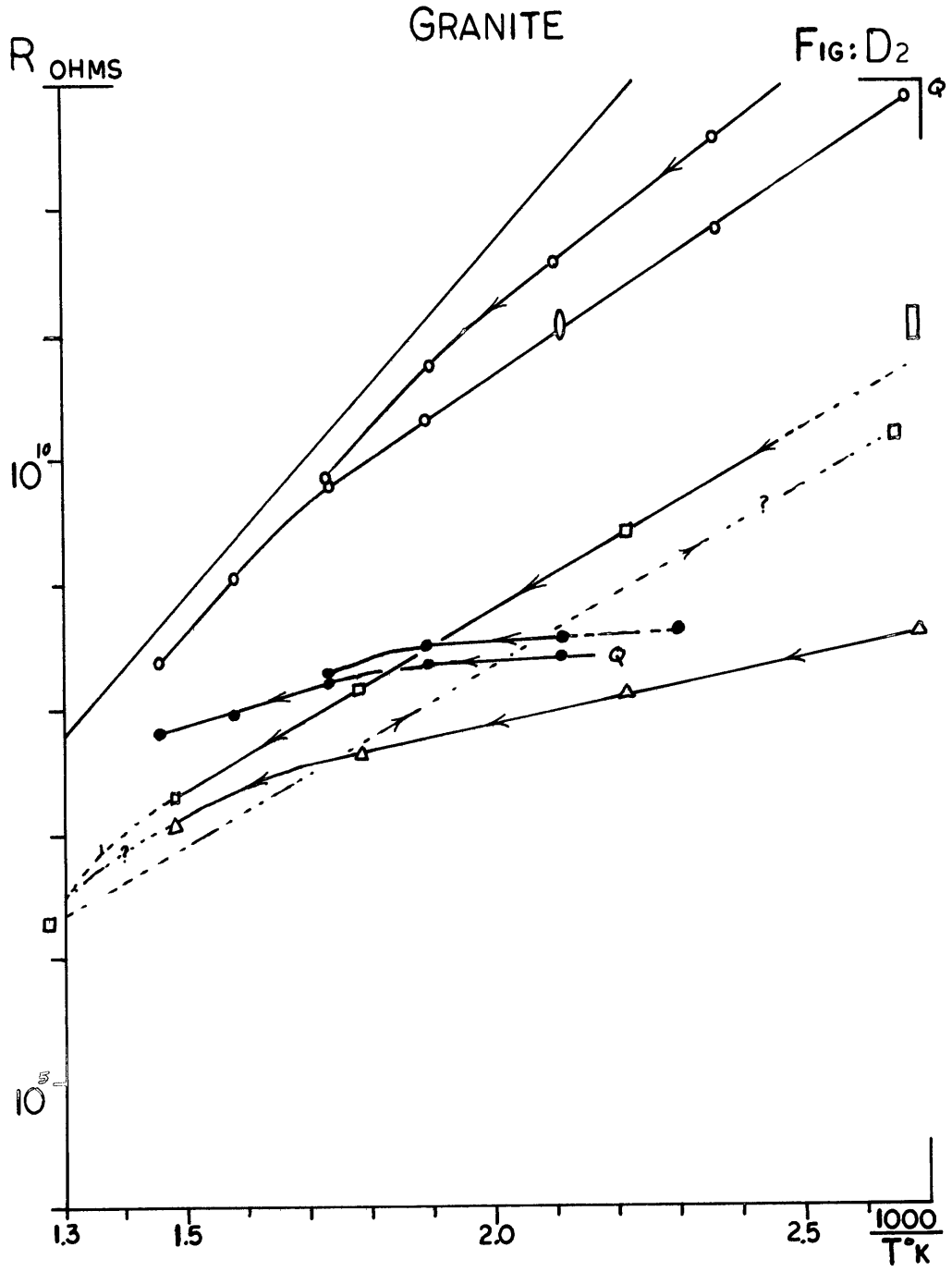
GRANITE
FIG: D2
R OHMS
10^10
10^5
1.3
1.5
2.0
2.5
1000/T°K
Q
Q
?
?

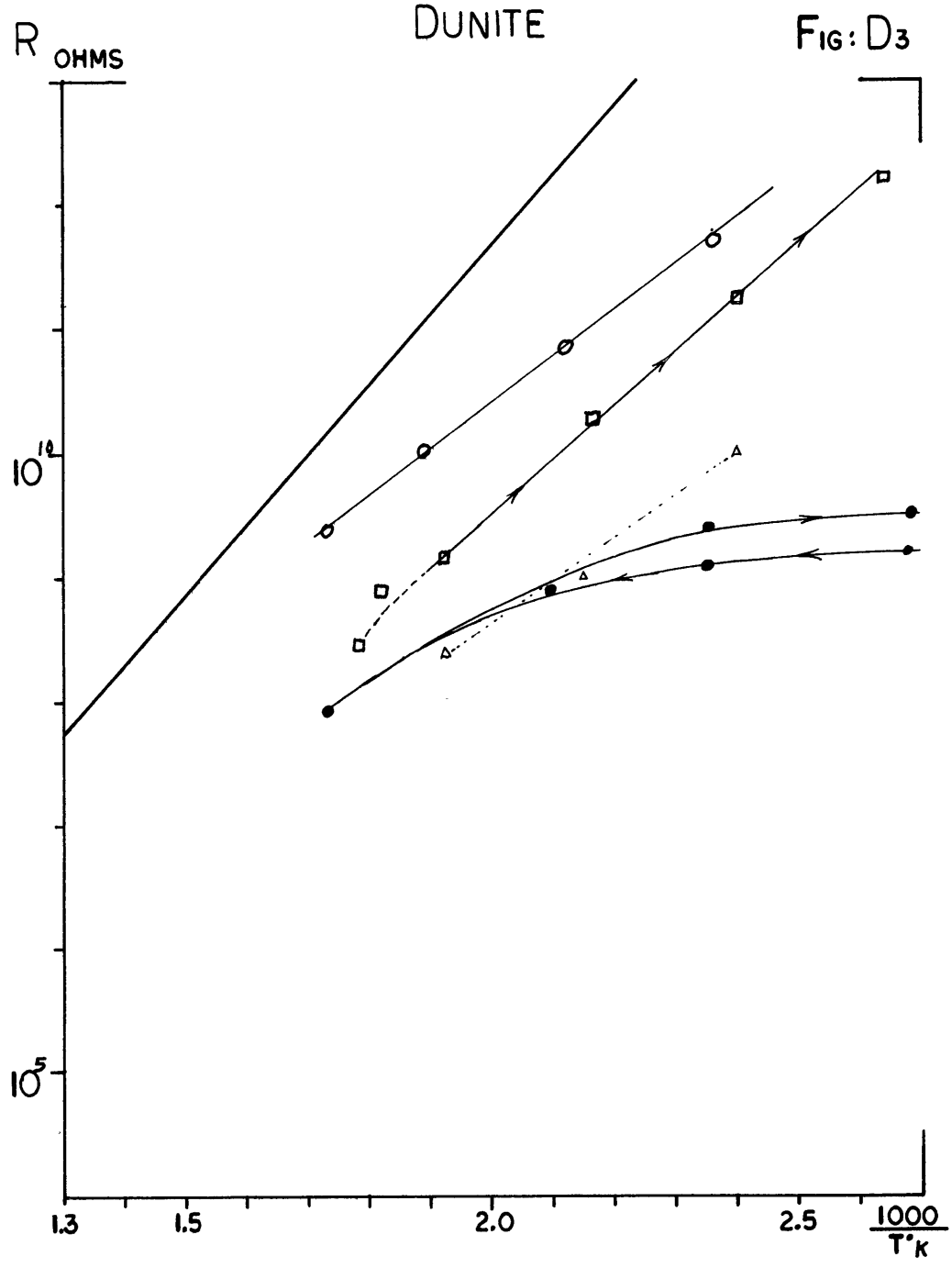
DUNITE
FIG: D3
R OHMS
10^{12}
10^{5}
1.3
1.5
2.0
2.5
1000/T°K

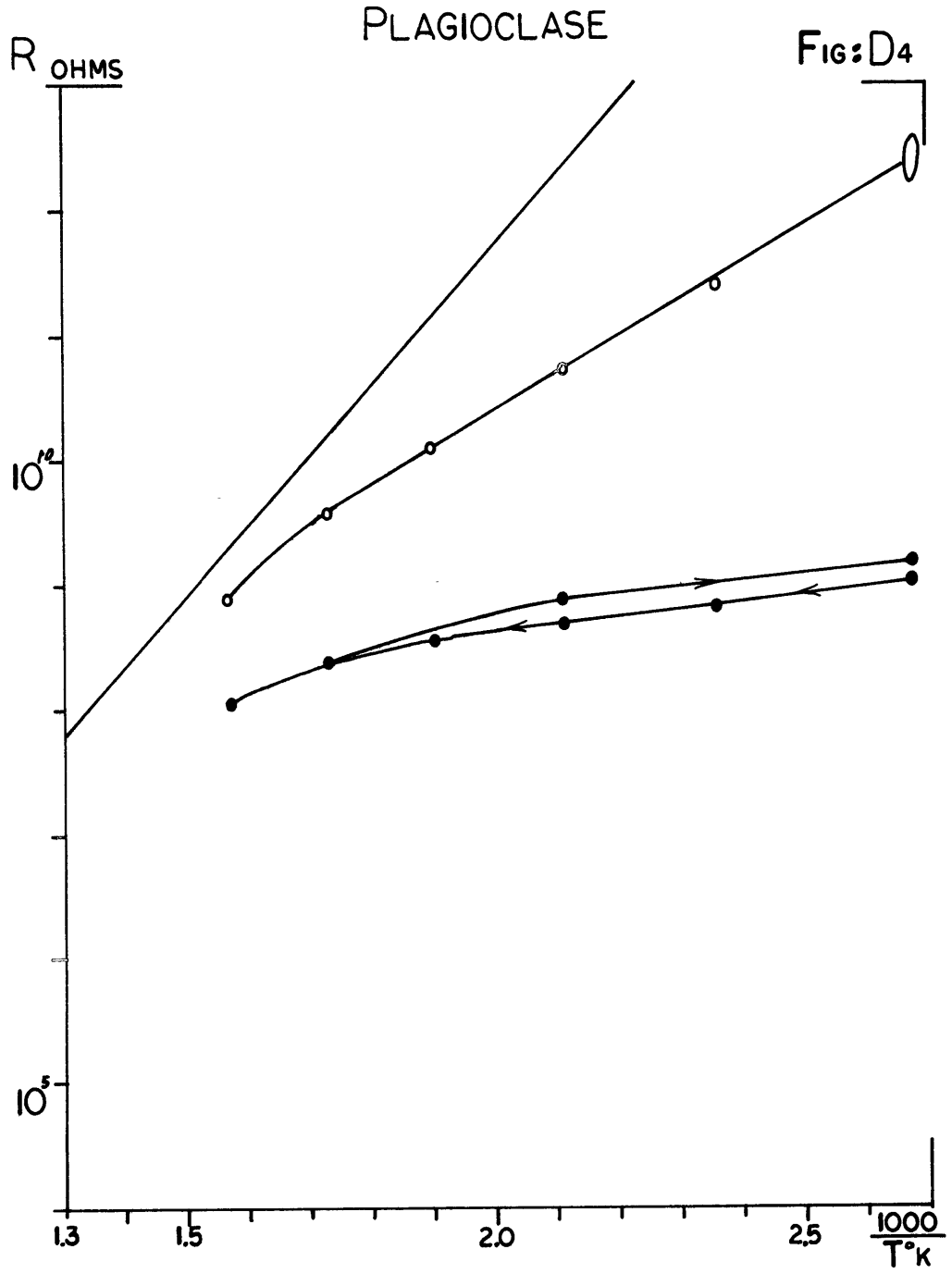
PLAGIOCLASE
FIG: D4
R OHMS
10^{12}
10^{5}
1.3
1.5
2.0
2.5
1000
T°K

RELAXATION MAXIMUMS

FIG: E1

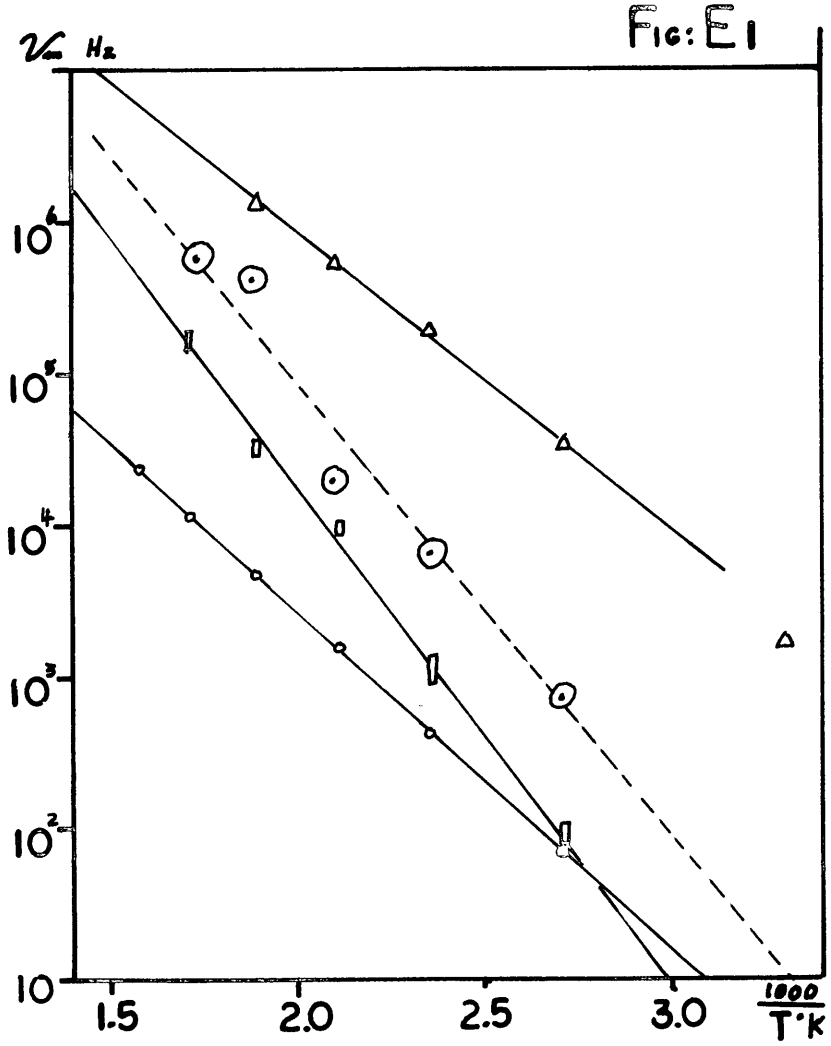

⊙ GRANITE

▯ BASALT M

○ HYPERSTENE

△ AUGITE

OHM'S LAW TEST

BASALT M

FIG: E2

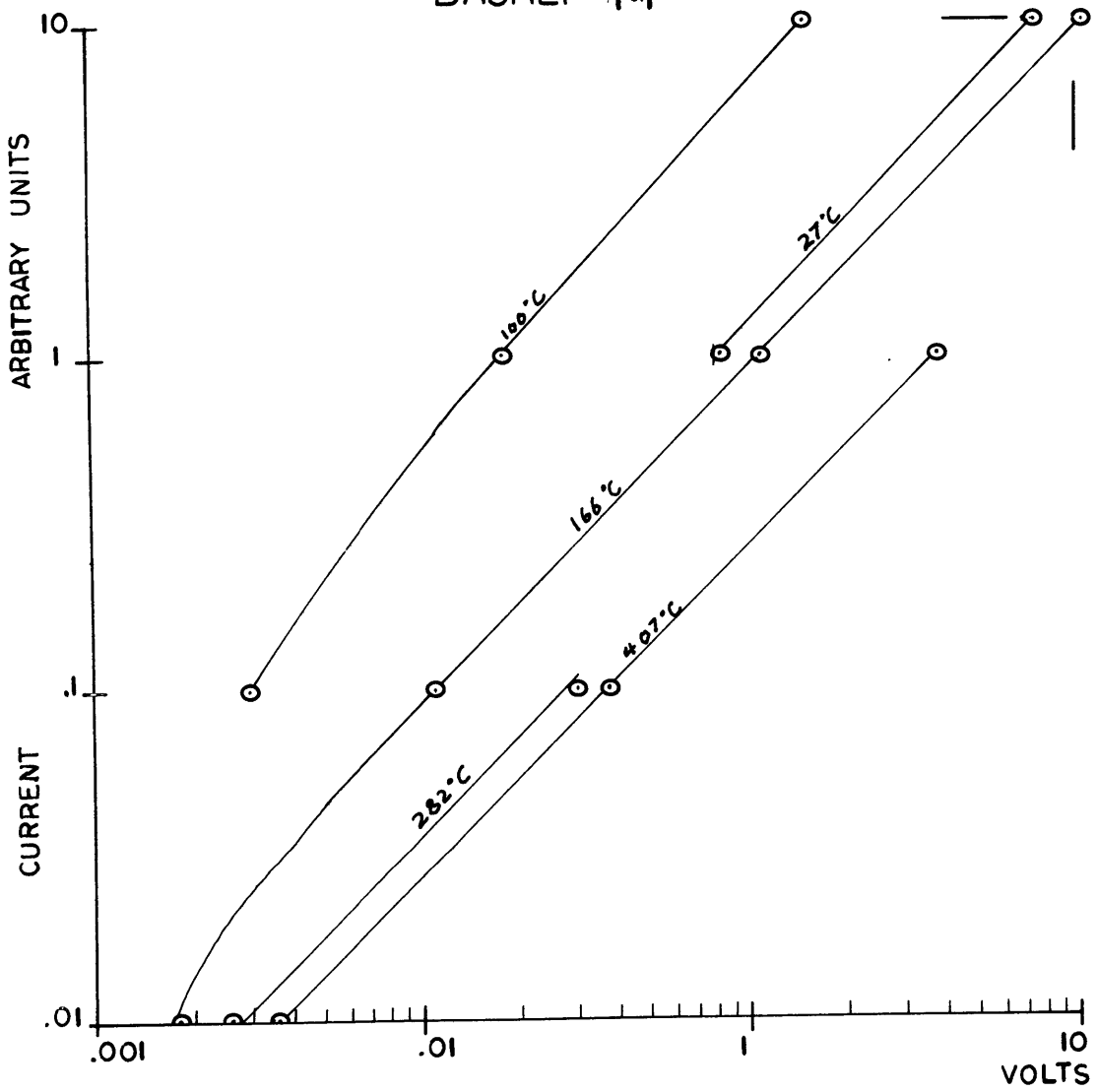

BASALT M
AT 200°C

FIG: E3

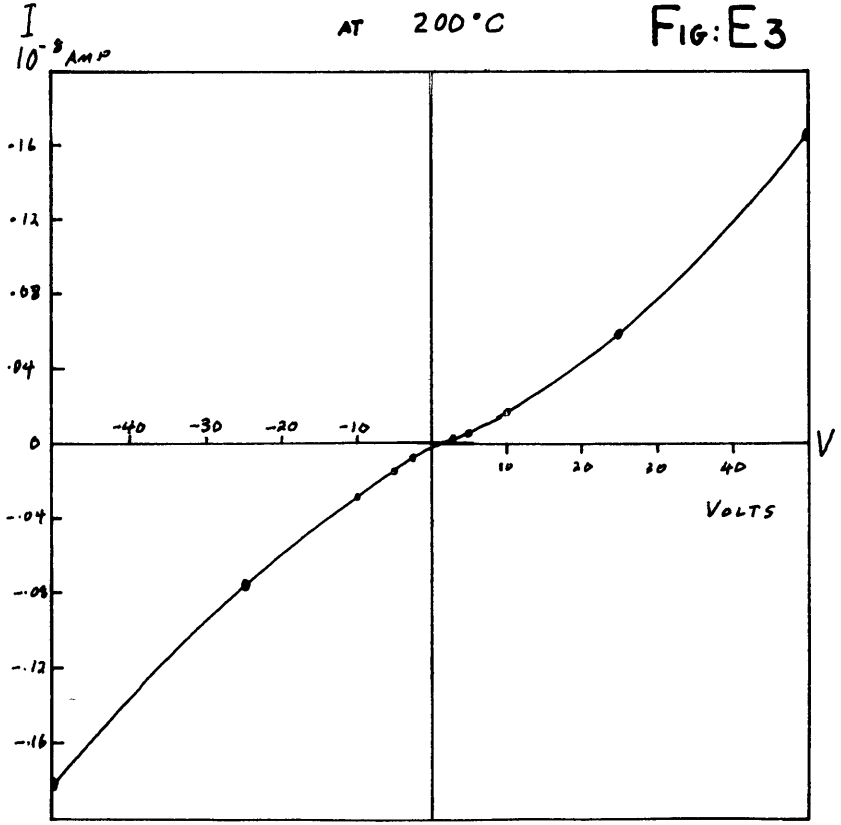

BASALT AA
0.5% H_2O

FIG: E4

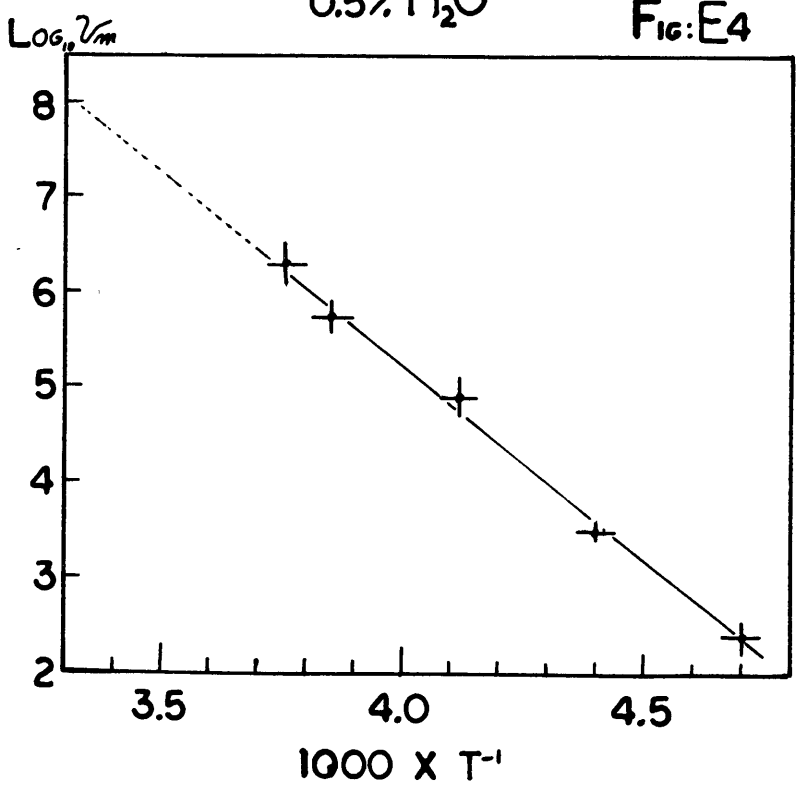

FIG: E_5

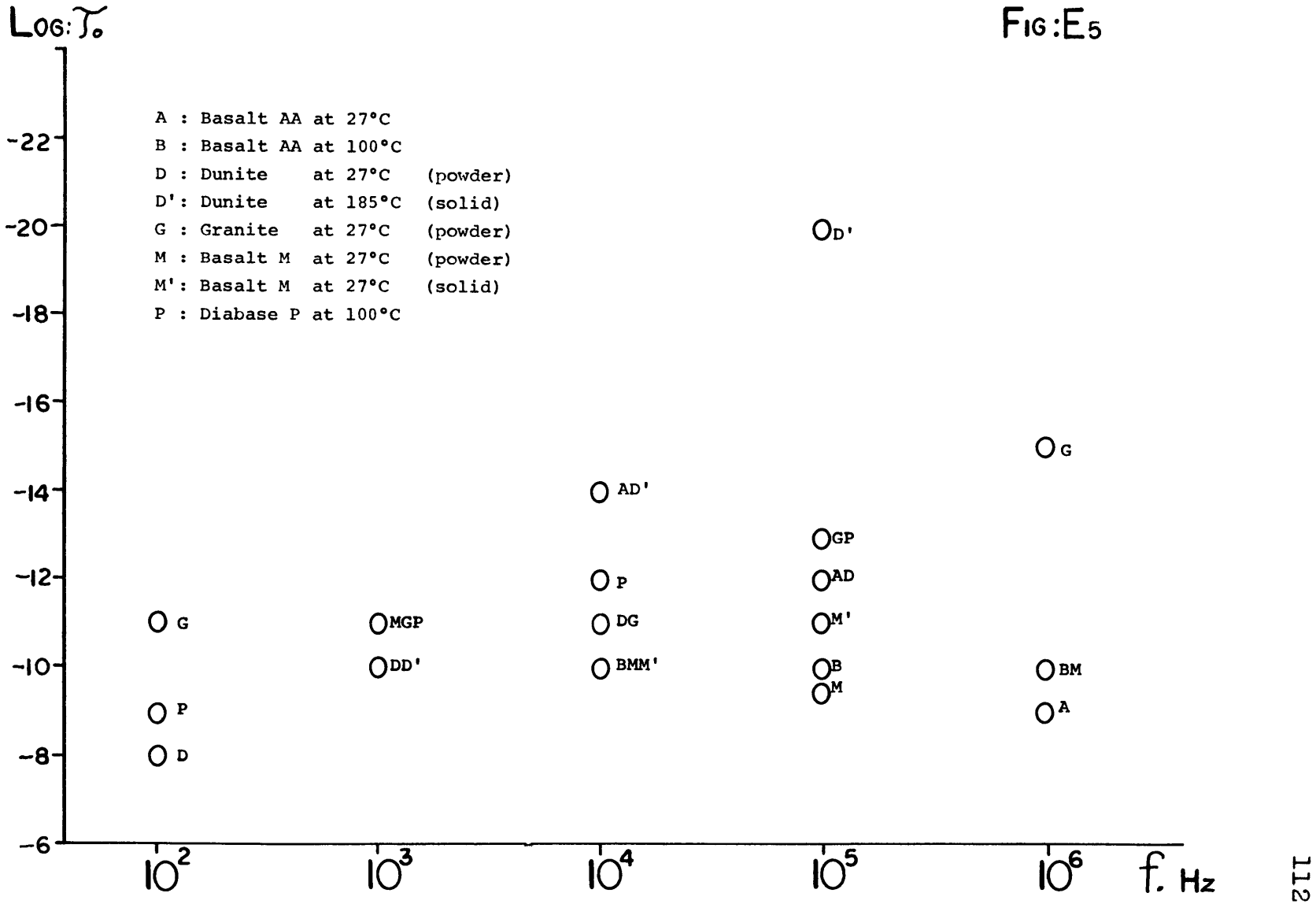
Log: τ_o
A : Basalt AA at 27°C
B : Basalt AA at 100°C
D : Dunite at 27°C (powder)
D': Dunite at 185°C (solid)
G : Granite at 27°C (powder)
M : Basalt M at 27°C (powder)
M': Basalt M at 27°C (solid)
P : Diabase P at 100°C
-22
-20
-18
-16
-14
-12
-10
-8
-6
G
P
D
MGP
DD'
AD'
P
DG
BMM'
D'
GP
AD
M'
B
M
G
BM
A
10^2
10^3
10^4
10^5
10^6
f. Hz

BASALT AA

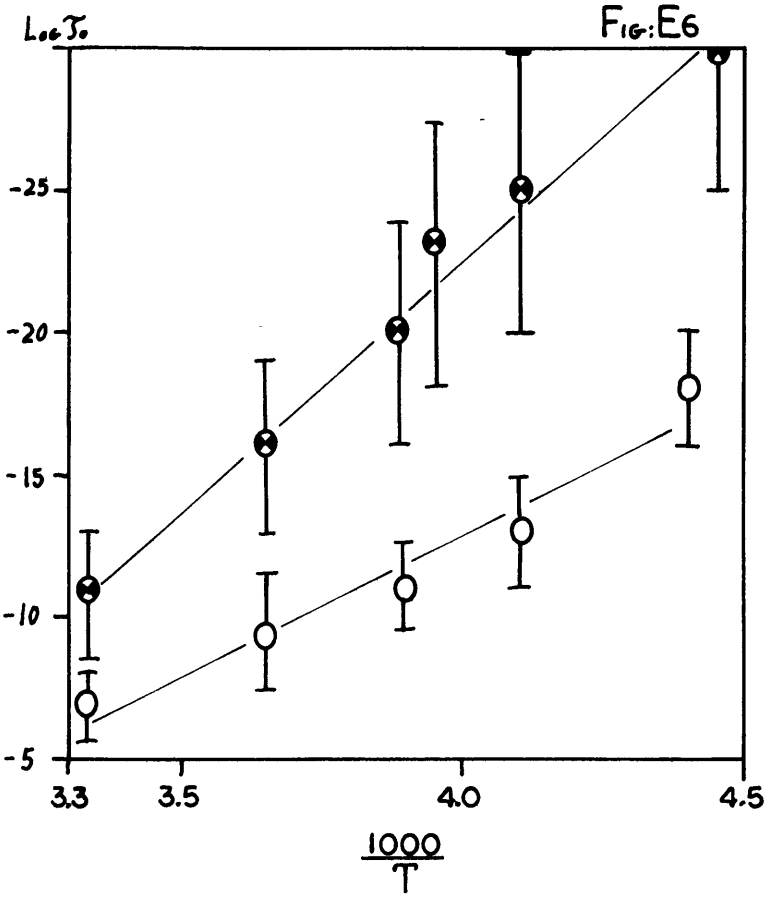

DRY 3000 Hz

0.1% H_2O 300 Hz

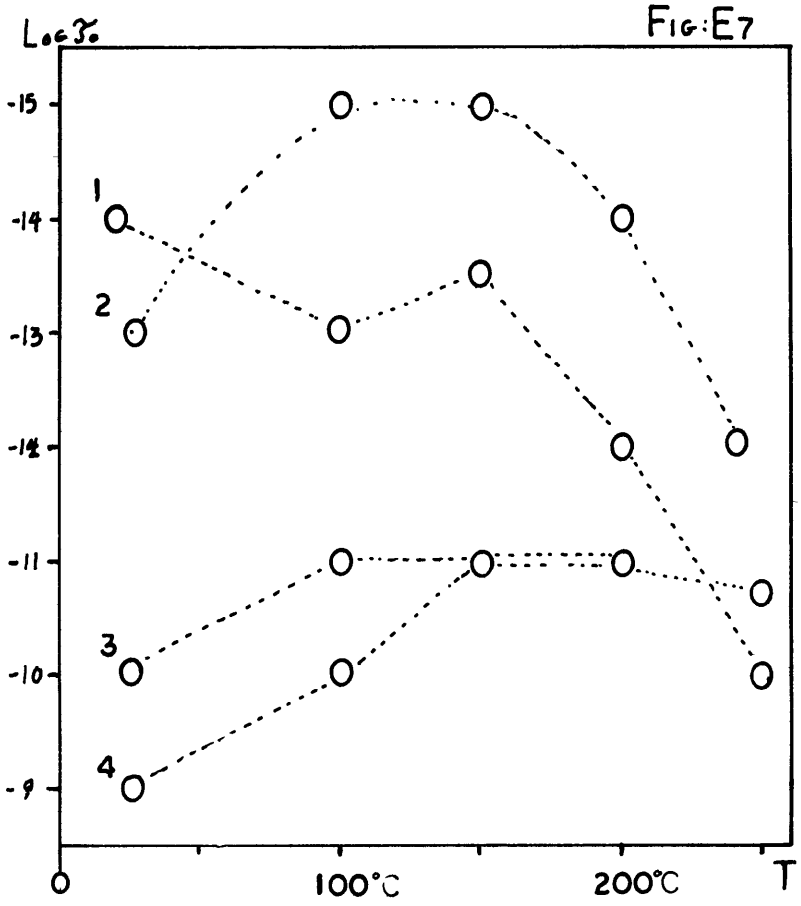

1 : Diabase at 10^5Hz
2 : Granite at 10^5Hz
3 : Basalt M at 10^6Hz
4 : Basalt AA at 10^6Hz

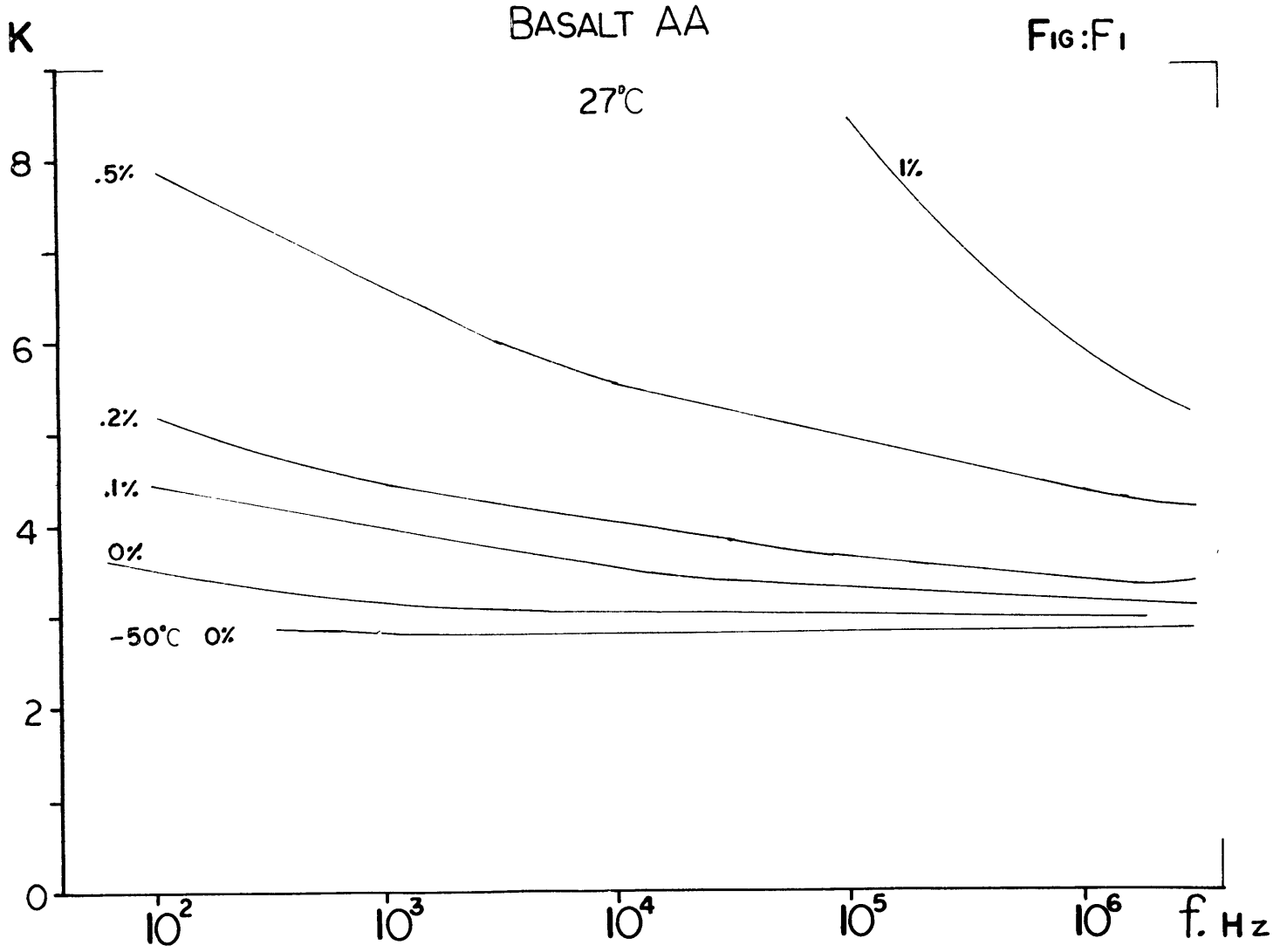
BASALT AA
FIG:F1
27°C
K
8
6
4
2
0
.5%
1%
.2%
.1%
0%
-50°C 0%
10^2
10^3
10^4
10^5
10^6
f. Hz

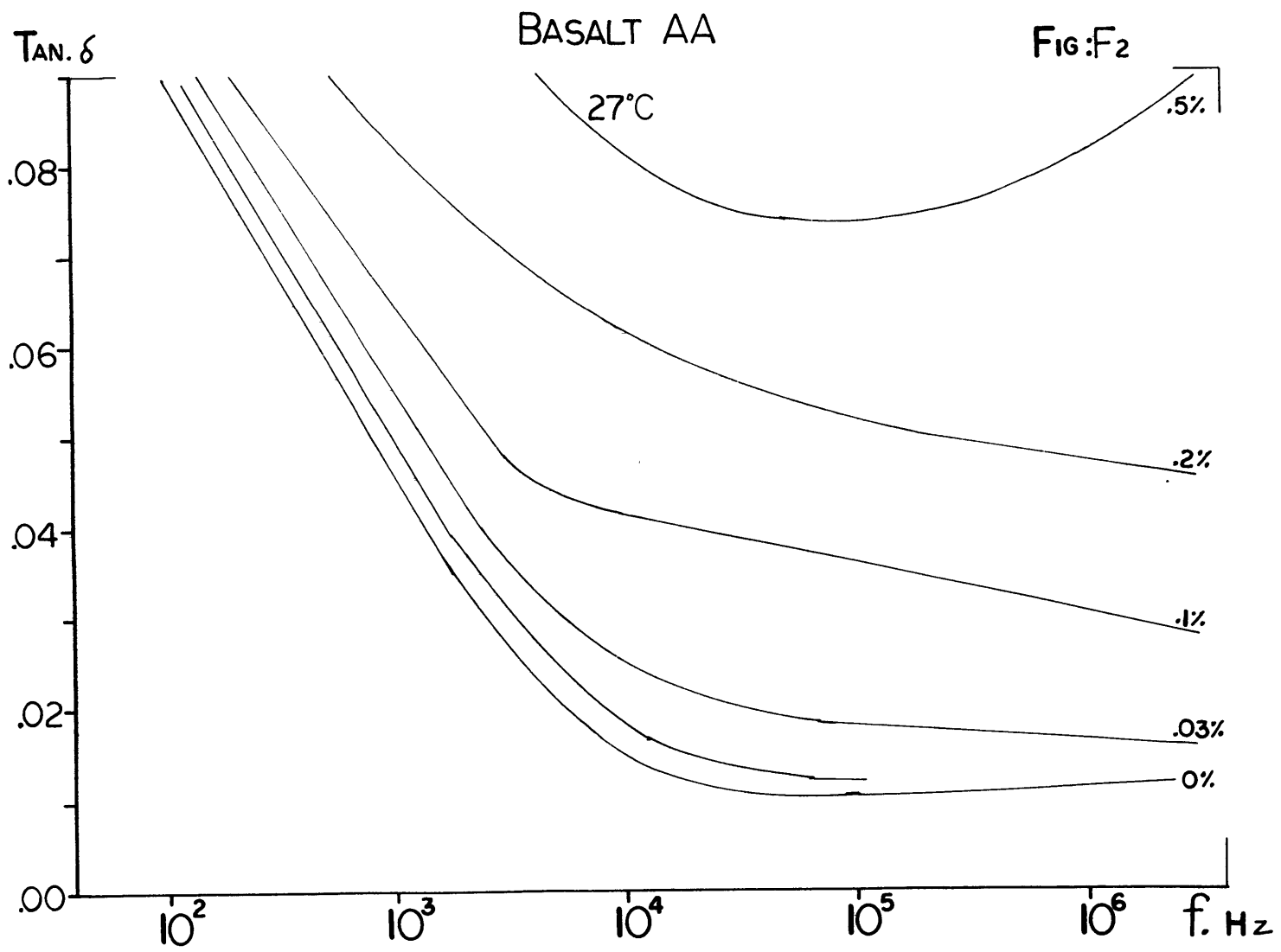
BASALT AA
FIG: F2
TAN. δ
27°C
.5%
.2%
.1%
.03%
0%
.08
.06
.04
.02
.00
10^2
10^3
10^4
10^5
10^6
f. Hz

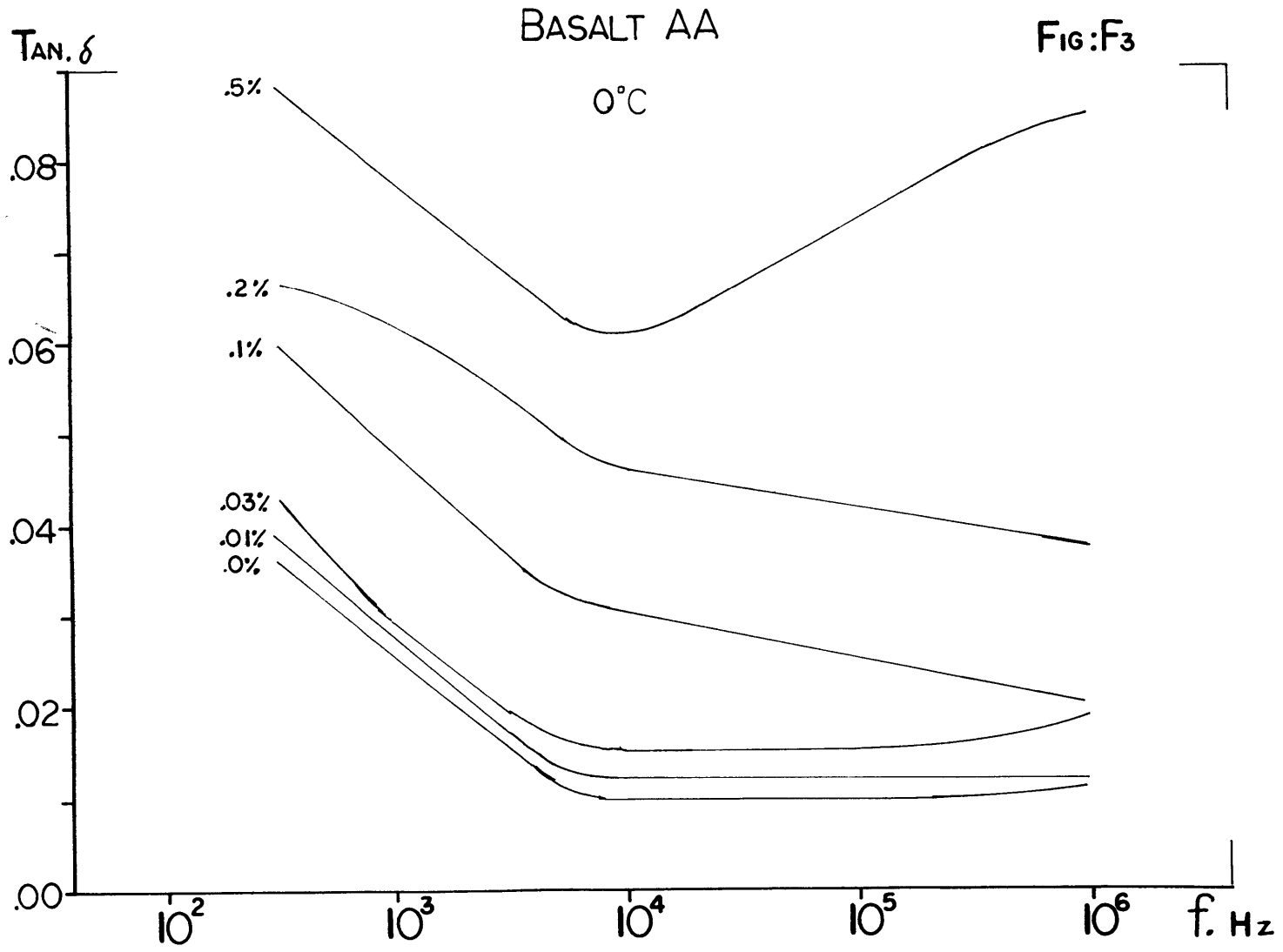
BASALT AA
FIG:F3
0°C
TAN. δ
.5%
.2%
.1%
.03%
.01%
.0%
.08
.06
.04
.02
.00
10²
10³
10⁴
10⁵
10⁶
f. Hz

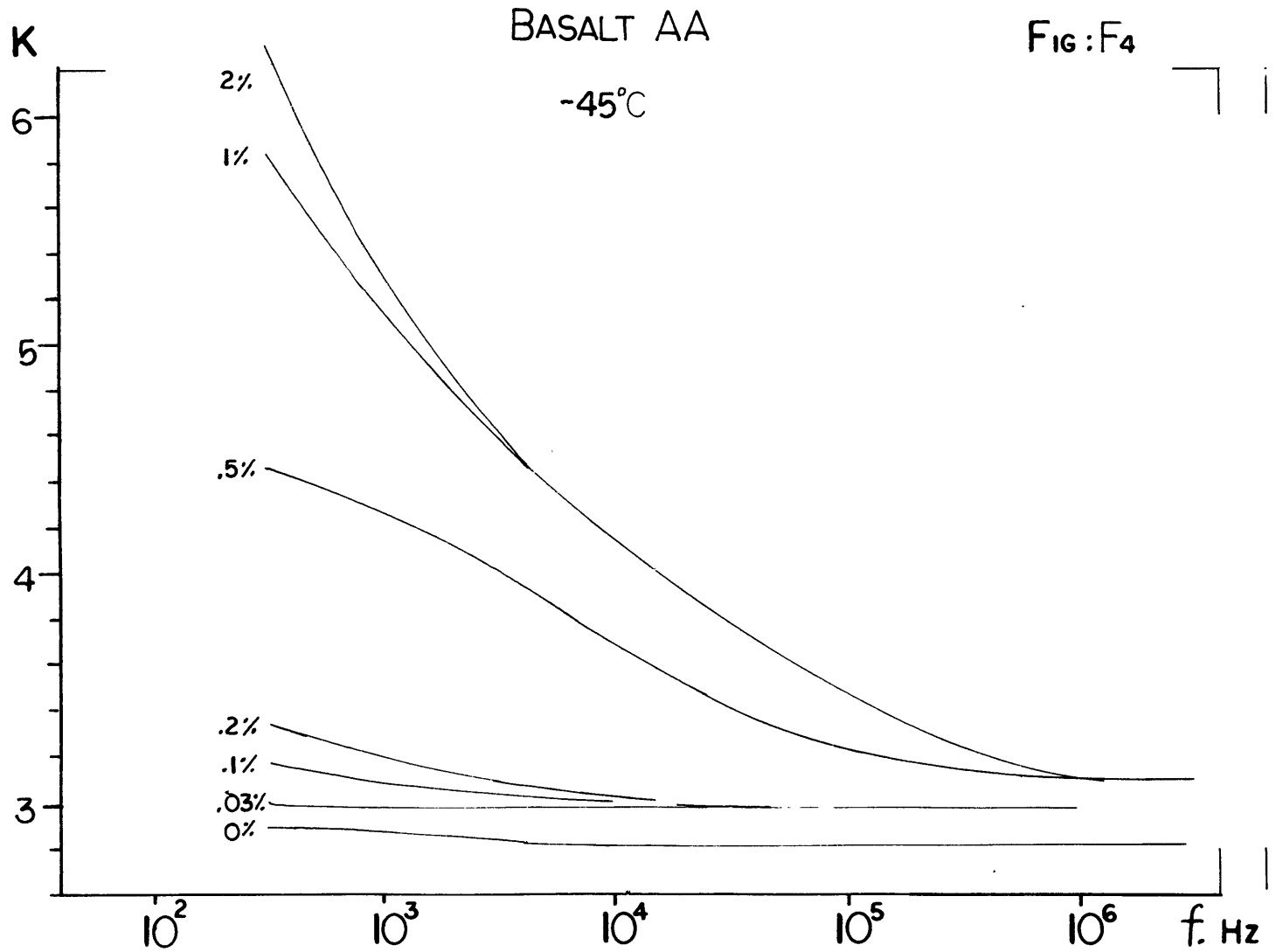
BASALT AA
-45°C
FIG : F4
K
6
5
4
3
2%
1%
.5%
.2%
.1%
.03%
0%
10^2
10^3
10^4
10^5
10^6
f. Hz

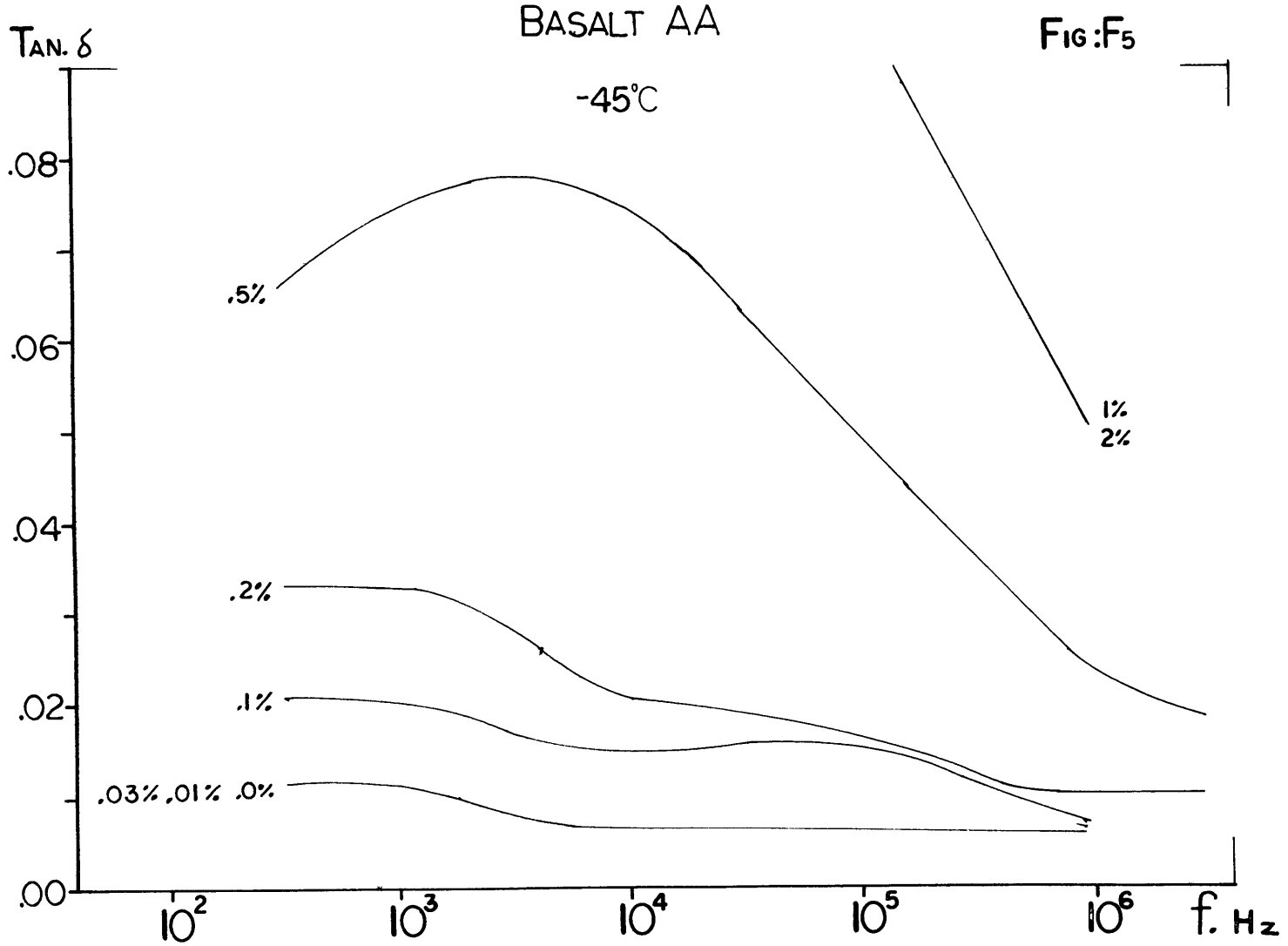
BASALT AA
-45°C
FIG:F5
TAN. δ
.08
.06
.04
.02
.00
.5%
1%
2%
.2%
.1%
.03%
.01%
.0%
10^2
10^3
10^4
10^5
10^6
f. Hz

FIG. G1

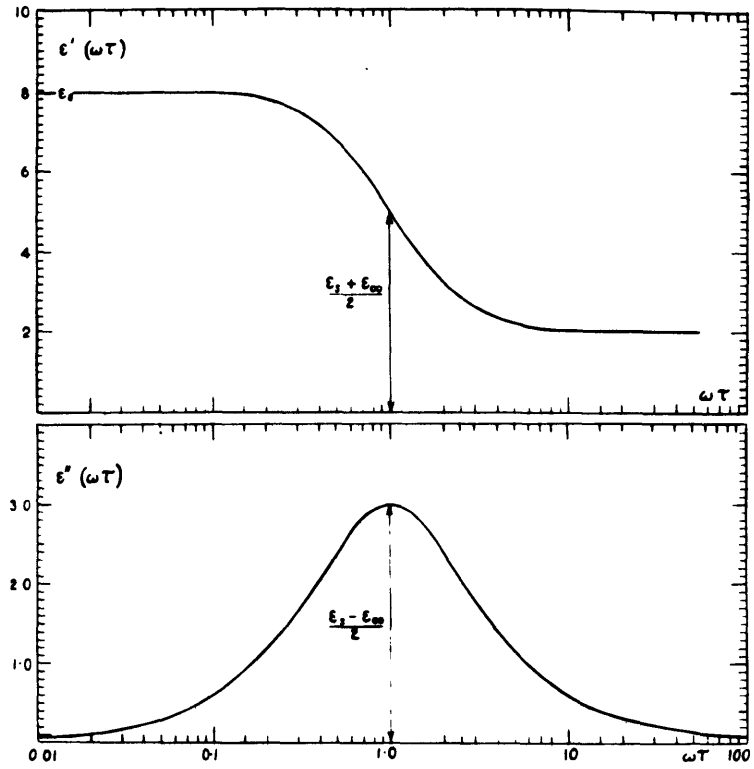

FIG. 2. (a) The real part of ε^* as a function of log $\omega\tau$ according to the Debye equations (2.21) and (2.22) for a dielectric with $\varepsilon_s = 8, \varepsilon_\infty = 2$; (b) The imaginary part of ε^* for the same dielectric.

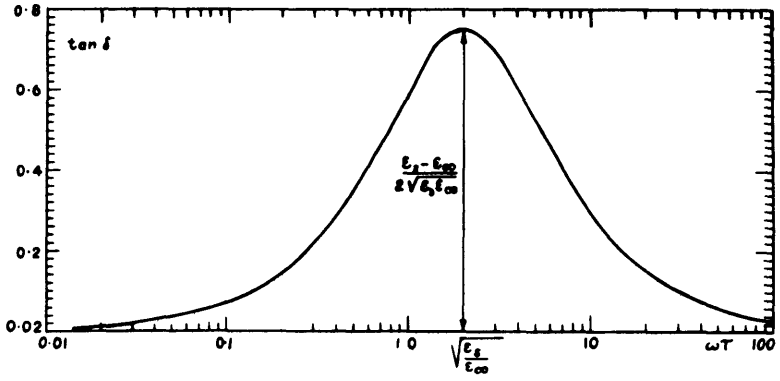

FIG. 3. The loss tangent for the dielectric illustrated in Fig. 2(a) and (b).

Fig:G2

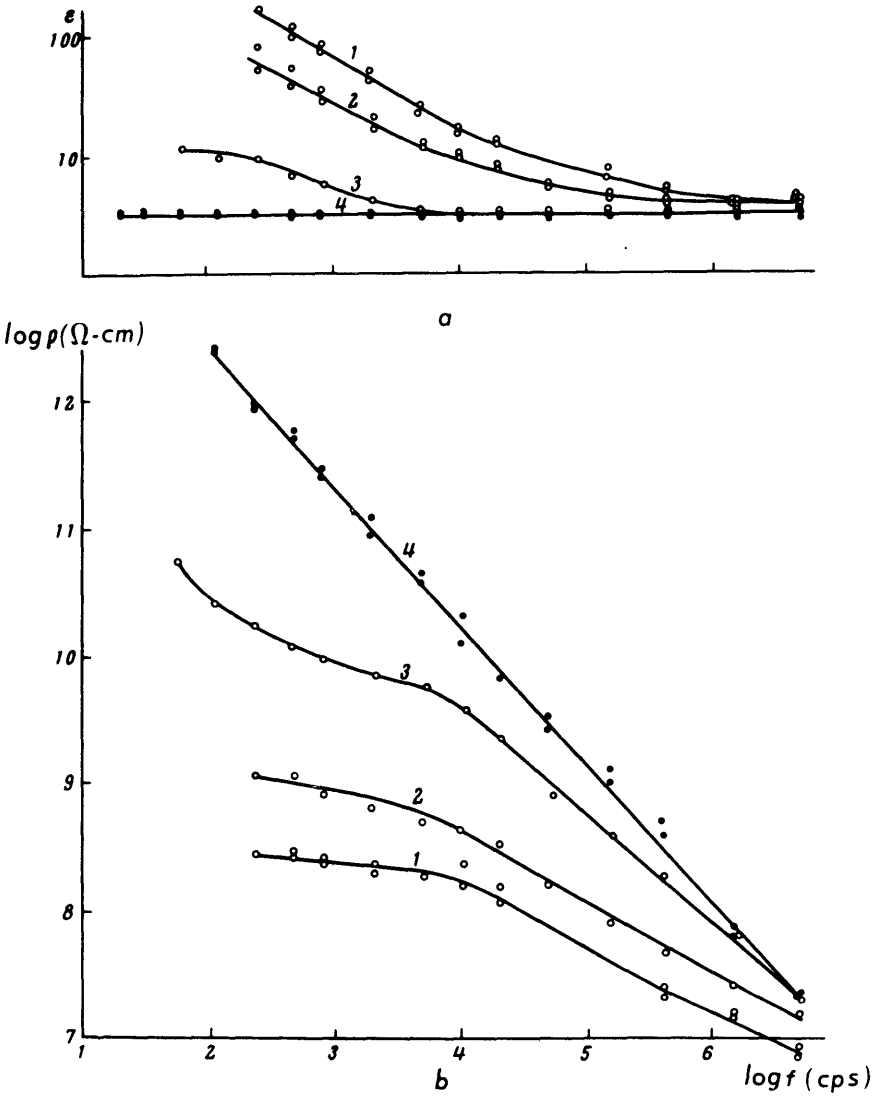

Fig. 92. Frequency dependence for the dielectric constant (a) and the resistivity (b) of a quartz sand. Water content in percent: (1) 12, (2) 0.4, (3) 0.03; (4) air dried with P_2O_5.

APPENDIX C

Table and Illustrations of Instruments.

	Title	Page
Fig.1	Sample Holder #3	123
Fig.2	Vacuum Inside Sample Holder #3 at Different Temperatures.	124
Fig.3	Sample Holder #4	125
Fig.4	Sample Set Up for Sample Holder #4	126
Fig.5	Furnace and Position of Sample Holder #3	127
Fig.6	Temperature Distribution in the Furnace (When Empty)	128
Table VII	Instruments Used.	129
Fig.7	Photography of the Laboratory.	130

FIG:1

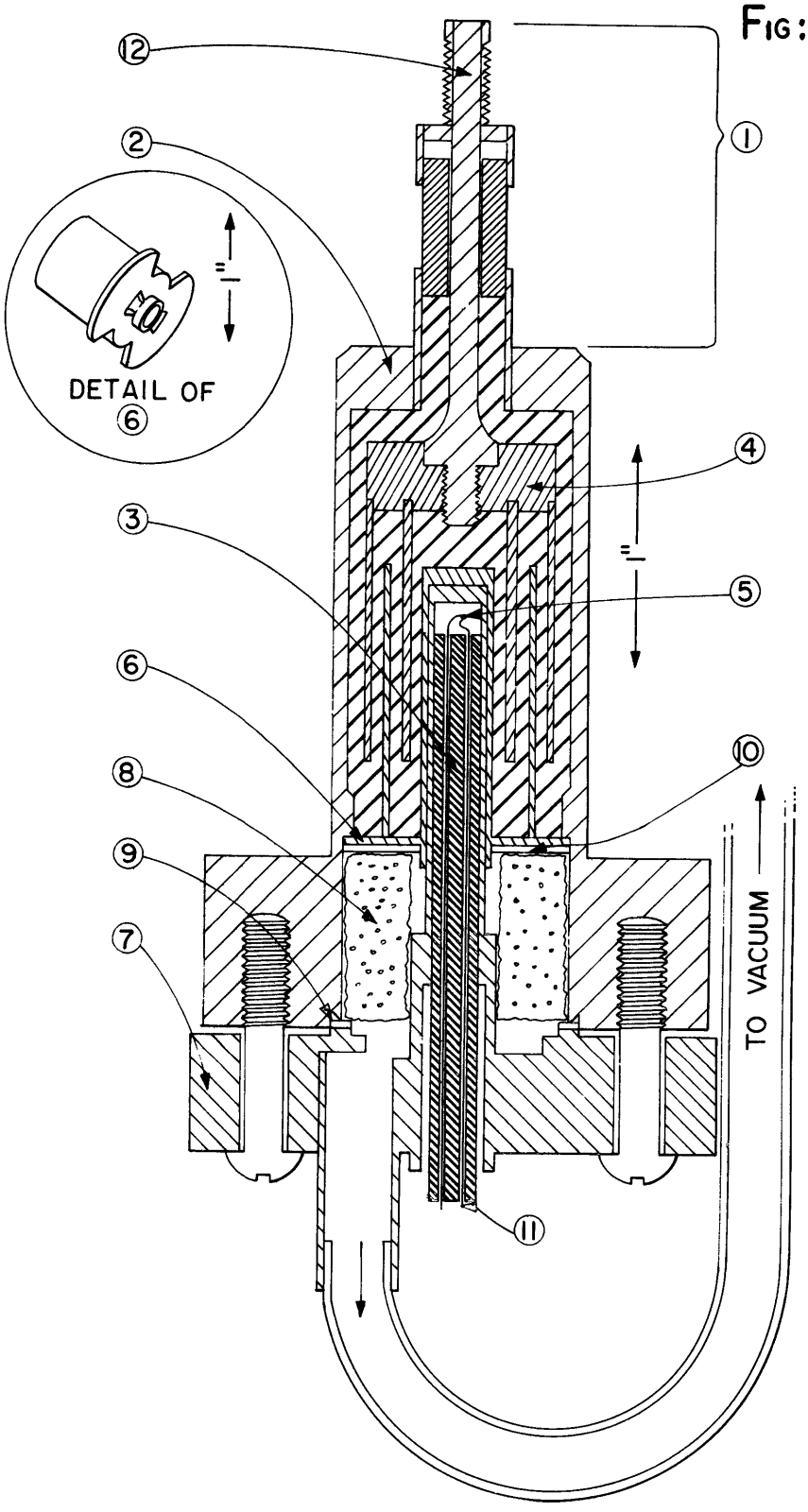

SAMPLE HOLDER # 3

FIG:2

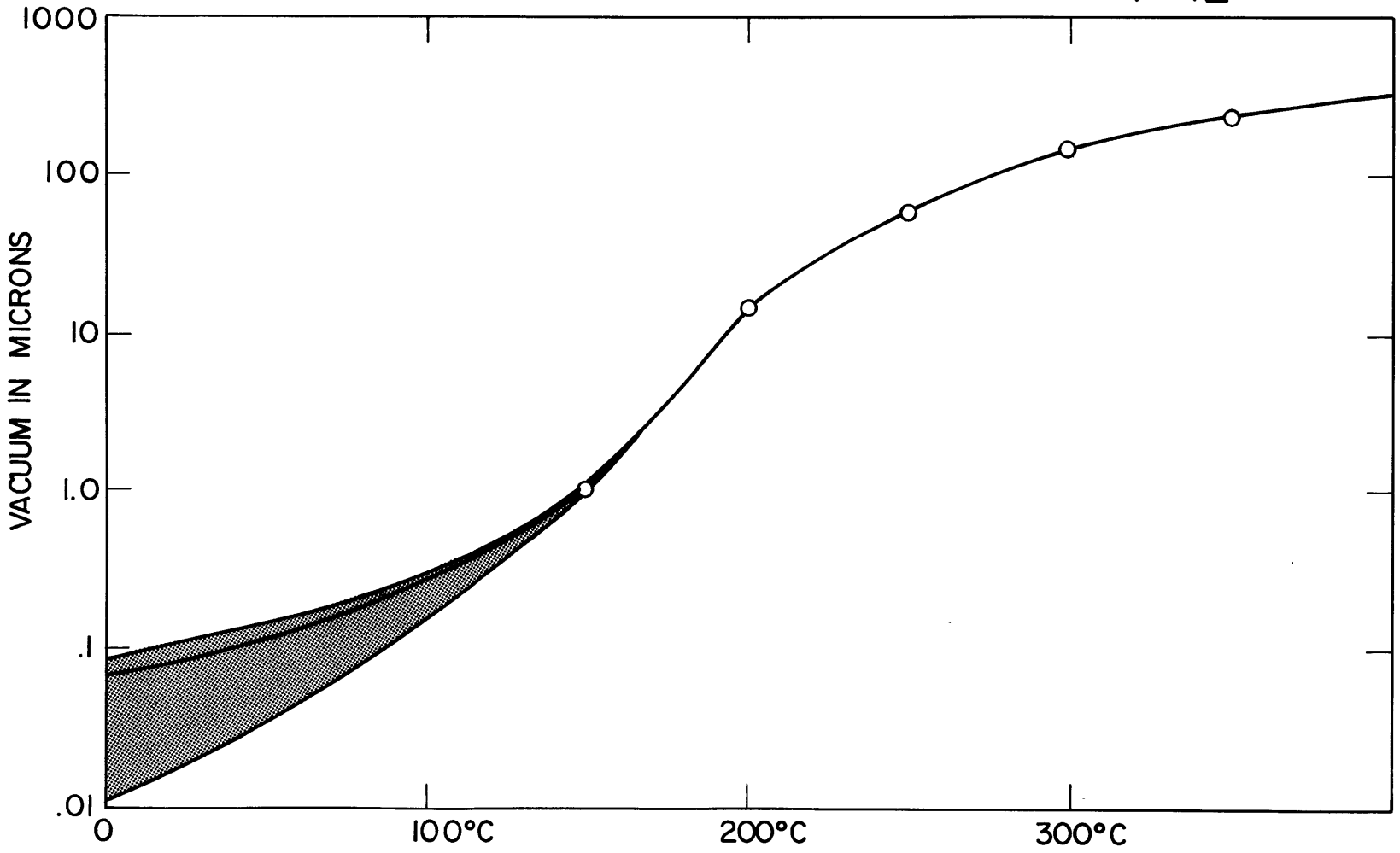

VACUUM INSIDE SAMPLE HOLDER # 3 AT DIFFERENT TEMPERATURES

SAMPLE HOLDER # 4
CROSS SECTION VIEW

FIG: 3

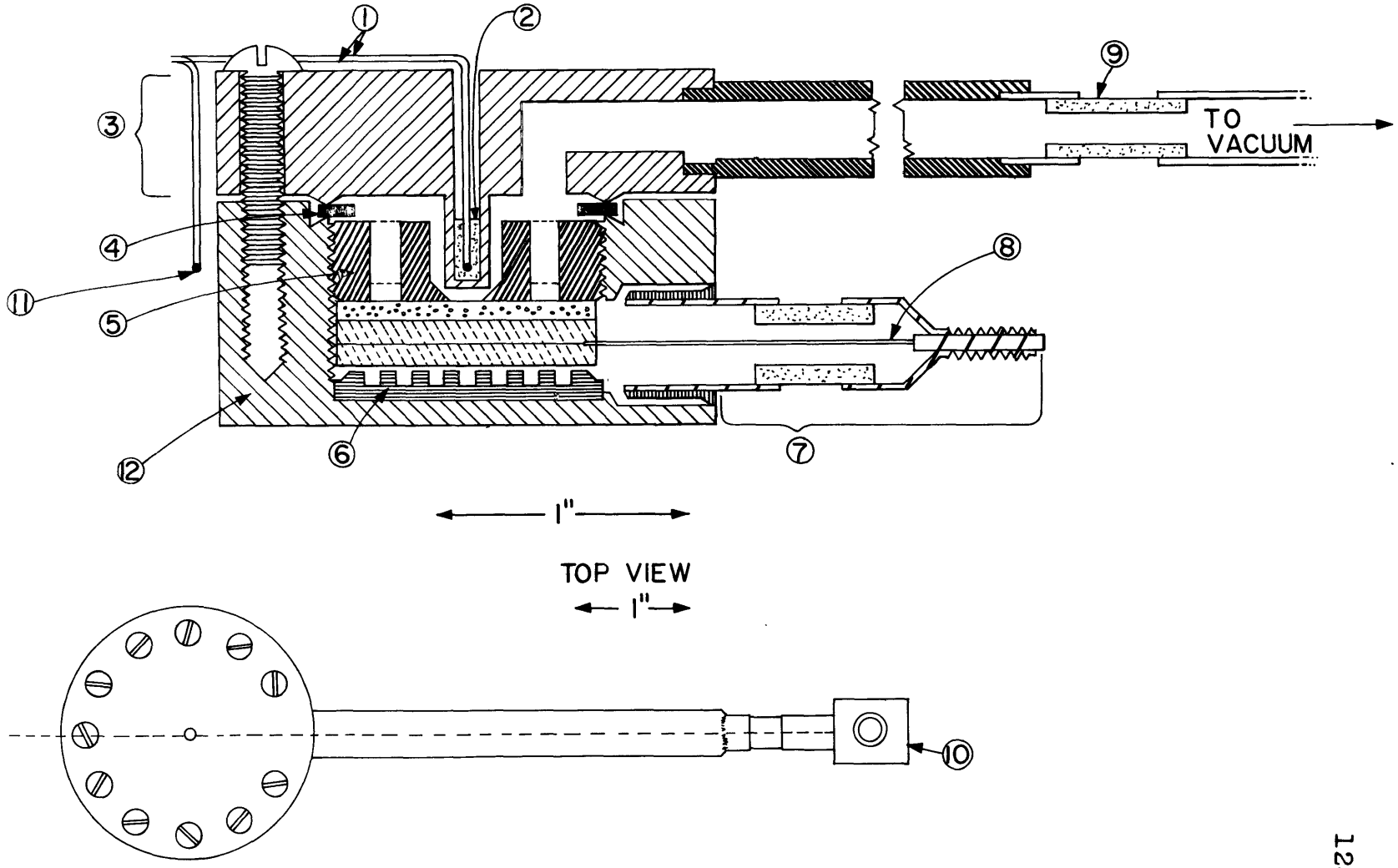

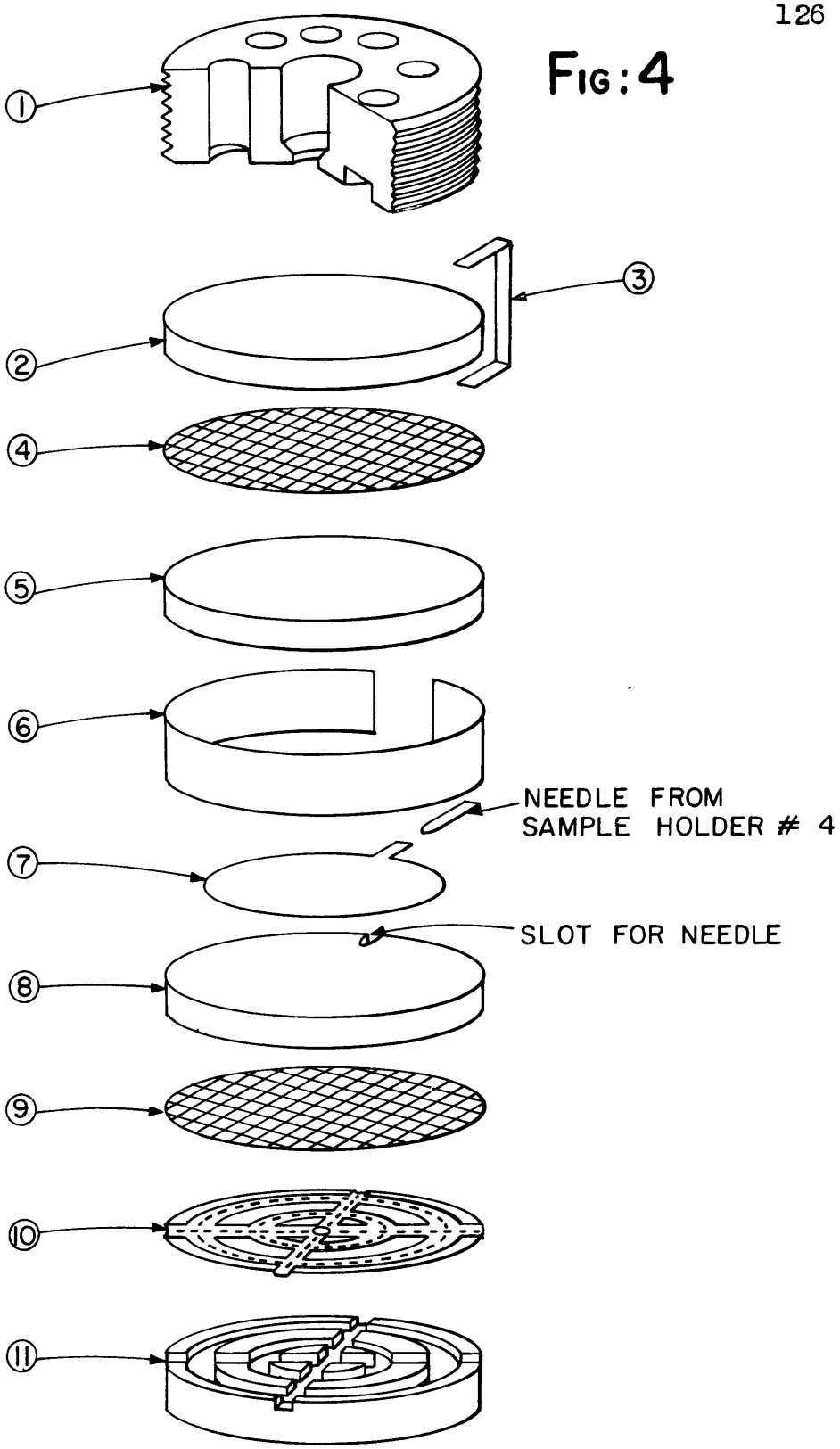

FIG: 4

SAMPLE SET UP FOR
SAMPLE HOLDER # 4

FIG: 5

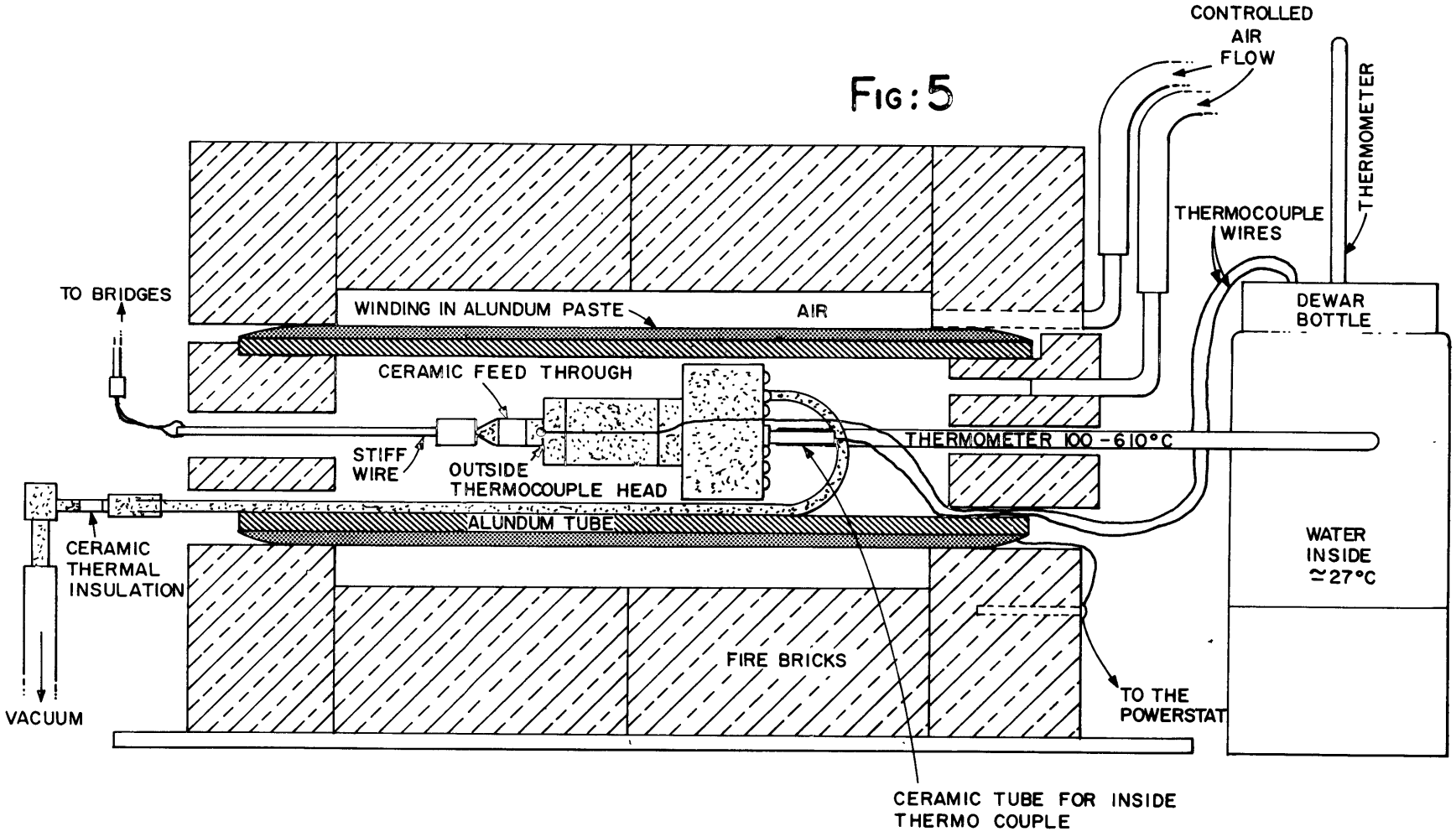

FURNACE AND POSITION OF SAMPLE HOLDER # 3

FIG: 6

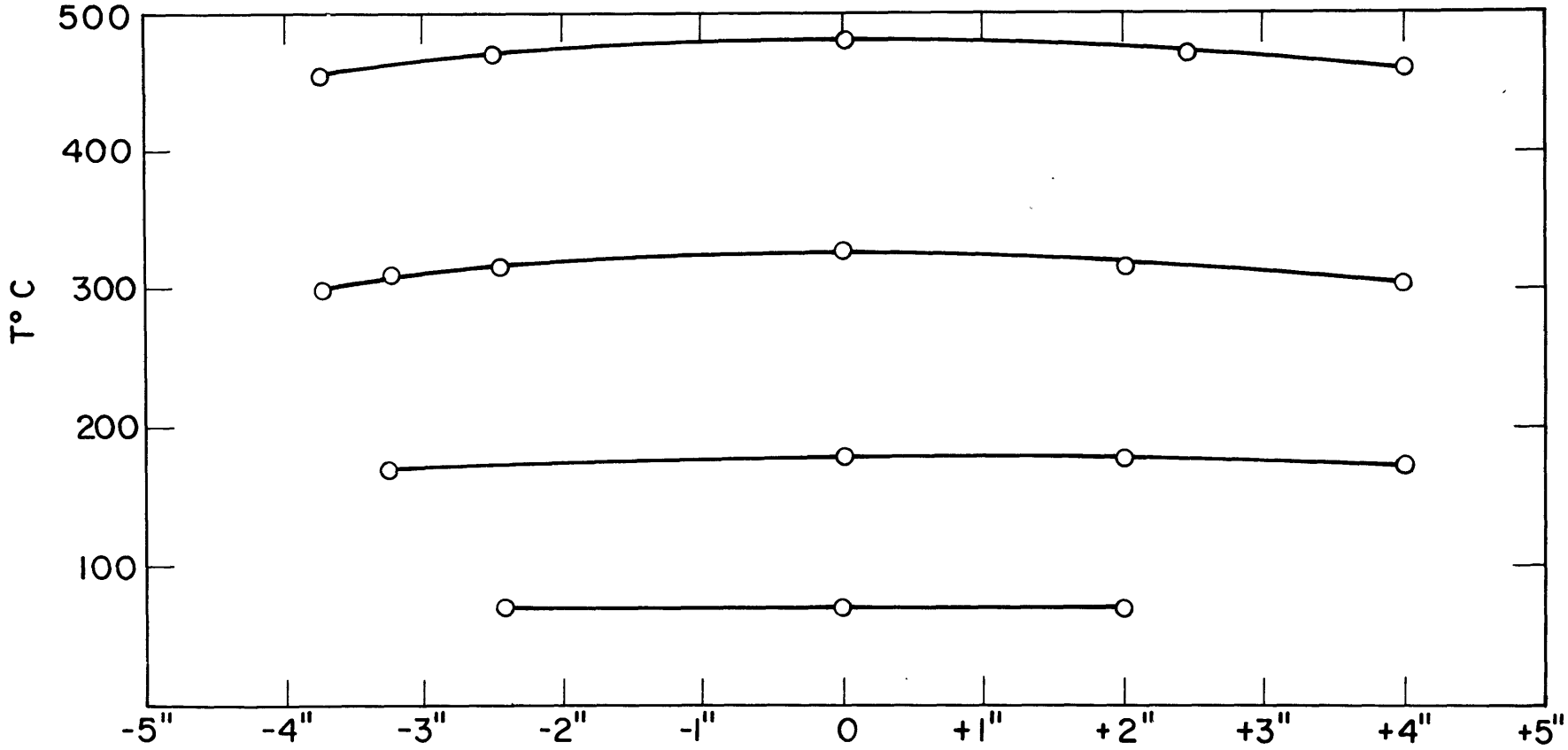

TEMPERATURE DISTRIBUTION IN THE FURNACE (WHEN EMPTY)

Table VII

Instruments Used

Instrument	Company	Model	Comments
Oscilloscope	H.P.	130A	
Oscillator	H.P.	650A	
Band Pass Filter	Allison Labs	2A	
A.C. Voltmeter, Ampl.	H.P.	400E	
Cap. Bridge	G.R.	716C	Low Frequency Bridge
Cap. Bridge	G.R.	716 C91	High Frequency Bridge
Null Detector	G.R.	1212A	
Electrometer	Keithley	600A	
Microvolt Meter	Keithley	150A	
Powerstat			0-140 volts 10 Amps.
Vacuum Pump	Hyvac	2	0.1μ guaranteed
Thermocouple Gauge Control	Veeco Instr.	TG6	
Thermometer 110-650°C	Fisher Sci.	15-016A	N_2 filled above Mercury column


CUT-RITE
CORNING
Gene Simmons

APPENDIX D

The Determination of K, tan δ from the Experimental Data

In order to determine K and tan δ , the correction factors given in the G.R. bridge manual are used. Since the bridge gives the value for the equivalent series circuit, they were transformed into parallel circuit equivalents and the wire and feed-thru capacitance subtracted. In the case of the solid samples, the loss factor and capacitance value of the reference capacitor were also taken into account. From the results, K and tan for the samples were determined. Resistance values which are lower by a factor of five than the resistance of the ceramic feed-thru are satisfactory and are given without any correction. Higher resistances are also given, but they are not as reliable.

The equivalent circuit connected to the UNKNOWN-DIRECT terminals of the type 716 bridge is illustrated below:

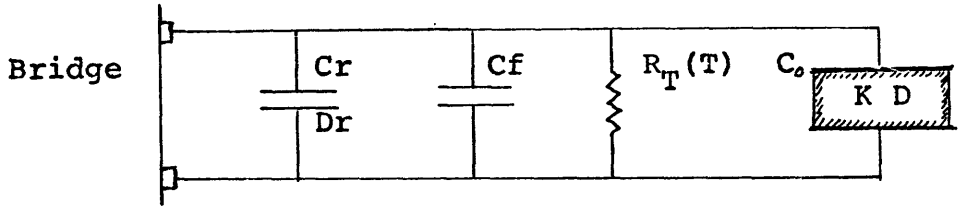

where:
- Cr is the capacitance value of the reference capacitor (for the case of solid sample)
- Dr is the loss tangent value of the reference capacitor (for the case of solid sample)
- Cf is the total capacitance of the feed-thru and of the connecting wires
- R_T(T) is the resistance value of the ceramic feed-thru
- C_O is the effective capacitance value of the sample holder when empty
- K is the dielectric constant of the sample
- D is the loss tangent of the sample.

APPENDIX E

Proposed General Form of tan (f) for Dry Sand and Low Density Rock, (at 27°C).

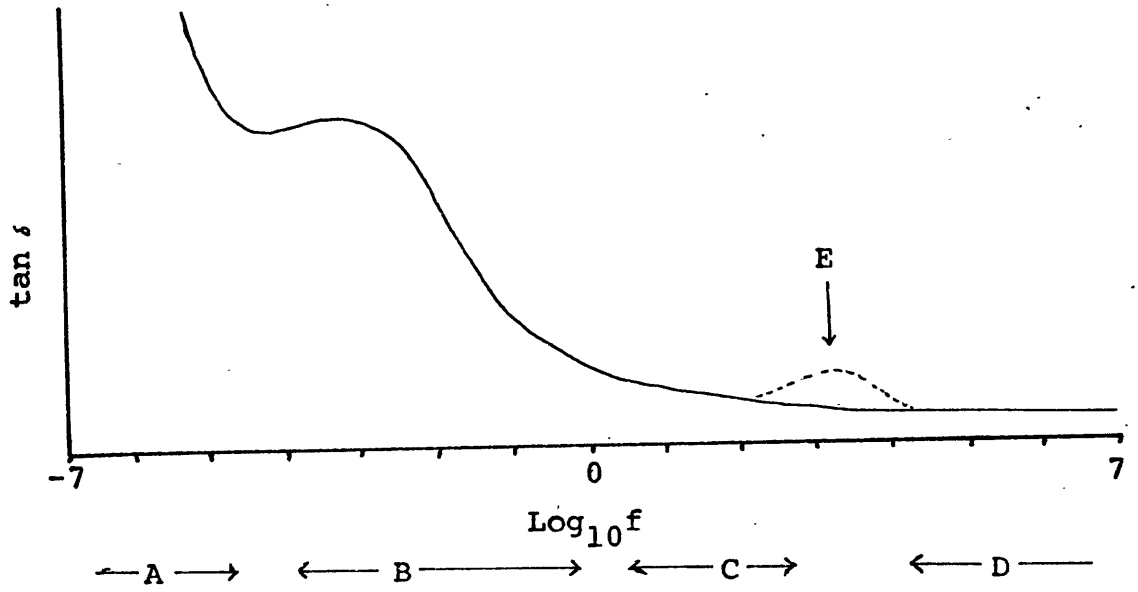

This figure shows qualitatively in a convenient form, the conclusion of this research for the case of dry sand and low density rocks.

The horizontal arrows indicate approximately the range of frequency of a given dominant loss mechanism for the present example.

A. A tan δ rise in the form: cst/f.
   Loss due to DC conductivity.

B. A broad relaxation maximum at very low frequency, 10^{-2} to 10^{-5} Hz.
   A Maxwell-Wagner effect of classical type, due to the inhomogeneity of conductivity within the rock, and/or of non-classical type, such as the Wenden mechanism (28).

C. Small dependence of tan δ to frequency.
   A Maxwell-Wagner effect, due to a wide distribution of conductivity of minor

constituents and alterations within the rock.

D. Frequency independent tan δ .

A mechanism involving ionic or molecular movements such as the Garton's mechanism.

E. Relaxation maximum outside the relaxation maximum in B.

A mineral effect by: a classical Maxwell-Wagner effect due to a higher conductivity of the mineral than the other constituents of the rocks (i.e. biotite or some augite or any mineral with high chemical impurity content) or, a relaxation maximum due to some lattice imperfection or a chemical impurity in the mineral.

At higher temperature, these features will move toward higher frequency at different rates.